# THE CREEP OF POTASH ROCK FROM NEW BRUNSWICK

by

**Fei Yin**

A Thesis
Submitted to the Faculty of Graduate Studies
in Partial Fulfilment of the
Requirements for the Degree of

**MASTER OF SCIENCE**

Department of Civil and Geological Engineering
Faculty of Engineering, University of Manitoba
Winnipeg, Manitoba

THE UNIVERSITY OF MANITOBA

FACULTY OF GRADUATE STUDIES

*****

COPYRIGHT PERMISSION PAGE

**THE CREEP OF POTASH ROCK FROM NEW BRUNSWICK**

**BY**

**FEI YIN**

A Thesis/Practicum submitted to the Faculty of Graduate Studies of The University of Manitoba in partial fulfillment of the requirements of the degree of

**MASTER OF SCIENCE**

# ABSTRACT

The laboratory investigation on which this thesis is based has involved over 6 creep-years of experiments using potash rock from New Brunswick, Canada. The experimental programme consisted of two parts: incremented-stress creep tests designed to determine creep strain and creep strain rates, and a series of tests in which the sensitivity of creep as a function of stress history was explored. The duration of tests was between 7 and 298 days, with most tests lasting about three months.

The experiments have demonstrated that potash deformation is highly time-dependent even at a stress as low as 2 MPa. A typical creep curve consists of two parts, an initial phase during which the strain rate drops sharply and a second phase during which the strain rate still decreases, but at a very slow rate. The first phase is usually over in about 20 days. Both phases should by definition belong to the primary stage of creep. There is little support for the existence of steady-state creep in potash rock. Similarly, tertiary creep did not appear in this study. This may however be due to the fact that the tests were usually terminated after the stress sensors (mainly strain gauges) ceased to function. The amount of creep strain increases rapidly above the yield point that is around 8 MPa. Above the crack initiation point (around 12 MPa), lateral dilatancy dominates the creep process.

In the absence of steady-state creep, the creep rate is never constant in being a function of time. The stress-dependence of the creep rate was established at a number of time intervals in the form of a power function. The exponent of the stress changes but little beyond 10 days. It is 2.3 for the axial strain rate over the stress range of 2 to 15 MPa

and 4.93 for the lateral strain in the 10 to 15 MPa range. Below 10 MPa, the lateral strain rate is too small, in the order of the resolution of the instrumentation.

When the same stress steps were used in comparable stress-increment and stress-decrement tests, the measured strains were lower and the strain rates higher the in stress-decrement series of creep tests. When two creep tests were repeated at the same stress, the strains were always lower in the second test. The strain rate followed a more complex pattern than other rock types. When the repeated test followed a 6-month rest period at no stress, the strain rate of the repeated test was lower. When there was no rest between the two creep tests, the strain rate in contrast was higher than in the original test. A memory effect is indicated.

**TO MY FATHER**
**with cheer and with mourning**

# ACKNOWLEDGEMENTS

Any words could not express my gratitude and appreciation to my supervisor, Dr. Emery Z. Lajtai for his intelligent guidance, continuous encouragement and sincere compassion. Without his leadership and support this thesis would not have been possible. The knowledge that I learned from Dr. Lajtai is not only about creep but also about a career. His tireless correction of my English expression during these years enabled me to improve my ability to use both scientific and everyday English.

I am grateful also to the examination committee's members for taking their time to review my work and offering constructive criticisms. My specific thanks I give to Dr. B. Stimpson for his true help whenever needed, who once encouraged me and gave me the first chance to work in Canada.

I am very grateful to Mr. W. Grajewski, Mr. N. Piamsalee, and Mr. S. Sparrow for their help in the laboratory, assisting with technical aspects of the equipment and helping to overcome unexpected problems. I would like to thank Ms. Ingrid Trestrail who has helped me in many different ways. I would like to thank all professors and co-workers in this faculty, who build so warm an environment to work in.

Finally, I will express my love and thanks to my family: my parents, who have offered me spiritual support, my husband, who has given me love, understanding and selfless sacrifice, and my son, who often asked me "how about your experiment?"

# TABLE OF CONTENTS

Page

ABSTRACT ..... i

DEDICATION ..... iii

ACKNOWLEDGEMENTS ..... iv

TABLE OF CONTENTS ..... v

LIST OF FIGURES ..... viii

LIST OF TABLES ..... xiii

NOMENCLATURE AND ABBREVIATIONS ..... xv

CHAPTER 1 INTRODUCTION ..... 1

1.1 General Background ..... 1

1.2 The Research ..... 3

CHAPTER 2 LITERATURE SURVEY .....

AND EXPERIMENTAL METHODOLOGY ..... 5

2.1 Literature Survey ..... 5

2.2 Test Environment ..... 6

2.3 Specimen Preparation ..... 6

2.4 Data Acquisition ..... 7

2.4.1 Strain measurement ..... 8

2.4.2 The strain-gauge and the DT measurements ..... 10

2.5 Testing Equipment and Environmental Control ..... 14

CHAPTER 3 INCREMENTED-STRESS CREEP TESTS ..... 15

3.1 Introduction ..... 15

3.2 Experimental Procedure ..... 18

3.3 Experimental Results ..... 20

3.3.1 Series NB1 at 4 MPa and 7 MPa ..... 20

3.3.2 Series NB2 at 10 MPa and 13 MPa ..... 23

3.3.3 Series NB3 at 6, 9, 10, 9,15 and 16 MPa ..... 23

3.3.4 Series NB4 at 8 MPa, 11 MPa, 12 MPa, and 14 MPa ..... 29

3.3.5 Series NB6 at 3 MPa, 5 MPa, and 8 MPa ..... 33

3.3.6 Series TP1 at 1 MPa and 10 MPa ..... 33

3.3.7 Series TP2 at 2 MPa and 12 MPa ..... 38

3.4 Discussion of Experimental Results ..... 40

3.4.1 Mechanisms of deformation in potash rock ..... 40

3.4.2 The theoretical stress-strain curves ..... 40

3.4.3 Construction of the stress-strain diagram ..... 41

3.4.4 Creep deformation ..... 45

3.4.5 The effect of loading history ..... 54

3.4.6 The strain rate ..... 58

3.5 Chapter Summary ..... 76

CHAPTER 4 DECREMENTED-STRESS AND REPEATED CREEP TESTS ..... 83

4.1 Introduction ..... 83

4.2 Experimental Procedure ..... 84

4.2.1 Creep tests under decremented-stress loading ..... 84

4.2.2 Repeated creep tests ..... 86

4.3 Experimental Results ..... 88

4.3.1 Decremented-stress creep test on specimen NB3 ..... 88

Decremented-stress creep test on specimen NB6 ..... 95

4.3.2 Repeated creep tests on specimen NB6 ..... 101

Repeated creep tests on specimen NB3 ..... 106

4.4 Discussion of Experimental Results ..... 109

4.4.1 Deformation in decremented-stress creep tests ..... 109

4.4.2 Deformation in repeated creep tests ..... 110

4.5 Chapter summary ..... 111

CHAPTER 5 CONCLUSIONS AND RECOMMENDATIONS ..... 112

5.1 Conclusion ..... 112

5.2 Recommendation for further research ..... 114

# LIST OF FIGURES


Page

2-1 The creep apparatus.....11

2-2 Comparison of creep strain measured by strain gauges and displacement transducers,(a)2MPa(b)15MPa..... 13

3-1 The schematic of different strain components and stages ..... 17

3-2 The 'bathtub curve' describing the creep rate.....18

3-3 Axial, lateral, and volumetric creep strain versus time on specimen PCA92-1M at 4 MPa and 7 MPa, (a) for NB1A, and (b) for NB1B.....21

3-4 The strain rate versus time, (a) specimen PCA92-1M, and (b) specimen PCA92-2M .....22

3-5 Axial, lateral, and volumetric creep strain versus time on specimen PCA92-2M at 10 MPa and 13 MPa, (a) for NB2A, and (b) for NB2B.....24

3-6 Axial, lateral, and volumetric creep strain versus time on specimen PCA92-3M at 6 MPa and 9 MPa, (a) for NB3A, and (b) for NB3B.....25

3-7 Axial, lateral, and volumetric creep strain versus time on specimen PCA92-3M at 10 MPa and 9 MPa, (a) for NB3C, and (b) for NB3D .....26

3-8 Axial, lateral, and volumetric creep strain versus time on specimen PCA92-3M at 15MPa and 16 MPa, (a) for NB3E, and (b) for NB3F .....27

3-9 Creep strain rate versus time on specimen PCA92-3M, (a) axial strain rate, and (b) lateral strain rate.....28

3-10 Axial, lateral, and volumetric creep strain versus time on specimen PCA92-5M at 8 MPa and 11 MPa, (a) for NB4A, and (b) for NB4B ..... 30

3-11 Axial, lateral, and volumetric creep strain versus time on specimen PCA92-5M at 12 MPa and 14 MPa, (a) for NB4C, and (b) for NB4D ..... 31

3-12 Creep strain rate for specimen PCA92-5M, (a) axial, and (b) lateral... ..... 32

3-13 Axial, lateral, and volumetric creep strain versus time on specimen PCA92-6M at 3 MPa and 5 MPa, (a) for NB6A, and (b) for NB6B ..... 34

3-14 Axial, lateral, and volumetric creep strain and strain rate on specimen PCA92-6M at 8 MPa (a), and strain rates versus time (b) ..... 35

3-15 Axial, lateral, and volumetric creep strain versus time on specimen LS-61-41 at 1 MPa and 10 MPa, (a) for TP1-1, and (b) TP1-2 ..... 36

3-16 Creep strain versus time, (a) on specimen LS-61-41, and (b) on specimen LS-61-19 ..... 37

3-17 Axial, lateral, and volumetric creep strain versus time on specimen LS-61-19 at 2 MPa and 12 MPa, (a) for TP2-1, and (b) for TP2-2 ..... 39

3-18 Theoretical stress-strain curves ..... 42

3-19 The stress-strain curves of a uniaxial compression test using potash from the Lanigan mine ..... 43

3-20 Interpreted stress-strain curves of the multiple incremented-stress creep tests in uniaxial compression ..... 44

3-21 The total strain at the end of a creep test as a function of stress ..... 46

3-22 The total volumetric strain at the end of a creep test as a function of stress.....47

3-23 Incremented-stress axial creep curves.....48

3-24 Incremented-stress lateral creep curves.....49

3-25 The relationship of axial strain and lateral strain, (a) loading stage, (b) creep stage .....53

3-26 Strains generated by the first and the third incremented-stress (8 MPa) .....55

3-27 Strains generated by the first and the third incremented-stress (10 MPa) .....56

3-28 The strain rates generated by the first stress increment test and the third stress step test .....57

3-29 The axial microstrain versus time for specimen NB4D from 25 days record of test with linear function fitting.....59

3-30 The lateral microstrain versus time for specimen NB4D from 25 days record of test with linear function fitting.....60

3-31 The axial microstrain versus time for specimen NB4D with the power function.....61

3-32 Residual versus time for specimen NB4D with the power function.....62

3-33 Axial strain rate versus time for specimen NB4Dd with the power Function.....63

3-34 The lateral microstrain versus time for specimen NB4D with the power function .....64

3-35 Residual versus time for specimen NB4D with the power function.....65

3-36 Lateral strain rate versus time for specimen NB4Dd with the power function... 66

3-37 Lateral strain rate curves at different stress levels .....71

3-38 Axial strain rate curves at different stress levels.....72

3-39 The stress dependence of the axial strain rate.....73

3-40 The stress dependence of the lateral strain rate.....74

3-41 The axial strain rates at 10 days for specimen NB6.....77

3-42 The lateral strain rates at 10 days for specimen NB6.....78

3-43 The strain rates for specimen NB3 at the high stresses.....79

4-1 Data from five stage incremented-load tests and one stage decremented-stress tests for specimen PCA92-3M, (a) stress history, (b) axial strain versus time, inset shows NB3G. .....89

4-2. Data from five stage incremented-load tests and one stage decrement-stress tests for specimen PCA92-3M, (a) stress history, (b) lateral strain versus time, inset shows NB3G .....90

4-3 Axial and lateral microstrains for NB3B, NB3C and NB3D.....91

4-4 Volumetric microstrains for NB3B, NB3C and NB3D.....92

4-5 Strain rates of NB3B, NB3C, and NB3D where first increase stress from 9 MPa to 10 MPa, then decrease stress from 10 MPa to 9 MPa, (a) axial, and (b) lateral .....93

4-6 Volumetric strain rates of NB3B, NB3C, and NB3D.....94

4-7 Data from three stage incremented-load tests and two stages decremented-stress test for specimen PCA92-6M, (a) stress history, (b) volumetric strain versus time....96

4-8 Data from three stage incremented-load tests and two stages decremented-stress test for specimen PCA92-6M, (a) axial, (b)lateral ....97

4-9 Axial and lateral strain rates for specimen PCA92-6M....98

4-10 Volumetric strain rates for specimen PCA92-6M ....99

4-11 A summary plots of original creep tests; NB6A, NB6B, NB6C and repeated creep tests; NB6E, NB6F, NB6G under same stress path and test duration, (a) axial strain versus uniaxial stress, (b) lateral strain versus uniaxial stress..... 102

4-12 Axial and lateral strain rates for specimen PCA92-6M at the original and the repeated creep tests..... 103

4-13 Volumetric strain rates for specimen PCA92-6M and PCA92-3M during the original and the repeated creep test....104

4-14 A summary plots of the original creep tests; NB3A, NB3E and the repeated creep tests; NB3H, NB3I under same stress path and test duration, (a) axial strain versus uniaxial stress, (b) lateral strain versus uniaxial stress.... 107

4-14 Strain rates for specimen PCA92-3M 3M at the original and the repeated creep tests....108

# LIST OF TABLES


Page

2-1 Specimens for creep tests ..... 7

2-2 A comparison of creep strain measured by strain gauges (G) and displacement transducers (DT) ..... 12

3-1 The multiple stress increment creep tests on potash ..... 19

3-2 The ratios of creep strain to total strain ..... 50

3-3 The ratios of the lateral strain to the axial strain ..... 51

3-4 Comparison of the axial strain rate at different interval time ..... 67

3-5 Comparison of the lateral strain rate at different interval time ..... 68

3-6 Comparison of the axial and lateral strain rates at 60 days ..... 70

3-7 The exponent of the power function representing the stress-strain rate relationship ..... 75

3-8 Comparison of the volumetric strain at end of test ..... 81

3-9 The volumetric strain at end of the creep test above the yield stress ..... 82

4-1 Decremented-stress creep tests ..... 85

4-2 The repeated creep tests ..... 87

4-3 The strain rates in the decremented-stress creep tests ..... 100

4-4 Strains and strain rates during the incremented and the decremented-stress ..... 100

4-5 Comparison of strains and strain rates in the repeated creep tests ..... 105

# NOMENCLATURE AND ABBREVIATIONS

| | | |
|---|---|---|
| NB | - | New Brunswick potash |
| TP | - | Thailand potash |
| DT | - | displacement transducer |
| G | - | electrical-resistance strain gauge |
| LVDT | - | linearly variable displacement transducer |
| MPa | - | megapascal |
| $\mu\varepsilon$ | - | microstrain |
| $\sigma$ | - | uniaxial compressive stress |
| O | - | original test |
| R | - | repeated test |

# CHAPTER 1

# INTRODUCTION

## 1.1 General Background

All rocks have the capacity to creep, to deform slowly at constant load. Creep takes place under natural conditions in response to tectonic stresses and also through interaction between rock and engineering structures. Brittle rocks, such as gabbro and granite, suffer little time-dependent strain, whereas others such as salt, potash, coal, yield time-dependent strain, which greatly exceeds the strain produced through instantaneous elastic deformation. Rock pillars in mines, which initially appear stable may deteriorate with time under constant load and subsequently fail due to the development of large deformations (Reynolds, 1961).

The creep process has traditionally been divided into three stages; primary or transient, steady state or secondary, and tertiary or accelerating creeps. During the primary stage of creep, the strain rate decreases until it reaches a constant rate. The stage during which the strain rate is constant is called the steady state or secondary stage. The steady state strain, which usually accounts for most of the total strain observed during a long-term creep, may later change into tertiary strain. During tertiary creep, the strain rate increases at an accelerating rate until failure occurs.

At room temperature and pressure, salt rocks are the most ductile (deformation without fracture) of all the rock types. The measured creep strain in salt rocks consists of both brittle and plastic strain. The brittle strain is produced through microfracture, the

nucleation and propagation of the axial microcracks. The movement of dislocations on two slip planes of the salt crystal structure generates the plastic strain. Both processes depend on the stress level, the confining pressure, time, temperature, and humidity.

Rock creep can be studied both in situ and in the laboratory. The majority of studies on rock salt properties, both in the short and the long terms, are carried out in the laboratory on specimens prepared from samples taken from the rock mass by means of core drilling. The data obtained on the specimen in the laboratory are useful in the safe design of engineering structures in rock, but laboratory data should be handled with care. They may be different from that obtained in situ because the situ environment is too complex to model in the laboratory alone.

The laboratory creep test is a technique designed to assess the time-dependent deformation of materials at constant load and experimental conditions. However, some researchers have derived creep parameters from the measurement of the deformation of rock pillars and from the settlement of the ground surface over mined out areas (Ershanov, 1959). Rock creep parameters have also been obtained from large scale field tests, such as pressure meter tests in drill holes and the settlement under loading plates (Wang, 1986). The deformation parameters measured in large-scale field tests are more representative of rock behaviour than those derived from the small specimens in the laboratory. However, only a few creep tests have been performed in the field because of the high cost.

Creep tests have been carried out for many purposes. Parameters obtained from creep studies were used to predict slope failure. Saito (1965, 1969) has described the method for forecasting the failure of a rock slope by observing the course of creep in rock

slopes. In this particular example, only tertiary stage creep was observed because of the late installation of instrumentation.

Creep studies for salt rocks are particularly important, because the low permeability of salt rocks can be exploited for the temporary storage of petroleum products and for the long-term disposal of hazardous waste in underground caverns. Creep studies are important in the analysis and prediction of rock-bursts. Roux (1954) has shown that the time-dependent deformation may cause a gradual release of the abutment stress and hence diminish the danger of rock-bursts. The occurrence of rock-bursts between work shifts, when the ground is not influenced by mining operations can be explained satisfactorily through tertiary creep.

## 1.2 The Research

The purpose of this study was to understand the creep of New Brunswick potash and in addition to highlight the effect of stress history on creep. The creep of the salt rock was studied mainly by doing incremented-stress creep tests, where the uniaxial load is raised in steps in the range of 1 to 16 MPa. In a few tests, the uniaxial load was decreased in steps from high to low level of stress (stress-decrement creep test). In order to test the repeatability of creep deformation, the specimen was unloaded and then loaded again to the same stress.

The thesis is divided into five chapters:

Chapter 1 is an introduction that provides some information relevant about the creep test and an overview of the problem being investigated.

Chapter 2 includes a survey of the literature relevant to creep and describes specimen preparation, testing equipment, environmental control, and data acquisition.

Chapter 3 describes the experimental work and presents the measured creep data.

Chapter 4 addresses the influence of stress history. Emphasis is placed on the comparison of stress increment and decrement tests, and the analysis of repeated creep tests.

Chapter 5 summarises the research by drawing together all conclusions, and indicating possible directions for future research.

# CHAPTER 2

# LITERATURE SURVEY AND EXPERIMENTAL METHODOLOGY

## 2.1 Literature Survey

Interest in salt rock deformation and its application to underground engineering started in the late 1950's. The research, focussing on the creep and failure of salt rock, demonstrated that salt rocks are highly ductile, easy to deform, and that they creep extensively (Hardy 1958; Le 1965; Patchet 1970; Carter and Hansen 1983; Senseny 1988; Wawersik 1988; Duncan 1990; Lajtai and Duncan 1994).

Senseny (1984) studied the effect of specimen size on creep behaviour. He found that the specimen size had little influence on creep deformation during the steady state stage. But, during primary creep, the deformation of the smaller specimen was greater than the deformation of the larger specimen. Patchet (1990), Horseman (1988), Lux and Rokahr (1984) and Duncan (1990) studied the influence of humidity and temperature. Patchet found that, when model potash pillars were subjected to a 73% increase in relative humidity, the creep rate increased twenty-fold. Horseman has also investigated the effect of relative humidity. He found that an 89% increase in the relative humidity induced a 330% increase in the strain rate. Lux and Rokahr found that a change in temperature resulted in an instantaneous increase in the creep strain rate. Duncan (1990) showed that the increase in humidity changed the axial strain, but the lateral strain was largely unaffected.

## 2.2 Test Environment

Since the creep behaviour of salt rock is significantly affected by pressure, deviatoric stress, time, temperature, humidity and possibly the loading path (Wawersik and Hannum, 1980 and Duncan, 1990), this investigation has been carried out under controlled loading, temperature and humidity. The following controls were used:

1. Constant temperature of 18° C and constant (dessicant - dry) humidity.
2. The load maintained within ± 0.5% of the design load.
3. The measuring devices were strain gauges (CEA-06-250UW-350), to increase accuracy at small strains, and transducers to extend the range of strain measurements. A load cell monitored the applied stress.
4. The uniaxial compressive load ranged from 1 to 16 MPa.
5. Testing at each constant load ranged from 7 to 298 days. In total, the creep tests in this research involved 2500 days (over 6 years).

## 2.3 Specimen Preparation

Two types of potash were used in this investigation: 1) New Brunswick potash, identified by the letter NB, and 2) Thailand potash, identified by the letter TP. Table 2-1 lists the rock type, the specimen number and the size of the specimen. Golder Associates of Calgary supplied both sets of specimens.

The specimens were cylindrical. The cores were trimmed using a standard cutting saw with kerosene as the cooling fluid. The ends were ground parallel with a machinist's lap grinder. The finished size of the specimen was 210 to 245 mm in length and 100 mm

in diameter. These dimensions provided the required minimum 2: 1 length to diameter ratio.

Table 2-1. Specimens for the Creep Tests

| Rock Type | Specimen No. | | Length of Specimen (mm) | Diameter (mm) |
|---|---|---|---|---|
| New Brunswick Potash | PCA92-1M | NB1 | 230 | 100 |
| | PCA92-2M | NB2 | 220 | 100 |
| | PCA92-3M | NB3 | 225 | 100 |
| | PCA92-5M | NB4 | 215 | 100 |
| | PCA92-6M | NB6 | 245 | 100 |
| Thailand Potash | 63-LS-41 | TP41 | 230 | 100 |
| | 63-LS-19 | TP19 | 210 | 100 |

## 2.4 Data Acquisition

The data supplied by the electronic sensors was recorded by a HP computerised data acquisition system and the data were recorded on discs. For safety, the same data was sent to a printer for a hardcopy.

### 2.4.1 Strain Measurement

Generally, the creep deformation of rocks is quite small. The measuring devices should be accurate enough to read strains in the order of microstrains. The unit of strain used in this thesis is microstrain ($\mu\varepsilon$), where $\mu$ is the standard designation for $10^{-6}$, and $\varepsilon$ refers to strain. In this investigation, two types of strain-measuring devices were utilised: electrical resistance strain gauges and displacement transducers (DT).

The foil strain gauges were manufactured by the Measurements Group Inc., Raleigh, North Carolina. The gauge type is CEA-06-250UW-350. It is 20 mm in length with a resistance of 350 ± 0.3 Ω and a strain limit of ± 5% (50,000 $\mu\varepsilon$). Nine strain gauges were used for each specimen, four oriented to measure the axial strain and the rest oriented to measure the lateral strain. All gauges were positioned at the mid-height of the specimen to avoid possible end effects. The strain gauges were bonded to the potash specimen surface using M-Bond 200 Adhesive Kit, a high-strength epoxy adhesive manufactured by M-Line Accessories, Measurement Group Inc., Raleigh, North Carolina. Strain gauges were the principal strain measuring devices for this study.

A Hewlett Packard model 7DCDT-250 Linearly Variable Displacement Transducer (LVDT) was used to measure the axial displacement between the loading platen and the stationary frame. An MTS clip gauge, measuring the displacement of a chain wrapped around the circumference of the specimen at a place just below the strain gauges, measured the lateral displacement. These devices were used only in tests where deformations were expected to be high and there was a great risk of having the strain gauges fail.

The strain gauges and other electrical sensors were connected in a Wheatstone Quarter Bridge Circuit. Duncan (1990) has described the technique in detail. The full complement of instrumentation included 12 different transducers: 9 electric strain gauges, a load cell for the axial load, a linearly variable displacement transducer, and an MTS clip gauge.

The strain indicators were connected to a HP 3421A 20-channel data acquisition/control unit, which in turn was controlled by a HP-75 portable computer. During the test, the strain gauges, the load cell and the temperature devices were monitored with readings taken every minute for the first half an hour, every 10 minutes for the next four hours, and hourly for the rest of the test. For each reading, the elapsed time and the 12 transducer outputs were printed out and stored on floppy disk. Eventually, the data were transferred to a PC where most of the analyses and all the graphing were done using our EzGraph software. The data analysis following the tests handled about 700,000 measurements. Figure 2-1 shows the testing set-up, the measuring and the monitoring systems.

The four axial and the five lateral gauges were averaged to get the axial and the lateral strains. The volumetric strain was generated by taking advantage of the infinitesimal strain assumption; the volumetric strain is simply the sum of the axial strain and twice the lateral strain ($\varepsilon_V = \varepsilon_A + 2\varepsilon_L$) with the compressive axial strain, substituted as positive. The creep data used in the thesis come from nine series of creep tests, seven for the New Brunswick potash, identified by the letter NB, and two for Thailand potash, identified by the letter TP. Test series NB1, NB2, NB3, NB4, and NB6 used specimens

PCA92-1M, PCA92-2M, PCA92-3M, PCA92-5M and PCA92-6M, respectively. TP41 and TP19 are specimens 63-LS-41 and 63-LS-19, respectively. The letter A, B, C, D, E and F attached to the test name refer to load steps. For example, NB1A, refers to the first load step of a creep test on specimen PCA92-1M. Similarly, NB3C would refer to the third loading step of specimen PCA92-3M.

### 2.4.2 The strain-gauge and the DT measurements

Table 2-2 is a comparison of creep strain measured by strain gauges and transducers. In general, the strains measured by the electrical-resistance strain gauge were less than those measured by displacement transducers in both the axial and the lateral directions. The difference was the most remarkable when a high uniaxial stress (i.e. 15 MPa) was applied (Figure 2-2 (b)). An exception to this occurs at low stress 2 MPa, where the strains measured by the displacement transducers are smaller than those obtained by the strain gauges in both directions (Figure 2-2 (a)). Apparently, the MTS clip gauge and the LVDT device are not sensitive enough to detect the small strains occurring at very low stress. In general, strain gauges measure local strain while the transducers measure the average strain for the whole specimen. Strain gauges are usually glued to the specimen in locations where the surface is sound; grain-boundaries are avoided. There will be, therefore, a tendency for strain gauge measurement to underestimate the strain measured by the axial and lateral transducers.

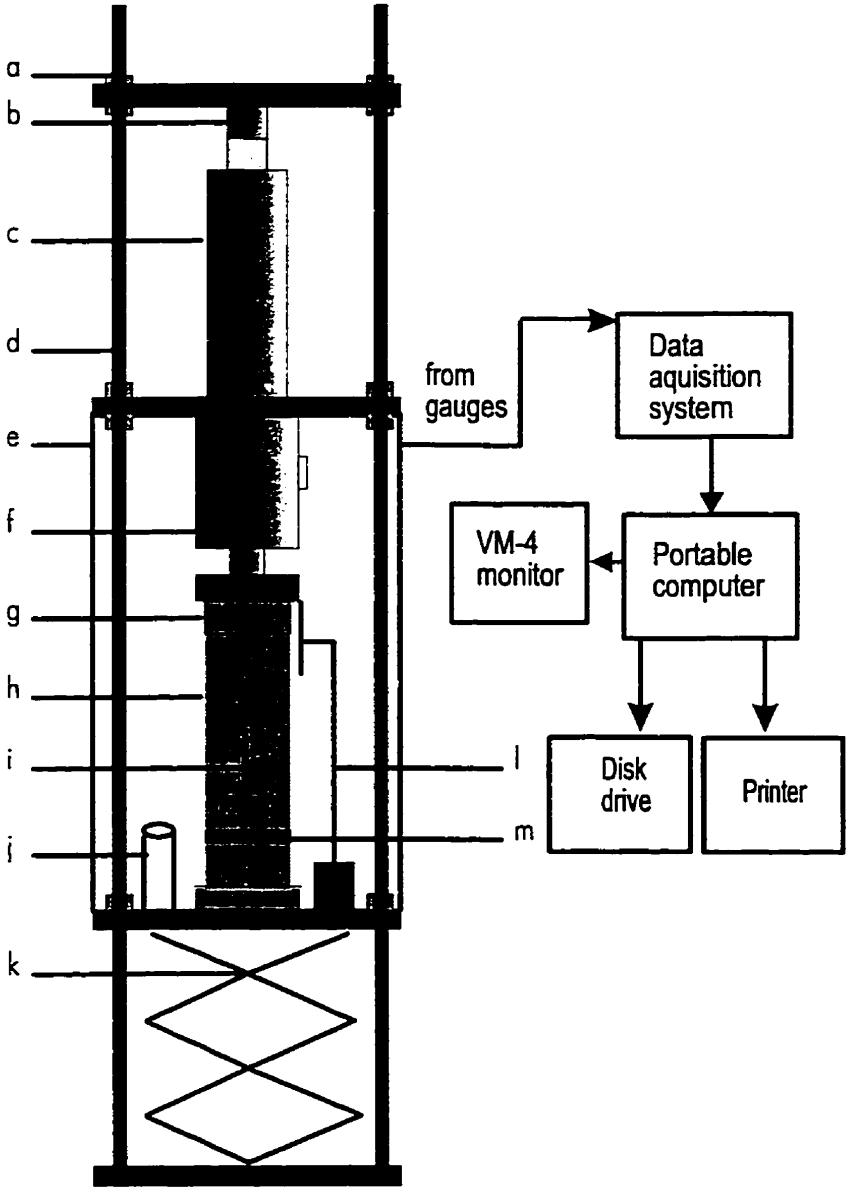


Figure 2-1. The creep apparatus. Major components: (a) nut, (b) steel platen, (c) press, (d) loading frame, (e) plastic bag, (f) load cell, (g) potash loading platen, (h) specimen, (i) strain gauge, (j) desiccant, (k) spring, (l ) displacement transducer, (m) MTS chain with clip gauge

Table 2-2. A comparison of creep strain

measured by strain gauges (G) and displacement transducers (DT)

| Specimen No. | Test No. | Measured method | Stress | Time | Axial | | Lateral | |
|---|---|---|---|---|---|---|---|---|
| | | | MPa | days | strain ( με) | ratio of DT/G | strain ( με) | ratio of DT/G |
| PCA92-5M | NB4C | G* | 12 | 85.2 | 1087 | | 827 | |
| | | DT** | 12 | 85.2 | 1308 | 1.2 | 995 | 1.2 |
| PCA92-2M | NB2B | G | 13 | 44.9 | 892 | | 550 | |
| | | DT | 13 | 44.9 | 1155 | 1.29 | 617 | 1.12 |
| PCA92-5M | NB4D | G | 14 | 49.4 | 2258 | | 1402 | |
| | | DT | 14 | 49.4 | 3274 | 1.45 | 2007 | 1.43 |
| PCA92-3M | NB3E | G | 15 | 70.8 | 2750 | | 3470 | |
| | | DT | 15 | 70.8 | 6413 | 2.33 | 5017 | 1.45 |
| 63-LS-19 | TP19 A | G | 2 | 17 | 393 | | 135 | |
| | | DT | 2 | 17 | 315 | 0.80 | 74 | 0.55 |
| 63-LS-19 | TP19 B | G | 12 | 48.6 | 5512 | | 4673 | |
| | | DT | 12 | 48.6 | 5859 | 1.06 | 7208 | 1.54 |

*G: strain gauge

**DT: displacement transducer

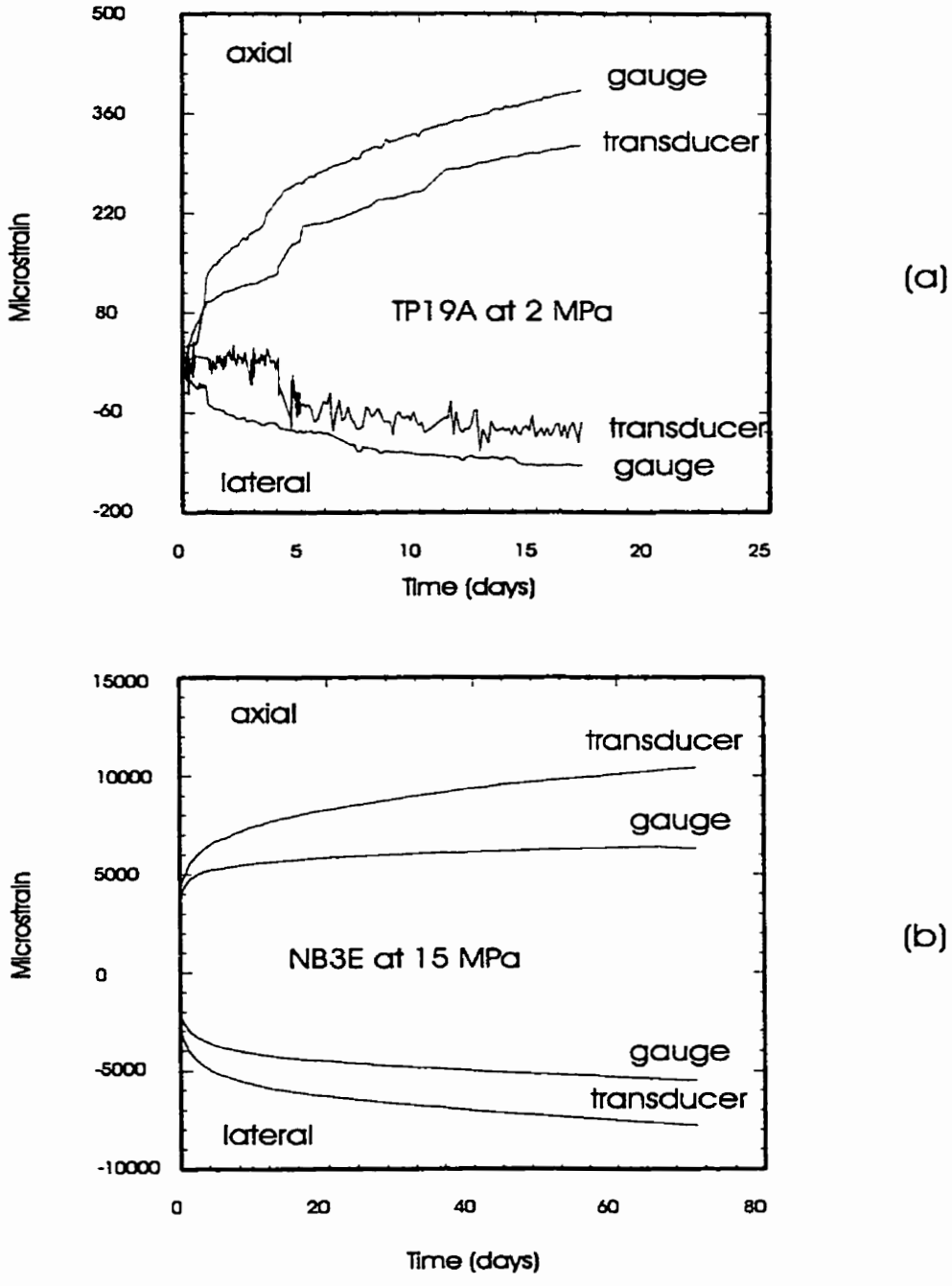


Figure 2-2. Comparison of creep strain measured by strain gauges and displacement transducers; (a) 2 MPa and (b) 15 MPa.

## 2.5 Testing Equipment and Environmental Control

Specimens were loaded in two loading frames where the specimen was placed in series with soft springs (Figure 2-1). Uniform loading was established by using loading platens with spherical heads. The four axial gauges served as a check on specimen alignment, i.e. whether the specimen was properly centred and not subjected to bending or torsion. Loading was applied with a portable hydraulic press. Once the desired load was reached, the nuts were tightened to lock-in the applied load. Constant loading was maintained by manually turning the nuts when necessary. Each adjustment caused a noticeable shift in gauge readings. Therefore, adjustments were kept to a minimum and made only when the load fell under 0.5% of the desired load.

The influence of changing temperature and humidity were avoided by installing a computerised temperature control system in the creep laboratory and by sealing the whole specimen assembly inside a plastic tent containing a desiccant (the commercial product Drierite). The temperature was maintained constant at 18°C for New Brunswick and at 30°C for the Thailand potash. The computerised temperature control system could hold these temperatures within ± 0.1°C of the set value.

# CHAPTER 3

# INCREMENTED-STRESS CREEP TESTS

## 3.1 Introduction

Under constant environmental conditions, the creep strain depends on time and the level of applied stress with respect to the strength of the specimen. To evaluate the stress-dependence of the creep strain, a series of creep tests at different stresses must be conducted. The experimental procedure for stress dependence may take several forms. Ideally, one would like to have a separate specimen for each creep test. When no multiple specimens are available, or specimen to specimen variation is great, the stress dependence may have to be evaluated from a single specimen. There are a number of ways doing this. In an incremented-stress creep test, after a specified time the applied load on the specimen is increased in steps from low to high stress levels. In contrast, in a decremented-stress creep test, the load is decreased from high to low stress levels. One variation on this procedure is that after the completion of the creep test at one stress level, the stress is reduced to nil before the stress is increased to the next level. In general, the creep strain is expected to depend on the previous stress history in ways that are not quite clear.

In the traditional sense, the creep curve represents the time-dependent behaviour of the axial, the load-parallel strain. This may be measured with strain gauges placed parallel with the loading (axial) direction. In older tests, the axial strain was deduced

from the convergence of the loading platens. The displacement would have been measured with dial gauges and more recently with LVDTs.

For the complete specification of the state of creep strain, however, all three principal strains are required. Because of the axial symmetry of the cylindrical test specimen, the two lateral principal strains are equal. Their variation with time can be measured either with strain gauges or with lateral strain transducers, which are placed along the circumference of the specimen. Using the infinitesimal approximation, the volumetric strain can be derived from measurements of the axial and lateral principal strains. This thesis follows the rock mechanics sign convention, in which extension (dilation) is negative and shortening (compression) is positive.

The creep curve has traditionally been divided into four parts (Figure 3-1). The strain in the loading region A-B is the instantaneous strain accumulated while loading the specimen up to the creep load. For salt rocks, instantaneous strain can be any combination of elastic, plastic and brittle (microcracking) strain. The time dependent strain (creep strain) itself is divided into three stages. The initial region (B-C) of the curve showing a declining strain rate is the primary or transient stage. In region C-D the strain rate is constant, the creep curve is linear. This is the stage of secondary or steady-state creep. The region D-E of the curve represents the tertiary creep stage, during which the strain rate increases at an accelerating rate. The actual shape of the creep curve depends on the stress level. At low stress, there may be no creep strain at all. For salt rocks, however, there is always some primary creep. At very high stress level, primary creep may change into tertiary creep without a steady-state interval.

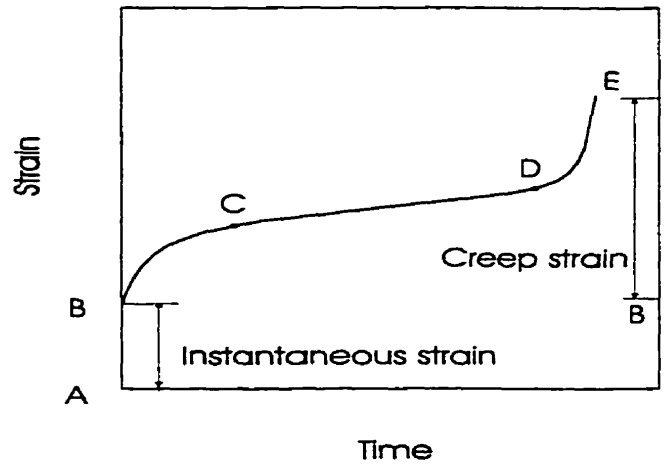


Figure 3-1. The creep curve. A-B is the instantaneous strain (loading strain). B-E is the creep strain. B-C is the primary, C-D is the steady-state, and D-E is the tertiary stage.

The strain rate is the slope of the creep strain - time curve. This slope was obtained by first fitting a power function to the creep curve, and then finding its first derivative, using the commercial computer code TableCurve. A creep rate curve has the bathtub shape (Figure 3-2). The three regions are referred to as the decelerating phase, constant phase, and the accelerating phase. The strain rate would be expected to start high at the beginning then reduce in magnitude through the primary stage, it should be constant during steady-state creep and then start increasing during tertiary creep. In this investigation, the creep rate curve consists of a section where the strain rate clearly drops and another where the strain rate appears to be nearing a constant rate. The accelerating phase never appeared.

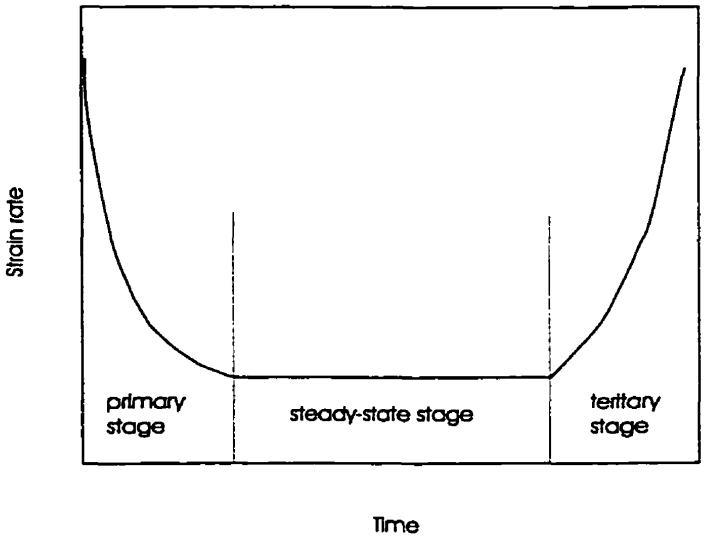


Figure 3-2. The bathtub curve describing the creep rate.

## 3.2 Experimental Procedure

Seven series of stress increment creep tests were performed in this study. Each series consisted of a number of creep tests at various loads while using the same specimen. New Brunswick potash was used for five of the creep series. These are NB1, NB2, NB3, NB4, and NB6 corresponding to specimens PCA92-1M, PCA92-2M, PCA92-3M, PCA92-5M, and PCA92-6M, respectively. Thailand potash was used for two series, TP41 and TP19 for specimens LS-61-41 and LS-61-19, respectively. Table 3.1 lists the specimen number, test number, the stress applied to the specimen, the stress history and the duration for each creep test.

Table 3-1. The incremented-stress creep tests

| Rock Type | Specimen No. | Test No. | Constant Stress (MPa) | Stress History (MPa) | Duration (days) |
|---|---|---|---|---|---|
| New Brunswick Potash | PCA92-1M | NB1A | 4 | 0→4 | 102 |
| | | NB1B | 7 | 4→7 | 68 |
| | PCA92-2M | NB2A | 10 | 0→10 | 102 |
| | | NB2B | 13 | 10→13 | 68 |
| | PCA92-3M | NB3A | 6 | 0→6 | 91 |
| | | NB3B | 9 | 6→9 | 171 |
| | | NB3C | 10 | 9→10 | 96 |
| | | NB3D | 9 | 10→9 | 173 |
| | | NB3E | 15 | 9→15 | 71 |
| | | NB3F | 16 | 15→16 | 143 |
| | PCA92-5M | NB4A | 8 | 0→8 | 91 |
| | | NB4B | 11 | 8→11 | 176 |
| | | NB4C | 12 | 11→12 | 96 |
| | | NB4D | 14 | 12→14 | 172 |
| | PCA92-6M | NB6A | 3 | 0→3 | 298 |
| | | NB6B | 5 | 3→5 | 120 |
| | | NB6C | 8 | 5→8 | 132 |
| Thailand Potash | LS-61-41 | TP41A | 1 | 0→1 | 21 |
| | | TP41B | 10 | 1→10 | 60 |
| | LS-61-19 | TP19A | 2 | 0→2 | 21 |
| | | TP19B | 12 | 2→12 | 49 |

## 3.3 Experimental Results

The creep data are presented in plots of creep strain versus time in Figures 3-3, 3-5, 3-6, 3-7, 3-8, 3-10, 3-11, 3-13, 3-14, 3-15 and 3-17. The creep strain for the start of each stress increment was zeroed to facilitate the comparison of the individual creep curves.

### 3.3.1 Series NB1 at 4 and 7 MPa

Testing of the New Brunswick potash specimen PCA92-1M lasted for 170 days. The specimen was first loaded to the constant stress level of 4 MPa and this load was kept constant for 102 days (NB1A). After this, the load was increased to 7 MPa (NB1B). (The specimen was not unloaded from 4 MPa). The duration of the test at this stress was 68 days. The results of the axial, lateral and volumetric creep strains are shown in Figure 3-3 (a) for NB1A and (b) for NB1B. Figure 3-4 (a) shows the axial and lateral strain rates. Note that the creep strain accumulated at 4 MPa is larger than at 7 MPa. Having relatively large strain during the first loading stage seems to be a typical feature of creep tests using salt rocks (Duncan, 1990). However, the strain rate at 4 MPa was appropriately smaller than at 7 MPa. The strain rates at the end of the tests were 1.42 x $10^{-12}$ /s and 4.7 x $10^{-12}$ /s for 4 and 7 MPa in the axial direction, and 0.5 x $10^{-12}$/s and 5.02 x $10^{-12}$ /s in the lateral direction. The creep strain in the lateral direction was quite large indicating unexpected dilation at 4 MPa. At 7 MPa the specimen had undergone the expected compression. Deformation was occurring approximately at constant volume.

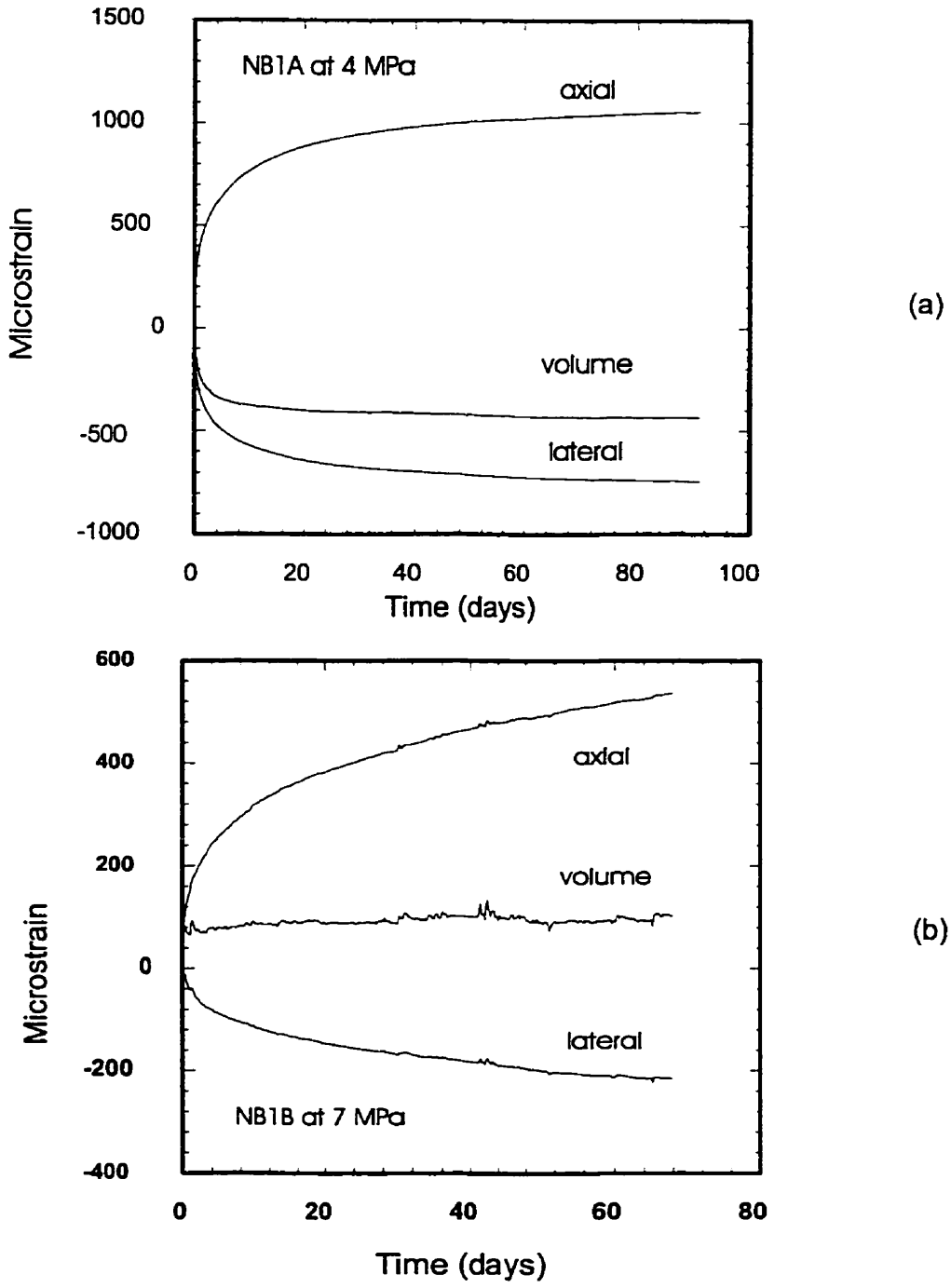


Figure 3-3. Axial, lateral and volumetric creep strain on specimen PCA92-1M at 4 MPa. and 7 MPa.

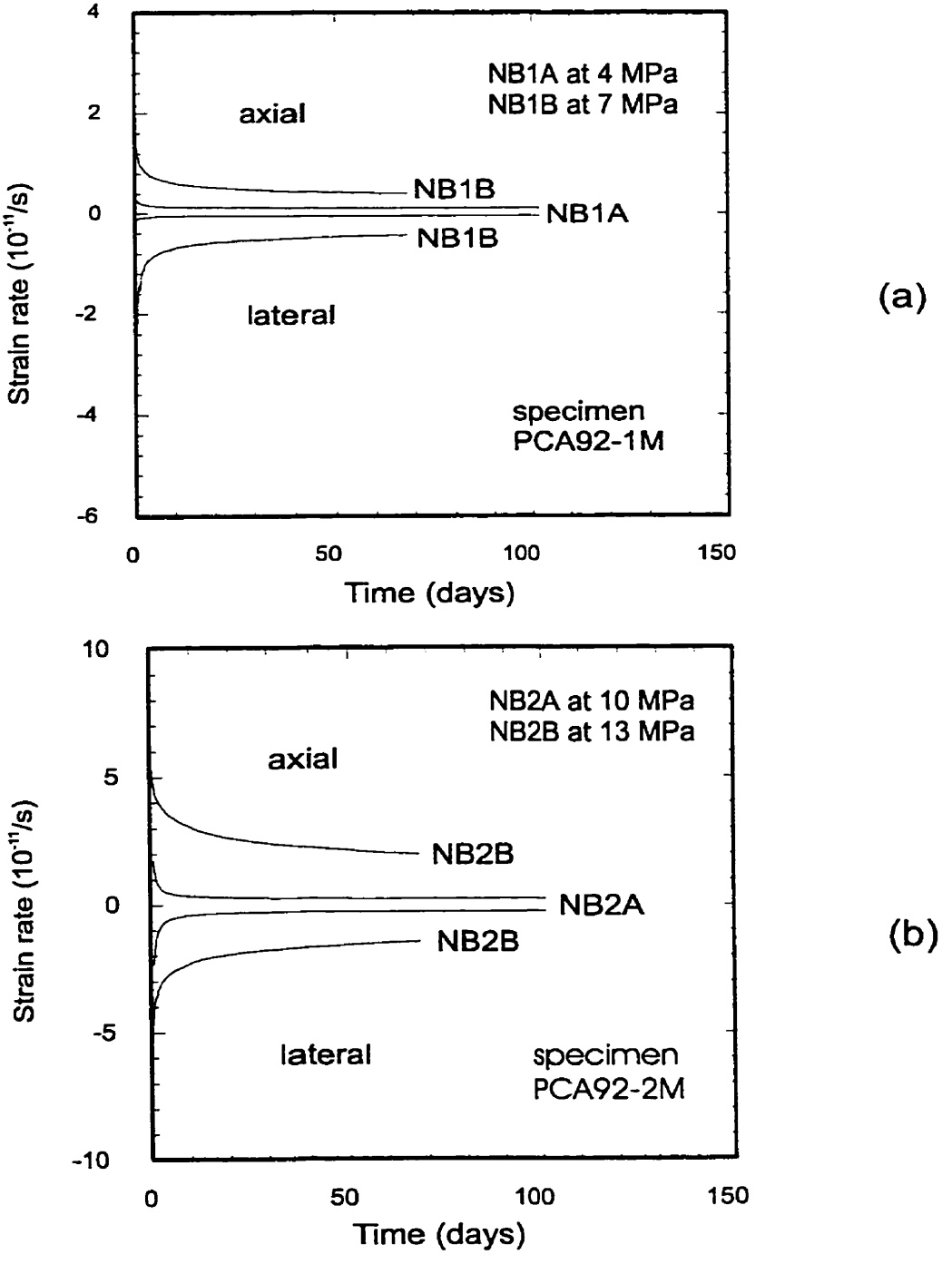


Figure 3-4. The strain rate for (a) specimen PCA92-1M and (b) PCA92-2M.

### 3.3.2 Series NB2 at 10 and 13 MPa

Testing of New Brunswick potash specimen PCA92-2M took 170 days. The specimen was first tested at the constant stress of 10 MPa for 102 days (NB2A). The load was then increased to 13 MPa (NB2B) and the test continued for another 68 days. The axial, the lateral and the volumetric creep strains are shown in Figure 3-5 (a) for NB2A and (b) for NB2B. Figure 3-4 (b) shows the axial and lateral strain rates. The total creep strain accumulated during the initial loading to 10 MPa was again larger than at 13 MPa. In both tests, the specimens were dilating. The strain rates at the end of the tests were 2.61 x $10^{-12}$ /s and 22.79 x $10^{-12}$ /s for 10 MPa and 13 MPa in the axial direction, and 3.08 x $10^{-12}$ /s and 16.7 x $10^{-12}$ /s in the lateral direction.

### 3.3.3 Series NB3 at 6, 9, 10, 9, 15, and 16 MPa

Testing of New Brunswick potash specimen PCA92-3M lasted for 745 days. This was the longest series involving six stages. Tests were performed at the uniaxial stress of 6, 9, 10, 9, 15, and 16 MPa. After the 10 MPa loading stage, the load was reduced to 9 MPa for 173 days in NB3D and then raised to 15 MPa. The duration of the tests was 91 days for NB3A, 171 days for NB3B, 96 days for NB3C, 71 days for NB3E and 143 days for NB3F. The results of the axial, the lateral and the volumetric creep strains are shown in Figure 3-6 (a) for NB3A, (b) for NB3B, Figure 3-7 (a) for NB3C, (b) for NB3E, and Figure 3-8 for NB3F. Figure 3-9 shows plots of the axial and the lateral strain rates for tests NB3A, NB3B, NB3C, NB3D, NB3E and NB3F.

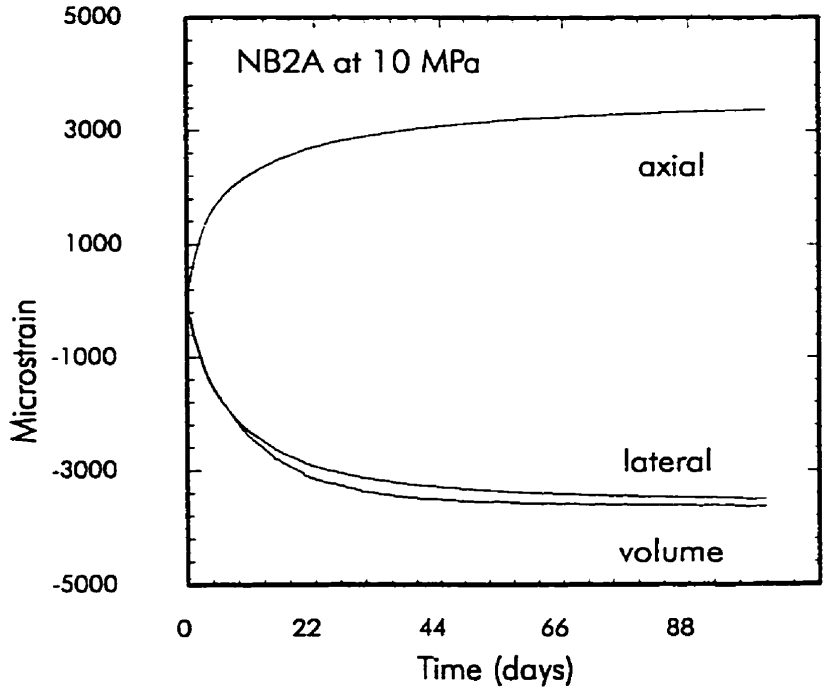


(a)

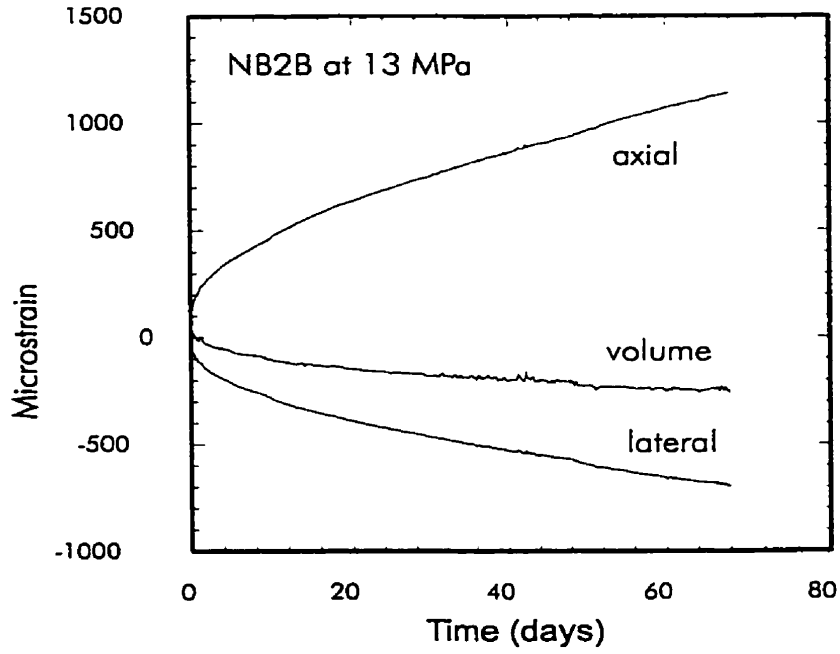


(b)

Figure 3-5. Axial, lateral and volumetric creep strain on specimen PCA92-2M at 10 and 13 MPa.

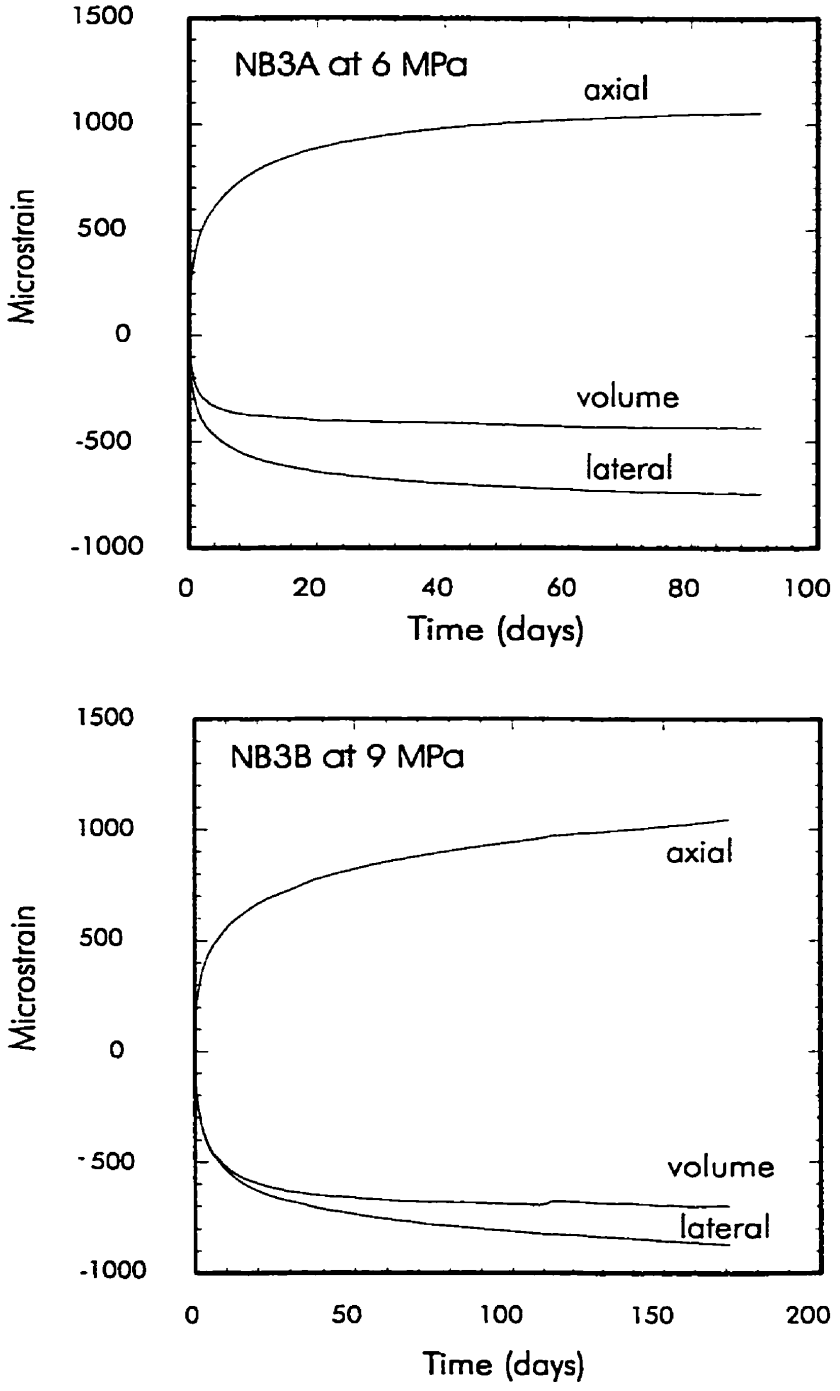


Figure 3-6. Axial, lateral and volumetric creep strain on specimen PCA92-3M at 6 and 9 MPa.

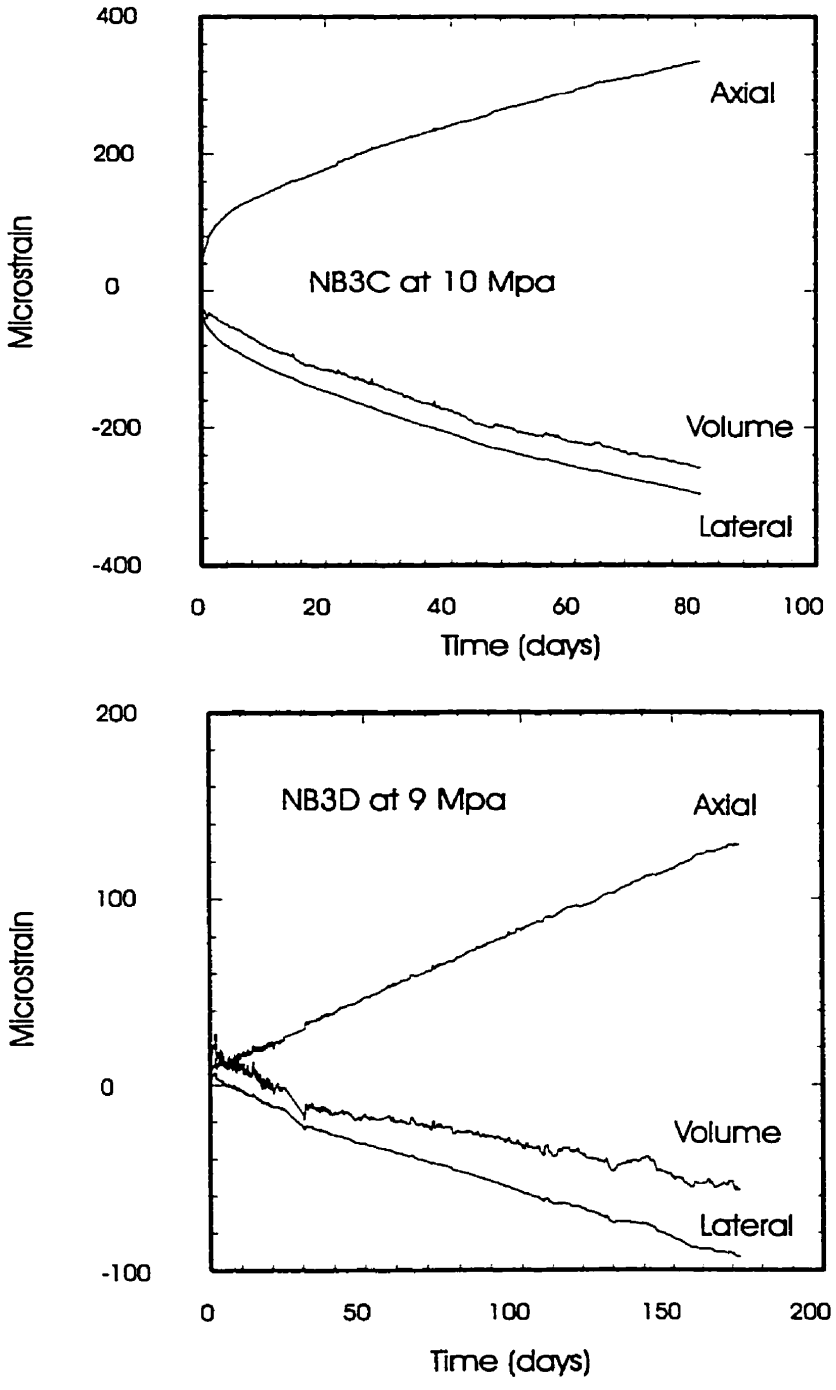


Figure 3-7. Axial, lateral and volumetric strain on specimen PCA92-3M

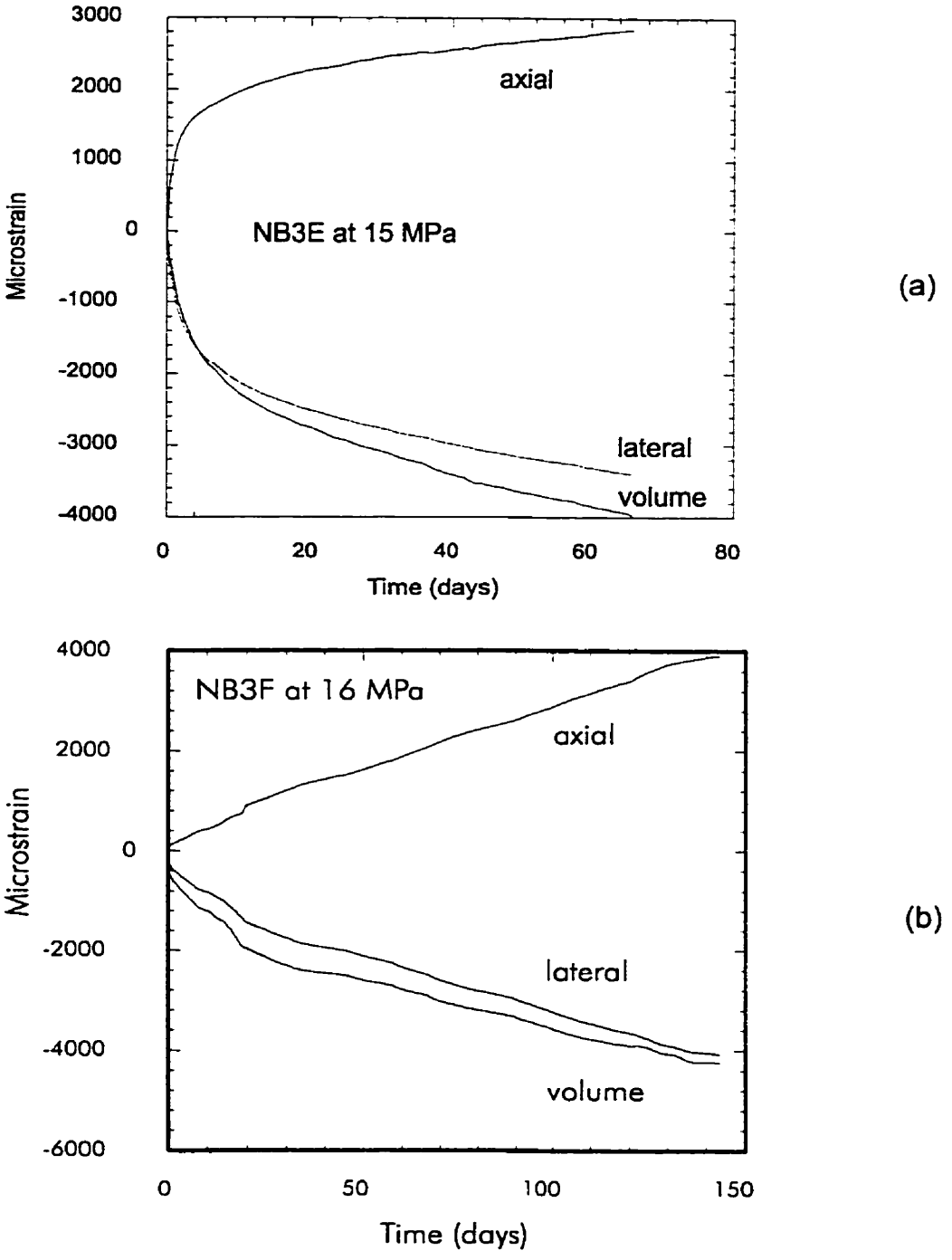


Figure 3-8. Axial, lateral and volumetric strain on specimen PCA92-3M at 15 and 16 MPa

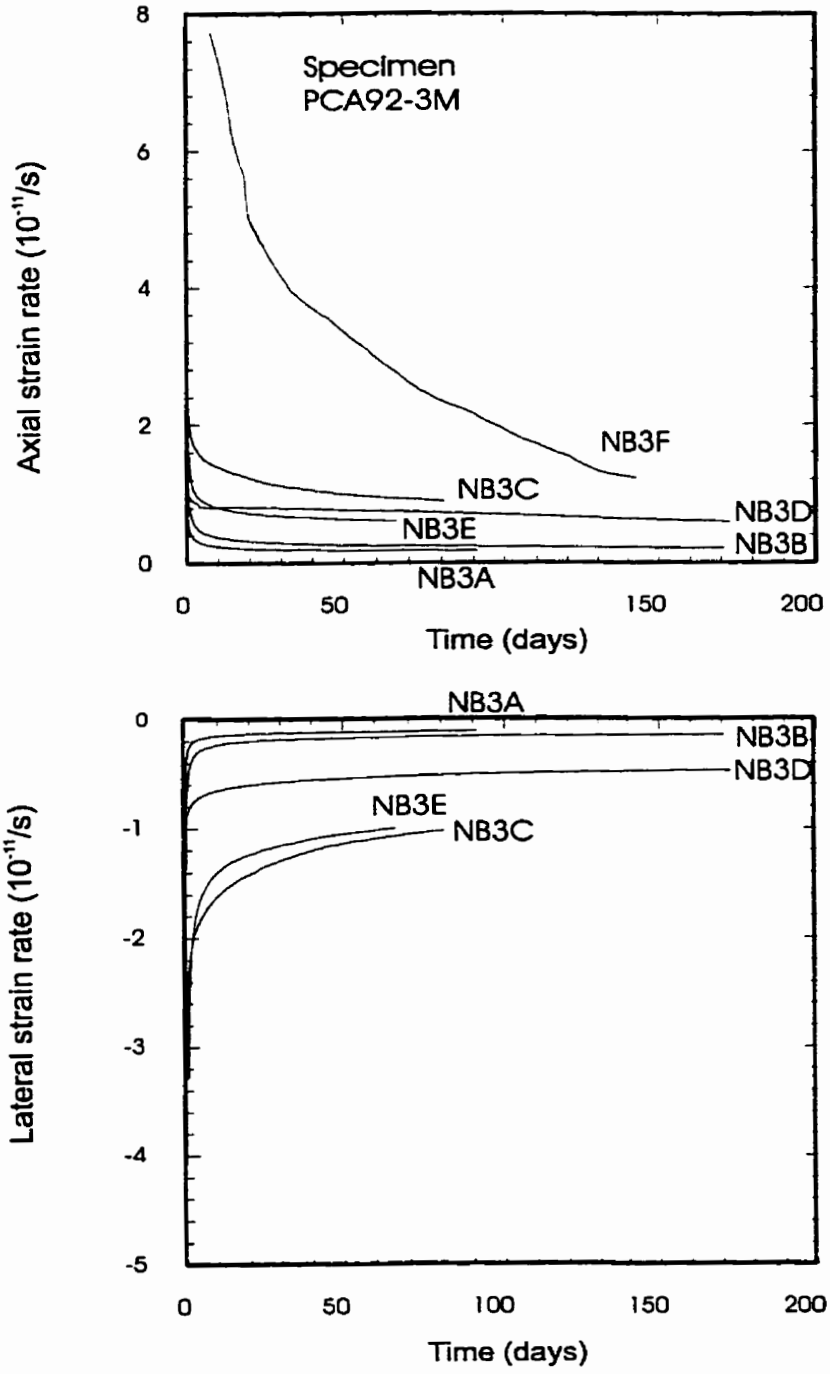


Figure 3-9. Strain rate versus time on specimen PCA92-3M; (a) axial, (b) lateral

The 16 MPa load in test NB3F caused very large strains. Maintaining the constant load was difficult, requiring frequent load adjustments. Two strain gauges debonded during the experiment and there is a question of their performance during the NB3E run at 15 MPa.

The strain rates at the end of the tests were 2 04, 2.44, 10.35, 6.89, 7.05 and 13.63 x $10^{-12}$ /s for 6, 9, 10, 9, 15 and 16 MPa in the axial direction, 1.3, 1.67, 11.9, 5.45, 11.6 and 130.2 x $10^{-12}$ /s in the lateral direction. For all the loading stages, even at 6 MPa, the specimen was dilating. The creep strain in the first loading stage was larger than in the third loading stage, but smaller than that in the second, fourth and fifth loading stages.

### 3.3.4 Series NB4 at 8, 11, 12, and 14 MPa

Testing of New Brunswick potash specimen PCA92-5M was performed for 535 days. The uniaxial stress in this stress-increment creep test was 8, 11, 12, and 14 MPa. The duration of the test was 91 days for NB4A, 176 days for NB4B, 96 days for NB4C and 172 days for NB4D. The axial, the lateral and the volumetric creep strains are shown in Figure 3-10 (a) for NB4A, (b) for NB4B, Figure 3-11 (a) for NB4C and (b) for NB4D. Figure 3-12 (a) shows the axial and the lateral creep strain rates. The strain rates at the end of the test were 1.71, 7.92, 14.66 and 17.56 x $10^{-12}$ /s for 8, 11, 12 and 14 MPa in the axial direction, and 1.15, 8.1, 24.4 and 23.5 x $10^{-12}$ /s in the lateral direction. During all loading stages, the specimen was dilating. The creep strain in the first loading stage was larger than in the third loading stage, but smaller than the strains observed in the second and fourth loading stages.

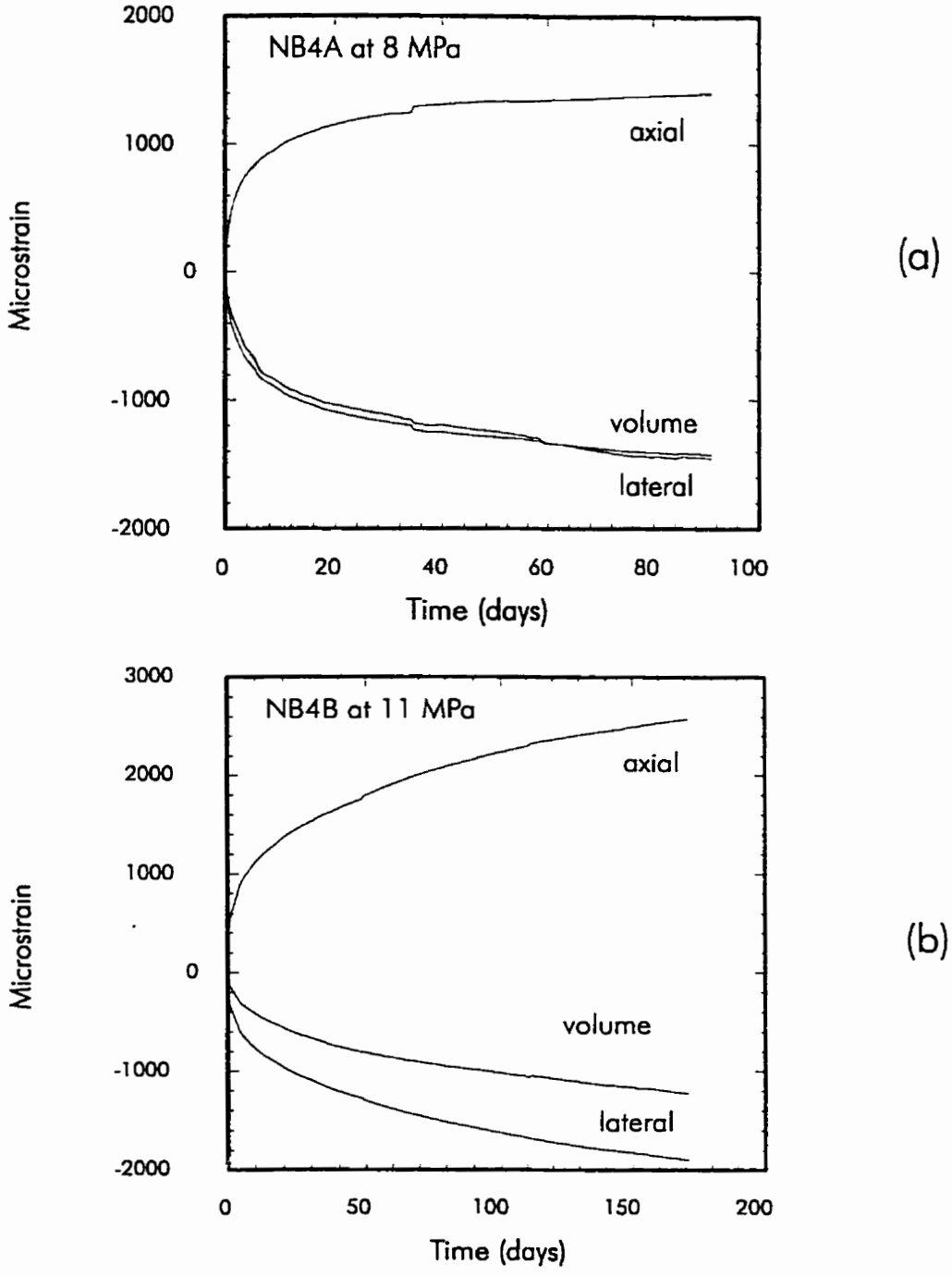


Figure 3-10. Axial, lateral and volumetric strain on specimen PCA92-5M

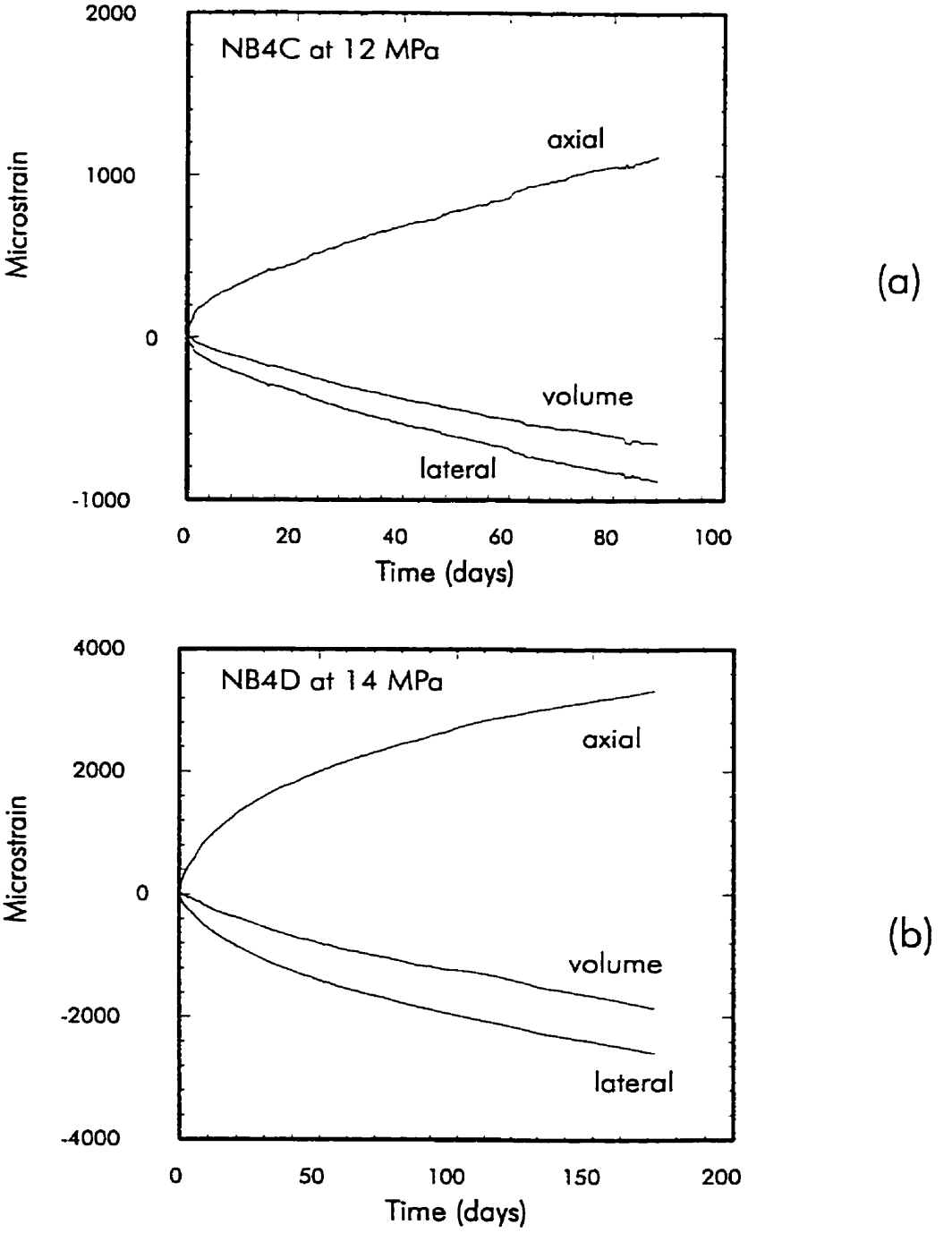


Figure 3-11. Axial, lateral and volumetric strain on specimen PCA92-5M.

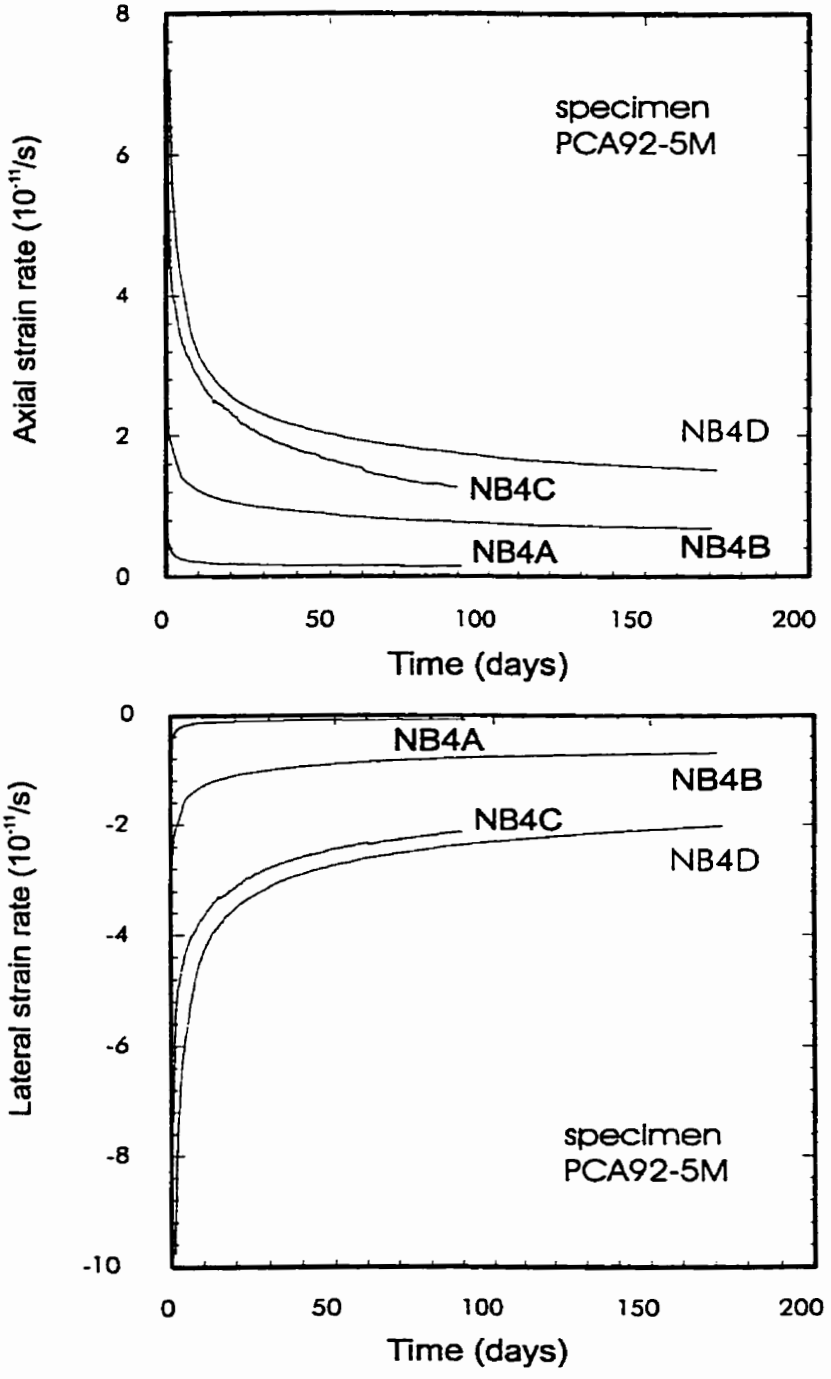


Figure 3-12. Strain rate for specimen PCA92-5M; (a) axial, (b) lateral.

### 3.3.5 Series NB6 at 3, 5, and 8 MPa

Testing on New Brunswick potash specimen PCA92-6M took 550 days. Multiple stress increment creep tests were performed at uniaxial stress levels of 3, 5, and 8 MPa. The duration of the test was 298 days for NB6A, 120 days for NB6B and 132 days for NB6C. The data shown in Figure 3-13 are the axial, lateral and volumetric creep strains, (a) for NB6A, (b) for NB6B. Figure 3-14 (a) gives the record for NB6C. The corresponding axial and lateral strain rates are given in Figure 3-14 (b). During all three loading stages, the volumetric strain was positive (compression). There was no dilation even with the 8 MPa load. The strain rates at the end of the tests were 3.41, 5.16 and 7.65 x $10^{-12}$ /s for 3, 5 and 8 MPa in the axial direction, and 2.42, 4.18 and 5.28 x $10^{-12}$ /s in the lateral direction. The axial strain in the first loading stage was the largest in this series, while the lateral strain in the first loading stage was larger than in the second stage, but smaller than in the third loading stage.

### 3.3.6 Series TP41 at 1 and 10 MPa

Testing of Thailand potash specimen LS-61-41 continued for 81 days. The specimen was first loaded to a stress level of 1 MPa. This load was maintained for 21 days (TP41A). Then, the stress was increased to 10 MPa (TP41B). The test lasted for another 60 days. The axial, lateral and volumetric creep strains are shown in Figure 3-15(a) for TP41A and in (b) for TP41B. Figure 3-16 (a) shows the corresponding strain rates. The strain rates at the end of the tests were 1.51 and 2.09 x $10^{-12}$ /s for 1 MPa and 10 MPa in the axial direction, and 0.51 and 2.22 x $10^{-12}$ /s in the lateral direction.

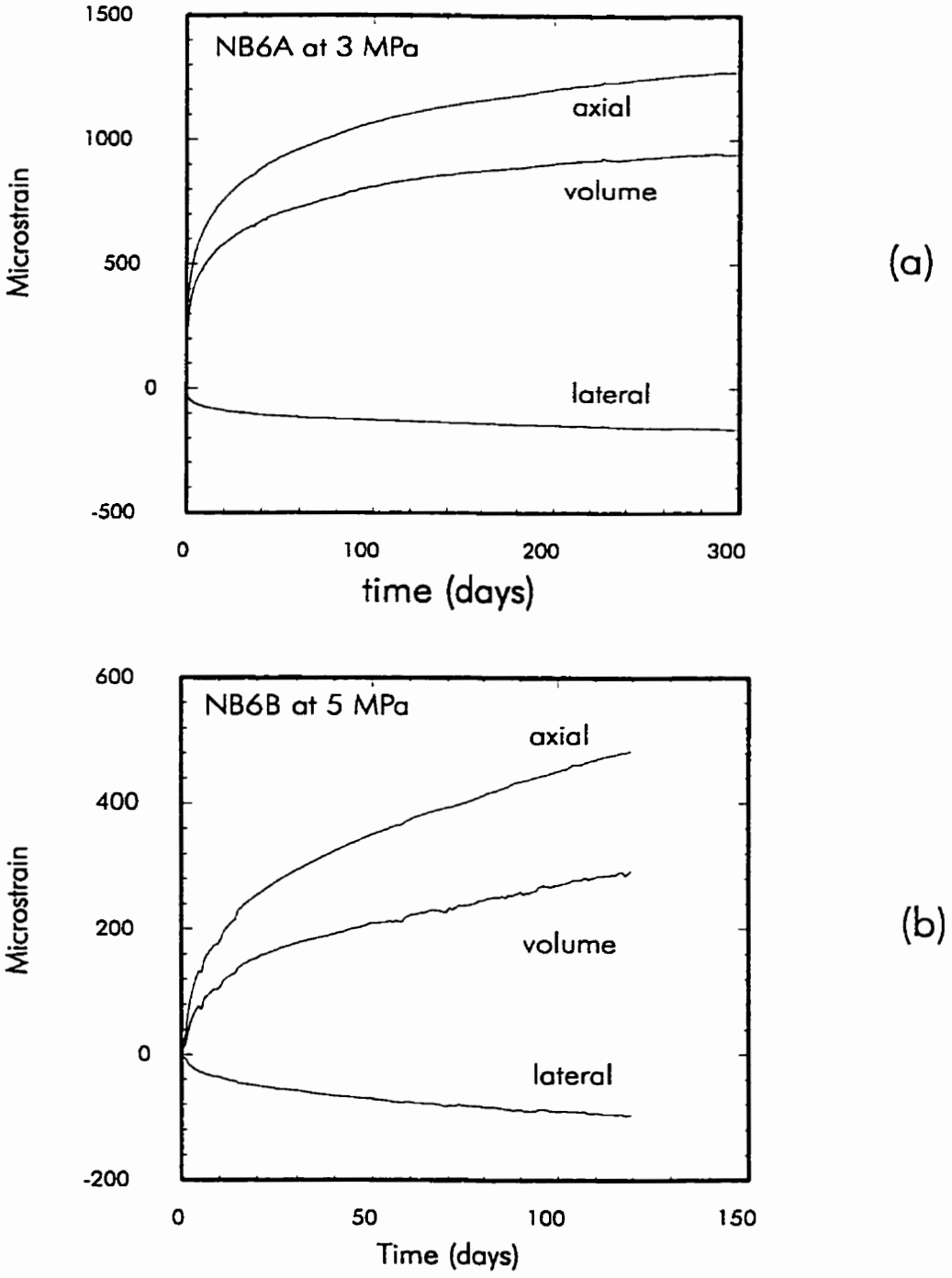


Figure 3-13. Axial, lateral and volumetric strain on specimen PCA92-6M at 3 and 5 MPa.

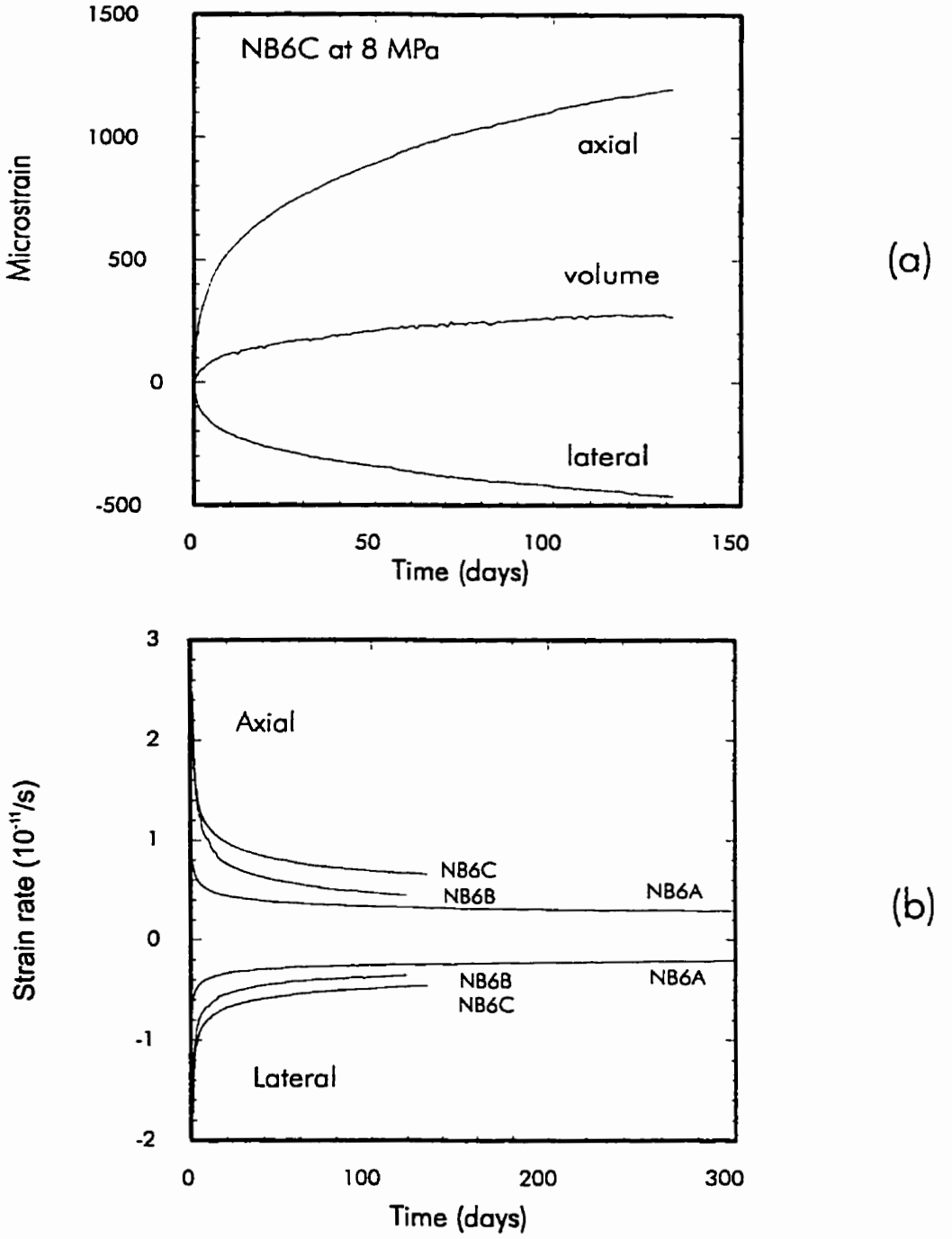


Figure 3-14. Axial, lateral and volumetric strain and strain rate on specimen PCA92-6M at 8 MPa; (a) strain (b) strain rate.

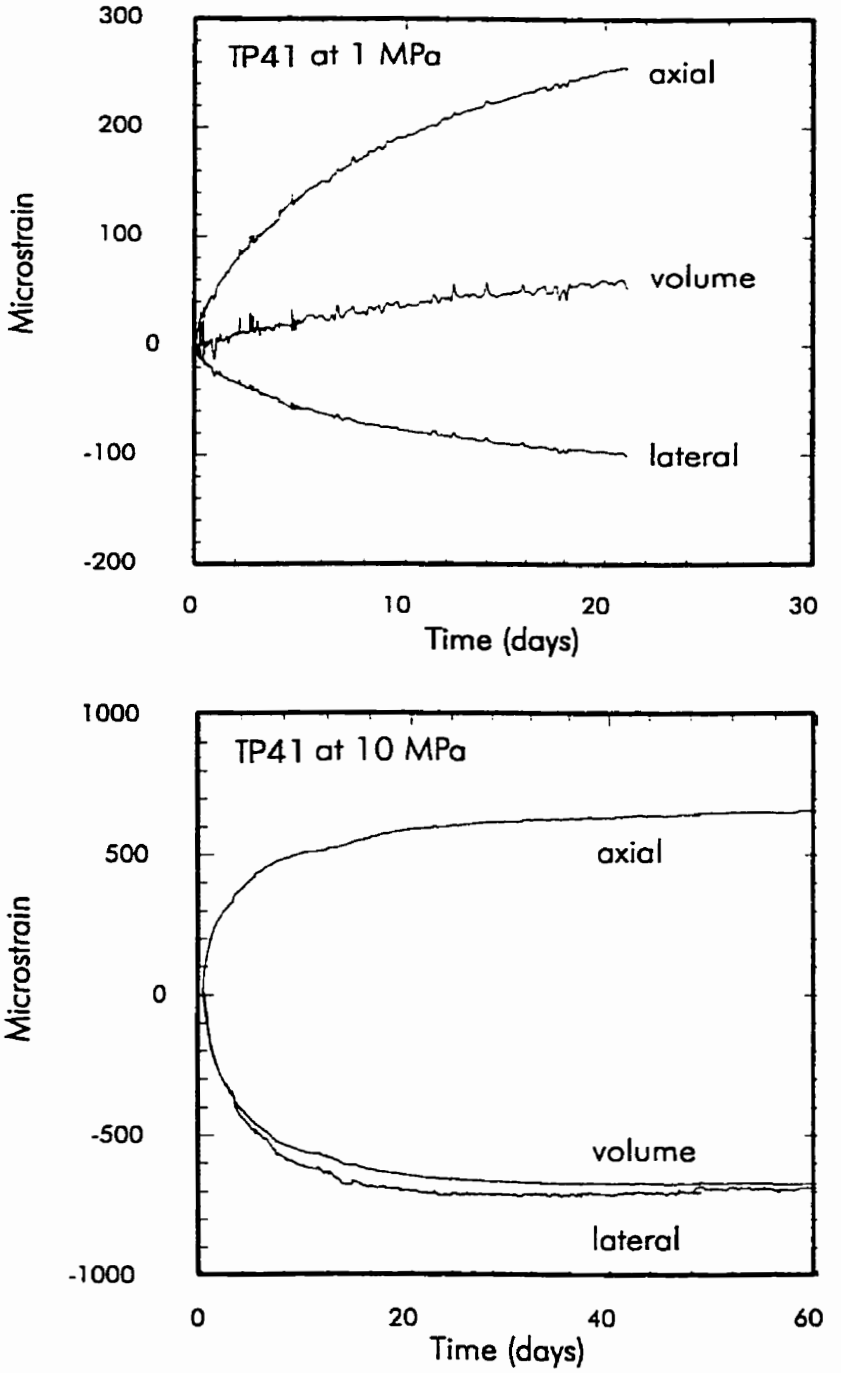


Figure 3-15. Axial, lateral and volumetric strain on specimen LS-61-41 at 1 and 10 MPa.

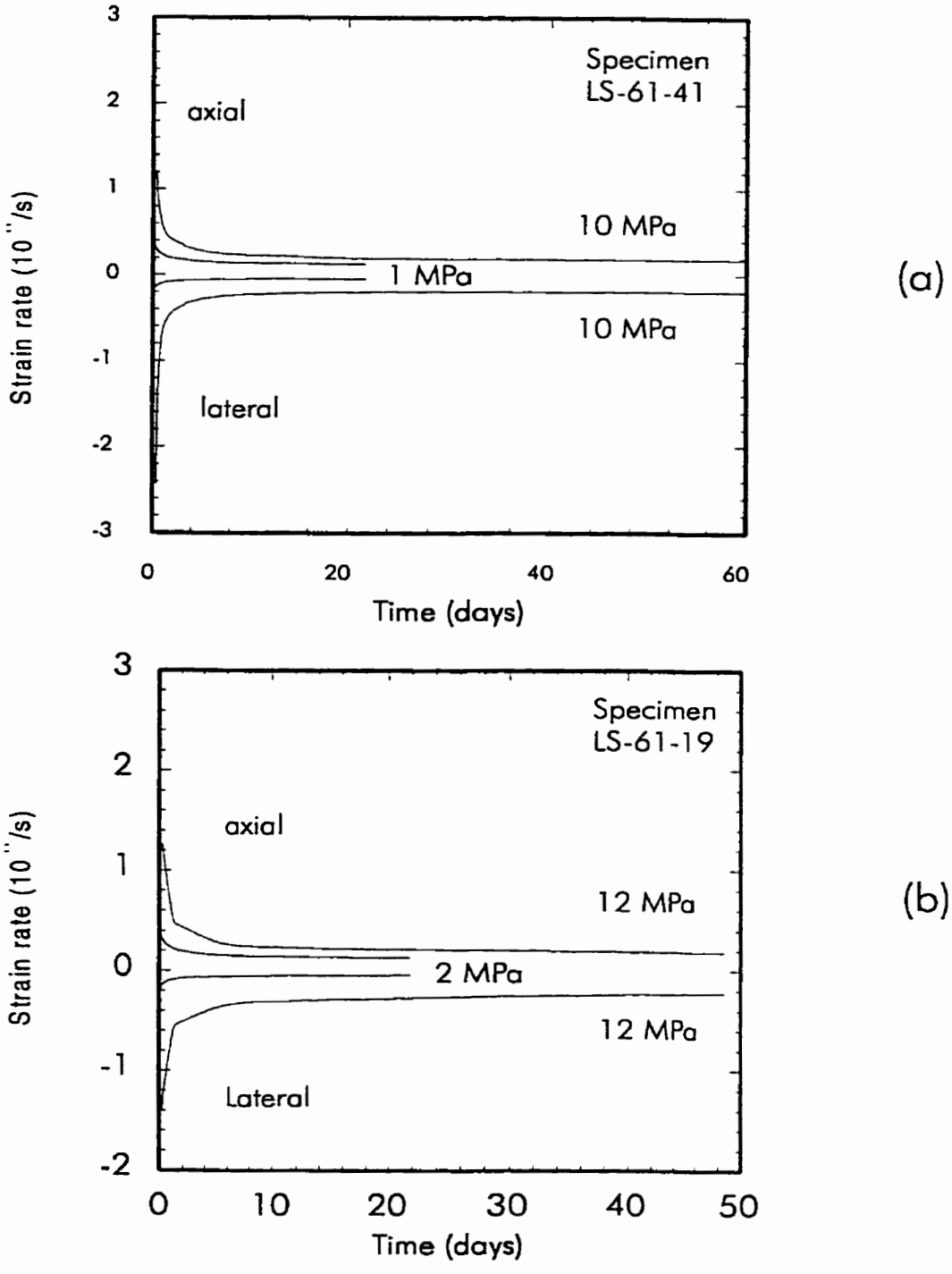


Figure 3-16. Creep strain rate; (a) for specimen LS-61-41 and (b) for specimen LS-61-19

At 1 MPa the specimen underwent volumetric compression. The creep strain in the lateral direction was quite large causing dilation at 10 MPa.

### 3.3.7 Series TP19 at 2 and 12 MPa

Testing of Thailand potash specimen LS-61-19 took 70 days. The specimen was first loaded to a stress of 2 MPa. This stress was kept constant for 21 days (TP19A). The load was then increased from 2 MPa to 12 MPa (TP19B). The creep test was continued for another 49 days. The axial, lateral and volumetric creep strains are shown in Figure 3-17(a) for TP19A and (b) for TP19B. The corresponding axial and lateral strain rates are plotted in Figure 3-16 (b). The strain rates at the end of the tests were 1.62 and 2.15 x $10^{-12}$/s for 2 MPa and 12 MPa in the axial direction, and 0.72 and 2.62 x $10^{-12}$/s in the lateral direction.

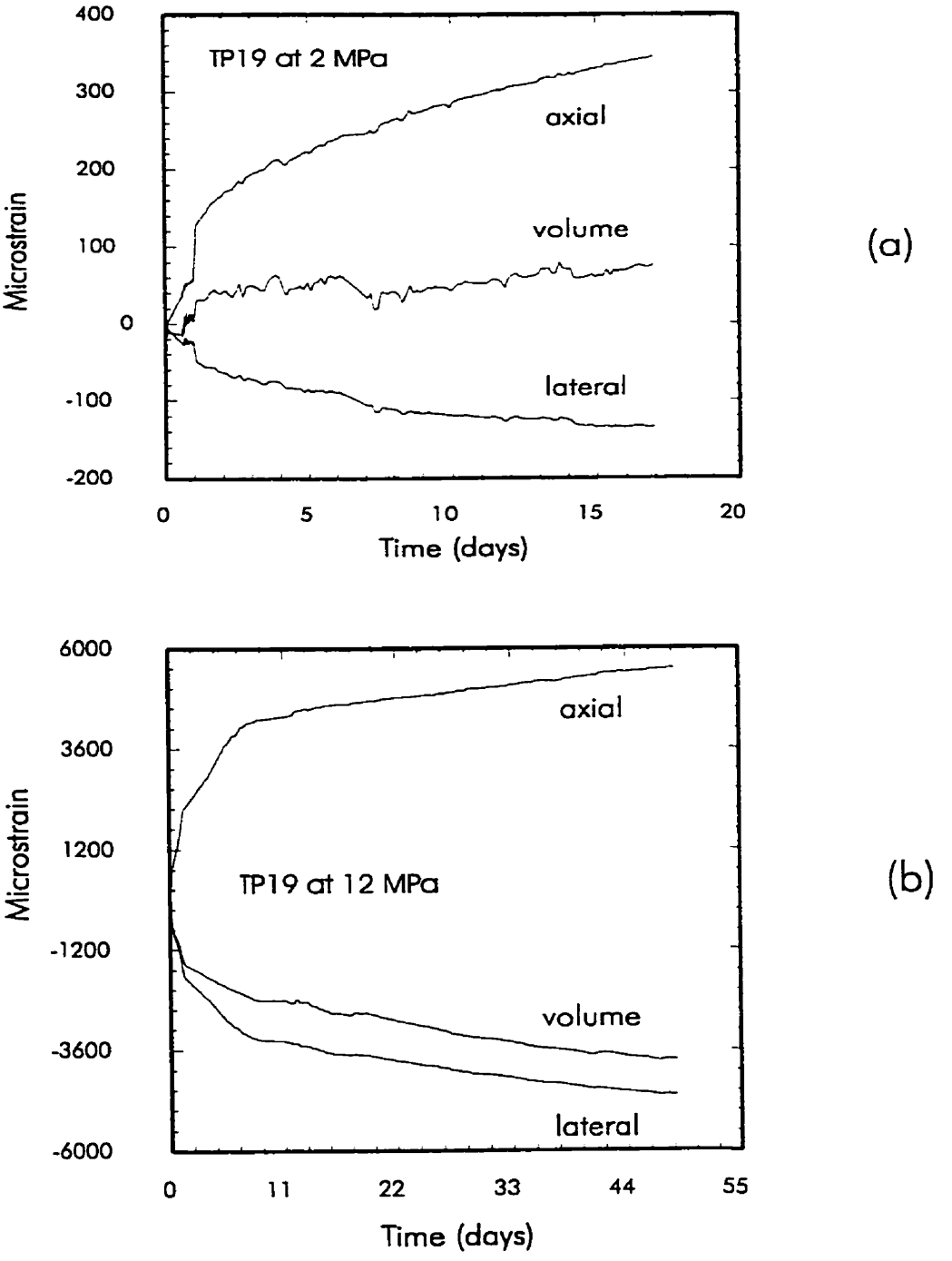


Figure 3-17. Axial, lateral and volumetric strain for specimen LS-61-19 at 2 and 12 MPa

## 3.4 Discussion of Experimental Results

### 3. 4. 1 Mechanisms of deformation in potash rock

In brittle materials, the time-dependent strain is generally quite small, but in potash rock and other salt rocks, creep deformation can be quite large and significant. In potash rocks deformation can be quite complex, producing elastic, plastic and brittle deformation. The entry and contribution of the three deformational mechanisms is stress-dependent.

Elastic strain is the strain (either linear or non-linear) that can be recovered once the load is removed. Most of the plastic strain in salt rocks results from the movement of dislocations on the two slip planes of the salt crystal (Hansen, 1985). The brittle deformation comes from microfracture, more specifically from the lateral dilation of tensile microcracks extending parallel to the uniaxial compressive stress. At ordinary temperature and pressure, potash rock shows many signs of microcracking, and the deformation is accompanied by both plastic and brittle strains (Cater and Hansen, 1983). There is no purely elastic, plastic and brittle behaviour at any stress level. The entry of the plastic (yield point) and the brittle (crack initiation point) strain producing mechanisms are only vaguely definable.

### 3.4.2 Theoretical stress-strain curves

Elastic behaviour dominates at low stress (Figure 3-18a). There is little creep at stresses lower than the yield point of the potash rock. Plastic deformation (Figure 3-18b) starts at the yield point. Theoretically it should continue at constant volume ($\nu = 0.5$). The

brittle mechanism enters at the crack initiation point and brittle deformation dominates the deformation process at high stress (Figure 3-18c). Axial microcracking does not affect the axial strain curve. Its entry must be deduced from the trend of the lateral and/or volumetric strain curves (Figure 3-18).

### 3.4.3 Construction of the stress-strain diagram

Only a small number of specimens were available for the testing program and they were all used for the creep tests; no uniaxial compression test was conducted. For potash from Lanigan, Saskatchewan (Lajtai et al, 1994), the stress-strain diagram in uniaxial compression has the typical features of an elastic-plastic-brittle material (Figure 3-19). The yield stress is around 10 MPa and this is little affected by the loading rate. Crack initiation on the other hand is strongly rate dependent and ranges between 13 and 18 MPa.

With no uniaxial compression test data available, an attempt was made to build a composite stress-strain diagram using the loading strains taken just before the beginning of the creep test. For each creep test, the starting creep strain was plotted in Figure 3-20. Although the data points scatter widely, a few observations can be made. There seems to be an increase in both the axial and the lateral strains at a stress level around 10 MPa. This could be the yield stress. The onset of dilation as indicated by the volumetric strain is around 13 MPa. The crack initiation point itself must be at a somewhat lower stress, perhaps at 12 MPa, but could be as low as 10 MPa.

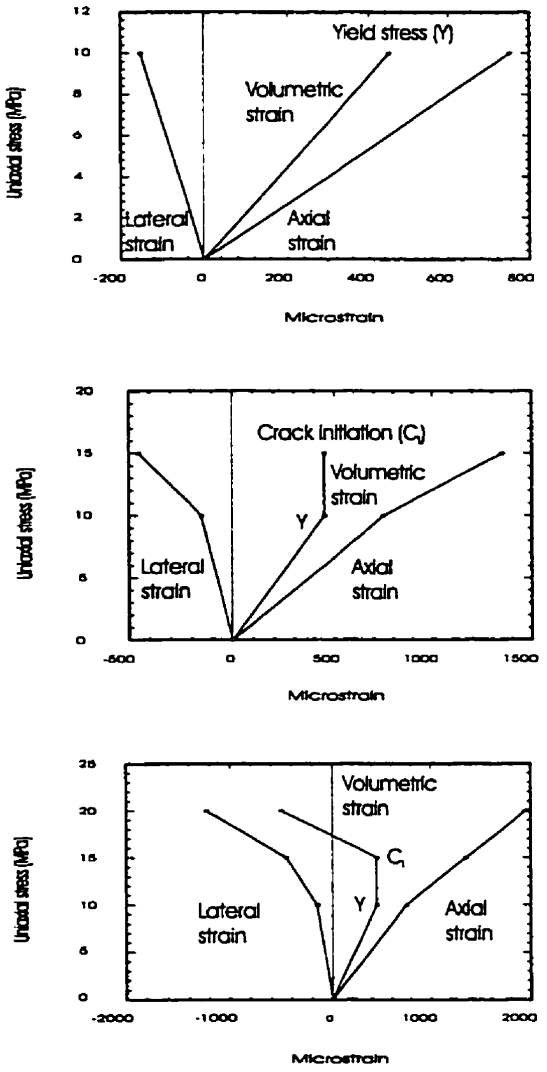


Figure 3-18. Theoretical stress-strain curves; (a) only elastic, (b) elastic-plastic and (c) elastic-plastic-brittle.

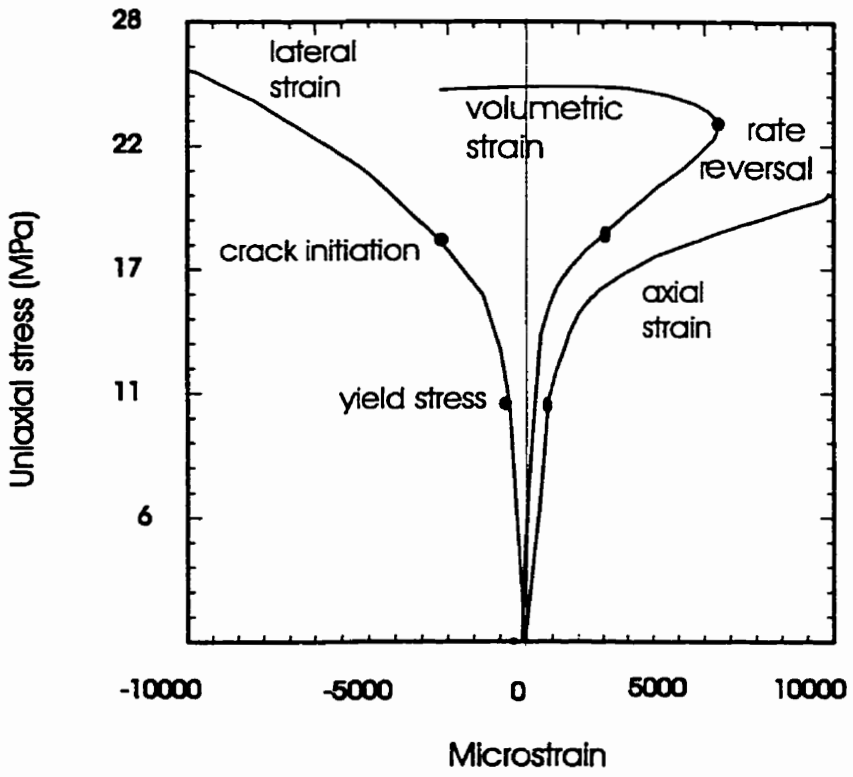


Figure 3-19. The stress-strain curves of a uniaxial compression test. The volumetric strain curve displays the three pre-failure milestones in the deformational history of potash: the yield stress, the crack initiation and volumetric strain rate reversal.

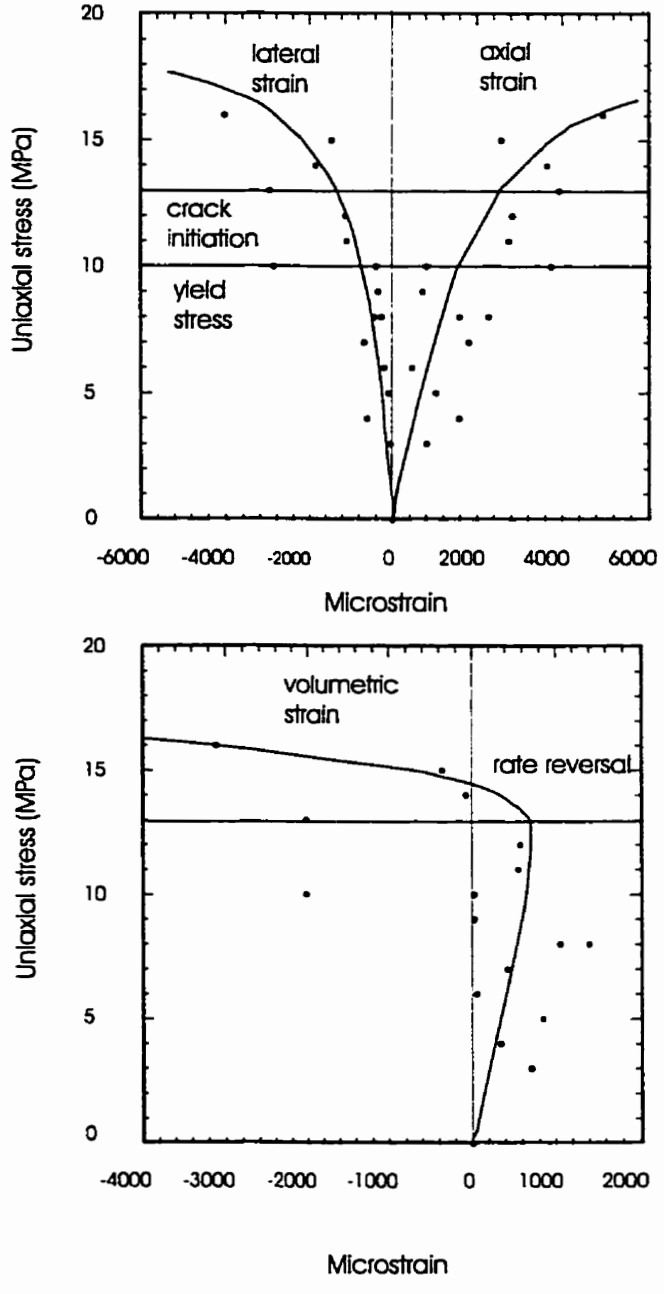


Figure 3-20. Interpreted stress-strain curves of the incremented-stress tests in uniaxial compression. The data come from all tests using the strain at the end of loading process.

### 3. 4. 4 Creep deformation

The total axial and lateral creep strains measured at the end of each creep test are plotted in Figure 3-21. As expected, the total axial and lateral creep strain increases with stress. In particular, the trend of the total lateral strain with increasing stress suggests that the increase in deformation with stress is not gradual and significant changes in trend are noticeable above 10 MPa.

Figure 3-22 shows the total volumetric strain as a function of uniaxial stress measured at the end of creep test. When the stresses are less than 8 MPa, the specimens suffer volumetric compression. Above this level dilatancy is indicated.

Figure 3-23, Figure 3-24 and Table 3-2 summarise the results of the creep tests. The results indicate that the creep strains in both axial and lateral directions are greater than the loading strains (accumulated while loading the specimen up to the creep load). The average creep strain was 61% of the total strain in the axial direction and 72% in the lateral direction. The creep strain for more brittle rocks is much smaller, e.g. 4% of the total strain for marble (Li, 1995), 9% for Portland limestone, 20% for Ormonde siltstone, 33% for Lea Hall sandstone (Hobbs, 1970), 38% for marlite and mudstone (Jia, 1989), and 50% for Hucknall shale (Hobbs, 1970). This observation indicates that potash deformation is the most time dependent among all rock types.

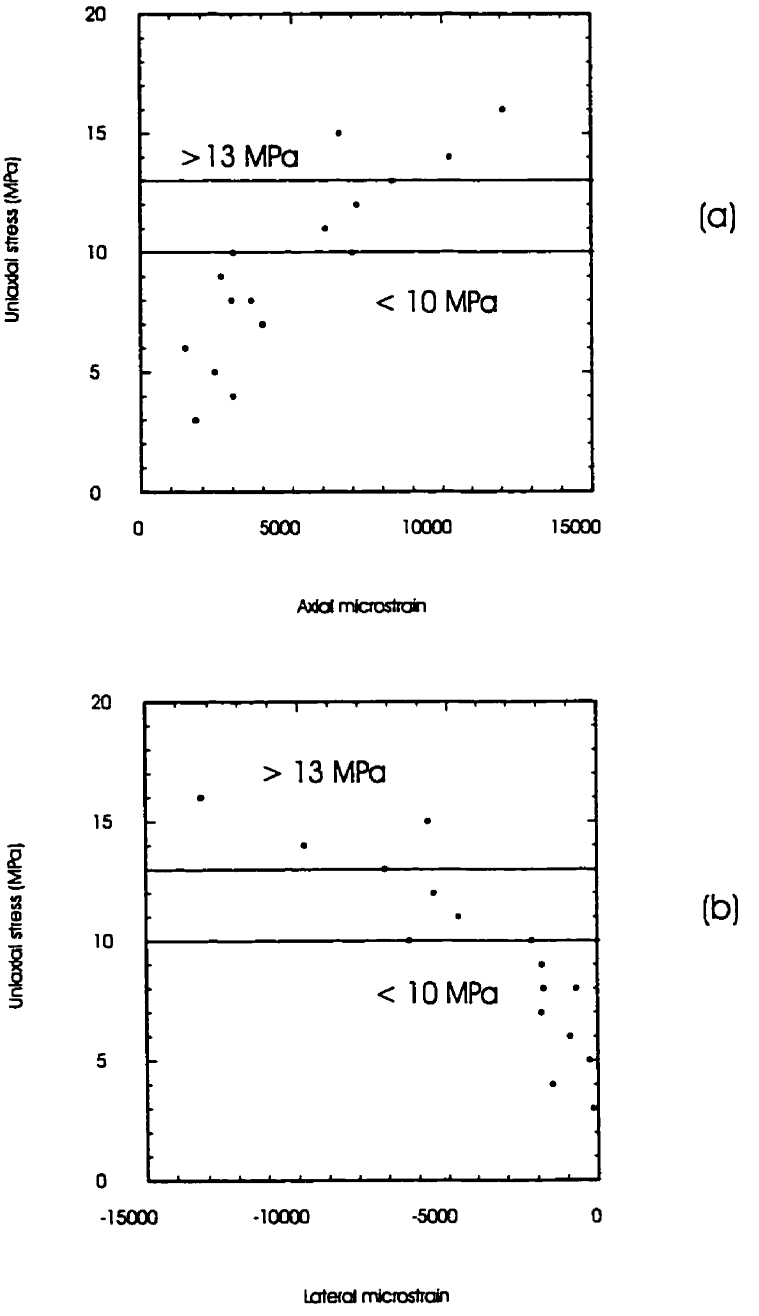


Figure 3-21. The total strain the end of a creep test as a function of stress; (a) axial (b) lateral.

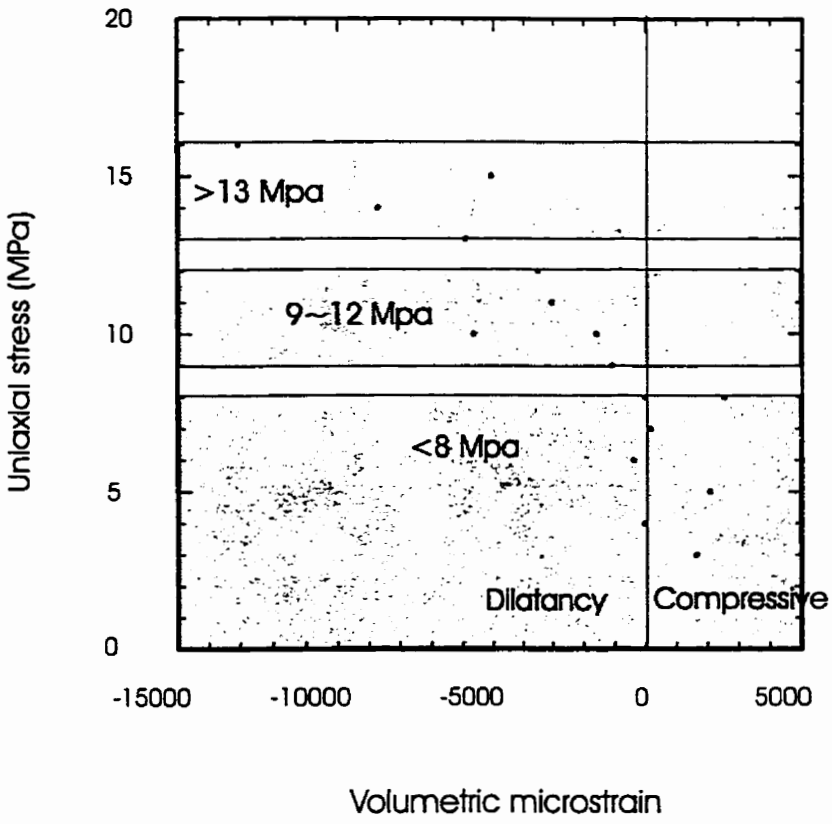


Figure 3-22. The total volumetric strain the end of a creep test as a function of stress for New Brunswick potash.

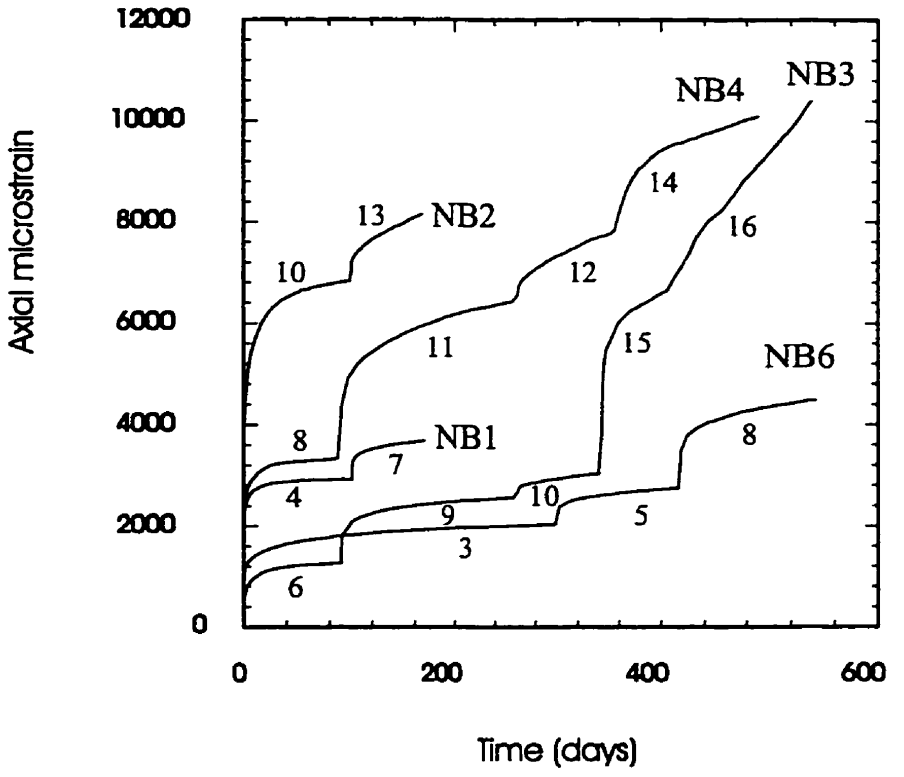


Figure 3-23. Incremented-stress axial creep Curves

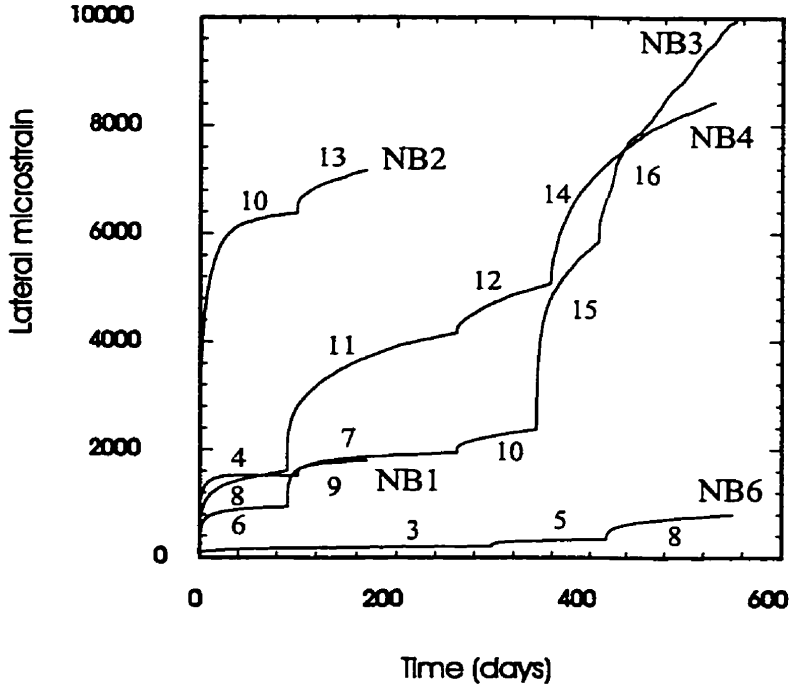


Figure 3-24. Incremented-stress lateral creep curves

Table 3-2. The ratios of creep strain to total strain

| Specimen No. | Test No. | Constant stress | Duration | Ratio of creep strain /total strain | |
|---|---|---|---|---|---|
| | | (MPa) | (days) | axial | lateral |
| PCA92-1M | NB1A | 4 | 102 | 0.48 | 0.59 |
| | NB1B | 7 | 68 | 0.52 | 0.62 |
| PCA92-2M | NB2A | 10 | 102 | 0.47 | 0.55 |
| | NB2B | 13 | 68 | 0.53 | 0.59 |
| PCA92-3M | NB3A | 6 | 91 | 0.70 | 0.79 |
| | NB3B | 9 | 171 | 0.75 | 0.82 |
| | NB3C | 10 | 96 | 0.76 | 0.84 |
| | NB3E | 15 | 71 | 0.77 | 0.92 |
| | NB3F | 16 | 143 | 0.65 | 0.70 |
| PCA92-5M | NB4A | 8 | 91 | 0.36 | 0.55 |
| | NB4B | 11 | 176 | 0.57 | 0.75 |
| | NB4C | 12 | 96 | 0.64 | 0.77 |
| | NB4D | 14 | 172 | 0.66 | 0.80 |
| PCA92-6M | NB6A | 3 | 298 | 0.61 | 0.76 |
| | NB6B | 5 | 120 | 0.63 | 0.74 |
| | NB6C | 8 | 132 | 0.65 | 0.73 |

Table 3-3. The ratios of the lateral strain to the axial strain

| Specimen No. | Test No. | Constant stress (MPa) | Duration (days) | Strain ratio of lateral/axial |
|---|---|---|---|---|
| PCA92-1M | NB1B | 7 | 68 | 0.47 |
| PCA92-2M | NB2B | 13 | 68 | 0.85 |
| PCA92-3M | NB3B | 9 | 68 | 0.71 |
| | NB3C | 10 | 68 | 0.72 |
| | NB3E | 15 | 68 | 0.87 |
| | NB3F | 16 | 68 | 0.96 |
| PCA92-5M | NB4B | 11 | 68 | 0.64 |
| | NB4C | 12 | 68 | 0.65 |
| | NB4D | 14 | 68 | 0.69 |
| PCA92-6M | NB6B | 5 | 68 | 0.12 |
| | NB6C | 8 | 68 | 0.24 |

Because each creep test had different duration, it is more meaningful to compute the same ratios for a fixed duration. Most of the creep tests went on longer than about 2 months. Table 3-3 gives the ratios of the lateral to the axial strains after 68 days of creep. The first loading stage is omitted. This ratio gets larger as the uniaxial stress increases.

The ratio of the lateral strain to the axial strain was less than 0.24 when the uniaxial stress was less than or equal to 8 MPa. An exception is NB1B. The ratio of the lateral to the axial strains increases rapidly from 0.64 to 0.96 in the stress range of 9 ~ 16 MPa.

The creep tests in this study showed only primary and possibly steady-state behaviour (Figure 3-4, 3-9, 3-12, 3-14 and 3-16). The strain rate gets greater as the uniaxial stress increases, except in test NB3E.

The relationship of the axial and the lateral strains is illustrated in Figure 3-25. During the loading stage, the axial strain is always larger than the lateral strain (Figure 3-25(a)), following the functional relationship of $\varepsilon_L = 1.12 \times 10^{-4} \varepsilon_A^{2.05}$. During the creep stage, if the stress is less than 12 MPa, the axial strain is greater than the lateral strain. However, when stress is larger than 12 MPa, the lateral strain is commonly larger than the axial strain (Figure 3-25b). The lateral strain in Figure 3-25(b) follows the relationship $\varepsilon_L = 6.1 \times 10^{-2} \varepsilon_A^{1.32}$.

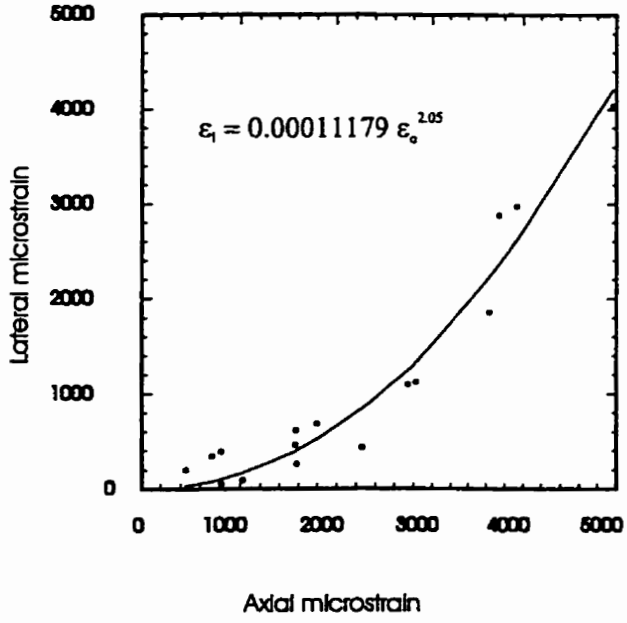


(a)

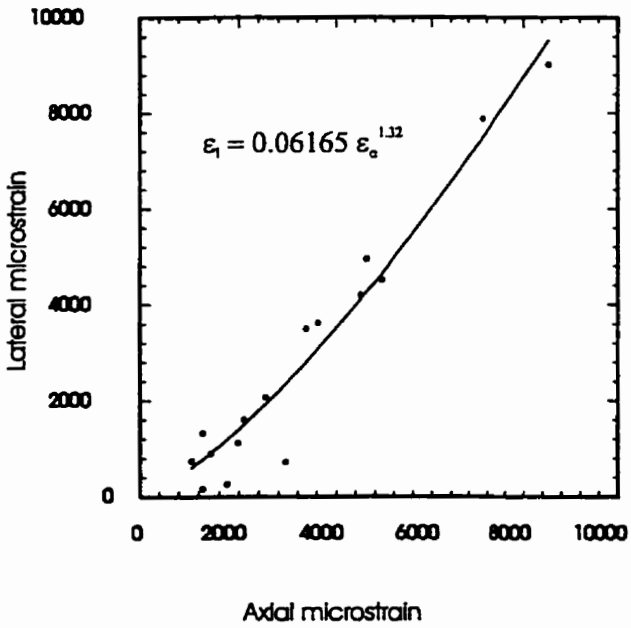


(b)

Figure 3-25. The relationship of axial and lateral strain; (a) the loading stage (b) the creep stage.

### 3. 4. 5 The effect of the loading history

The first loading stage in a creep test produces anomalously large initial strains. This can be demonstrated by comparing creep test series NB4 and NB6 at 8 MPa and NB2 and NB3 at 10 MPa (Figure 3-26 and 3-27). In NB4, the 8 MPa creep curve is the result of the first loading stage, in NB6, it is the third. Similarly, the 10 MPa creep curve of NB2 comes from the first loading stage and, in NB3 it comes from the third. As shown in Figure 3-26, the 8 MPa axial strain curves are somewhat similar but not the 8 MPa lateral strain curves. At 10 MPa both the axial and lateral strain curves are different (Figure 3-27).

The reason for the anomalous high creep strain during the first loading stage may be that extra strain is derived from the closing of microcracks that are the result of disturbance during specimen retrieval, drilling and machining.

Interestingly, the strain rates are influenced in an opposite way. The strain rates are smaller on the first loading. For example, when the same stress of 8 MPa is applied, the strain rates of the first load (NB4A) are smaller than that of the third load (NB6C) (Figure 3-28 (a)). The tests under 10 MPa have same trend (Figure 3-28 (b)).

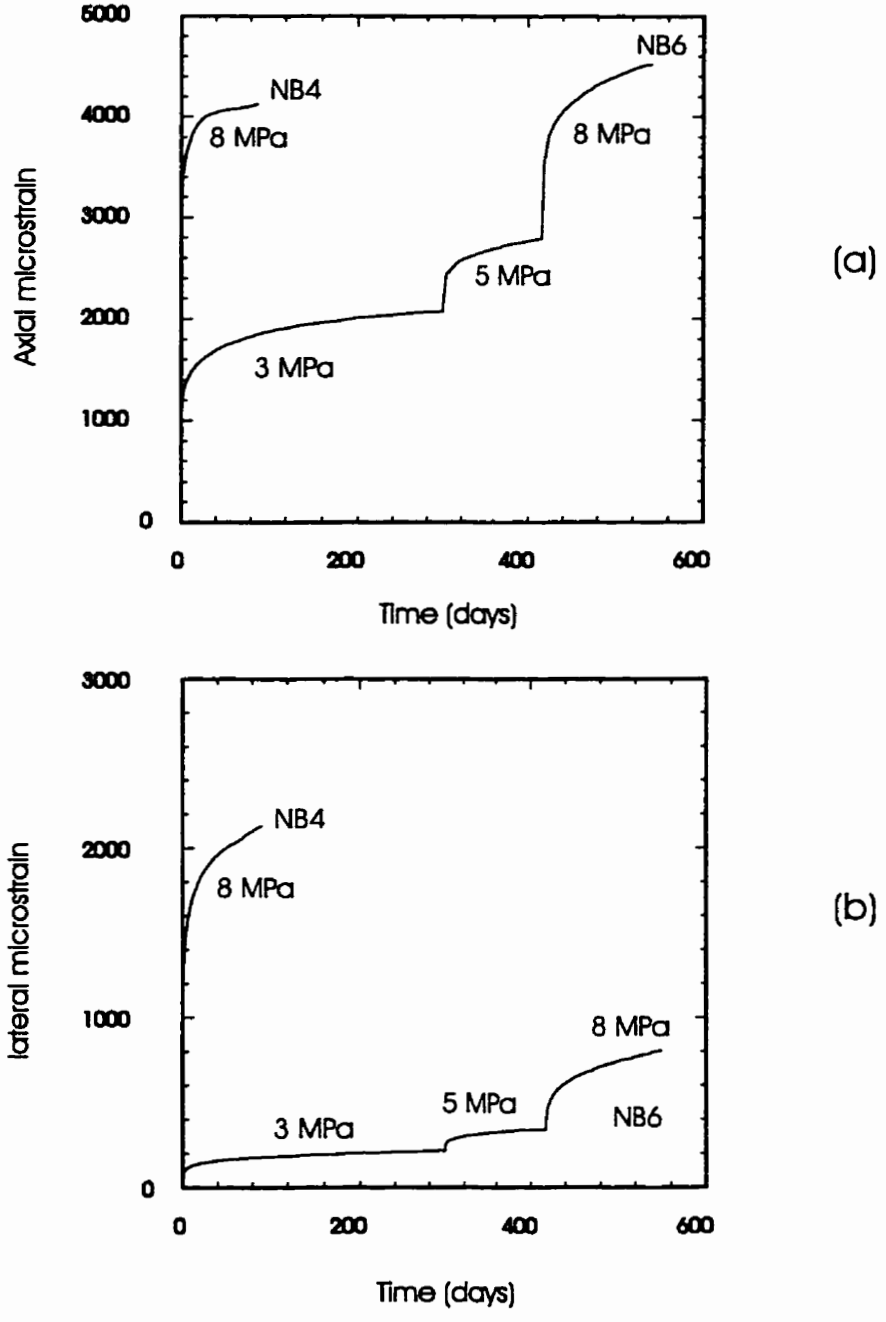


Figure 3-26. The creep strains generated by the first stress increment (once to 8 MPa) on specimen NB4 and the third stress step (3 steps to 8 MPa) on specimen NB6, (a) the axial strains, and (b) the lateral strains.

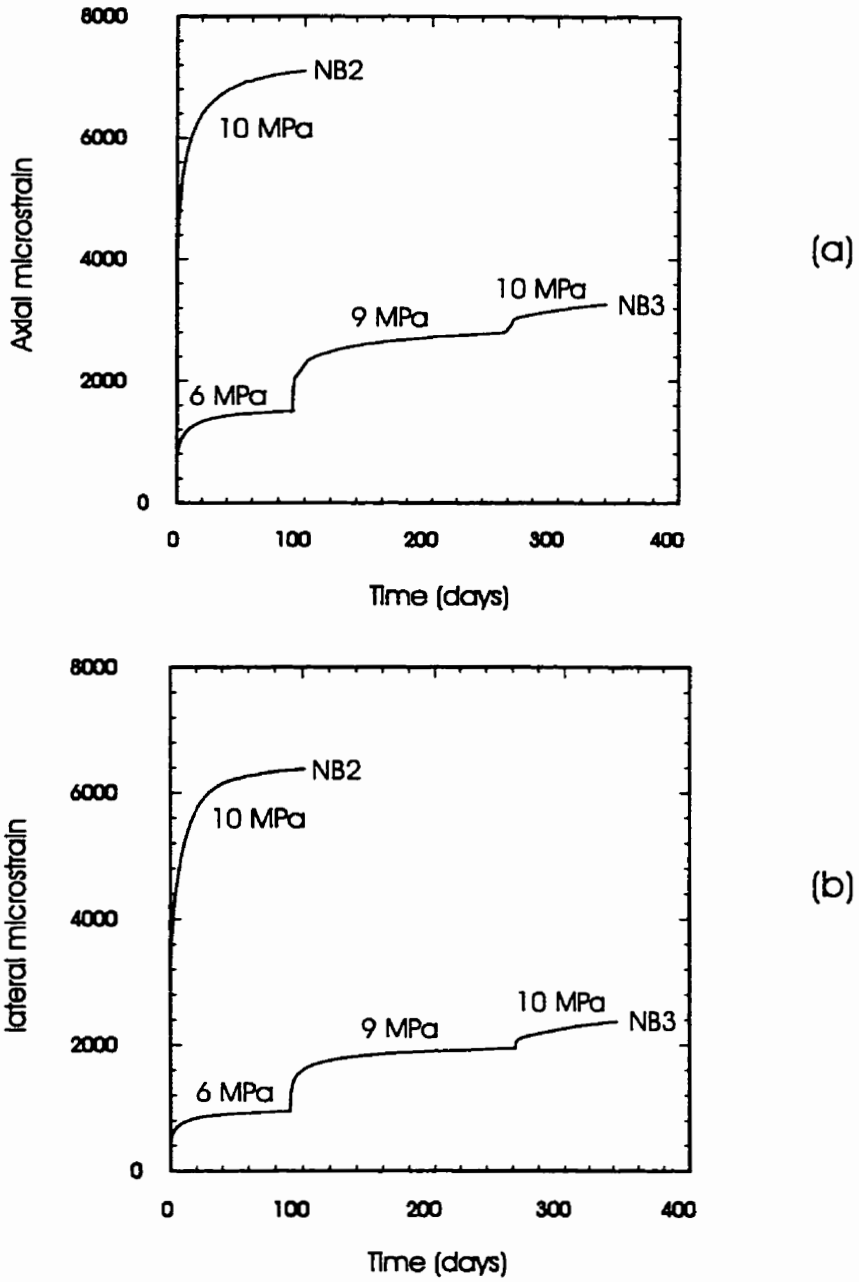


Figure 3-27. The creep strains generated by the first stress increment (once to 10 MPa) on specimen NB2 and the third stress step (3 steps to 10 MPa) on specimen NB3, (a) the axial strain, and (b) the lateral strain.

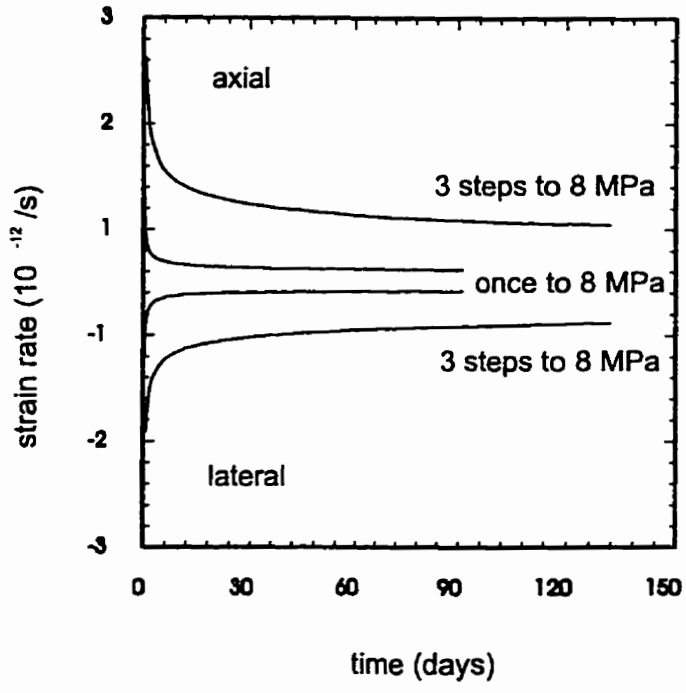


(a)

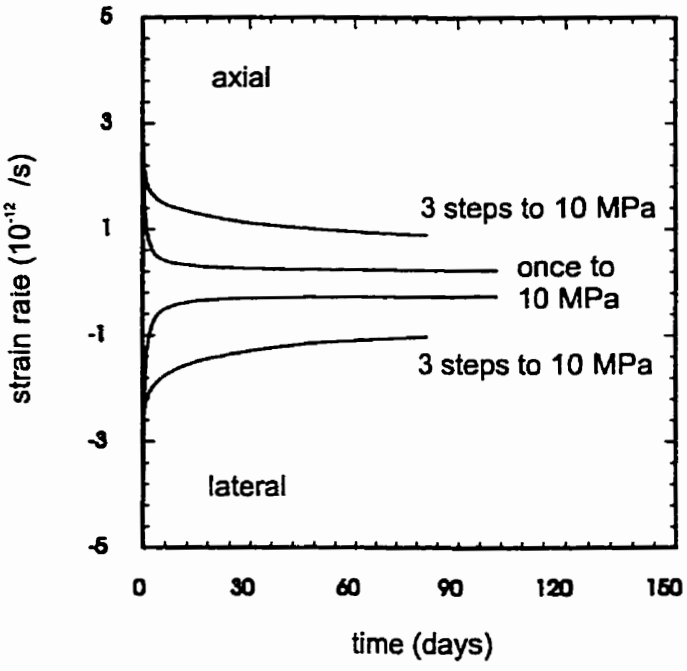


(b)

Figure 3-28. The strain rates generated by the first stress increment test and the third stress step test, (a) 8 MPa, and (b) 10 MPa.

### 3. 4. 6. The strain rate

Most creep tests are conducted to establish the relationship of steady-state strain rate versus stress. To derive the conventional stress versus steady-state strain rate relationship, the average rate would be taken at, or close to, the end of the test using approximately one-month interval of the data since, if there is steady-state creep at all, it would be likely to occur close to the end of the creep tests (Duncan, 1990). The procedure of selecting this interval is illustrated through Figures 3-29, 3-30, 3-31 and 3-34. There are linear sections in both the lateral and axial strain curves for the 73 to 97 days interval. In fact, linearity extends all the way to 120 days. If the test ended here, a good case could be made for the steady-state stage. The test however continued to 172 days. Clearly, both the axial and the lateral strain rates were declining at the end. A power function seems to fit the whole curve much better, as illustrated by the plot of the residuals (Figure 3-32, and 3-35). The corresponding strain rates are shown in Figure 3-33 and Figure 3-36.

A comparison of the axial and lateral strain rates at different stresses and time intervals for all specimens is given in Table 3-4 and Table 3-5. Because of equipment problems, some strains were not recorded; four creep tests do not have data at 0.2, 0.6 and 0.8 days. For the convenience of comparison, only 170 day's data was considered for test NB6A even though it was tested for 298 days.

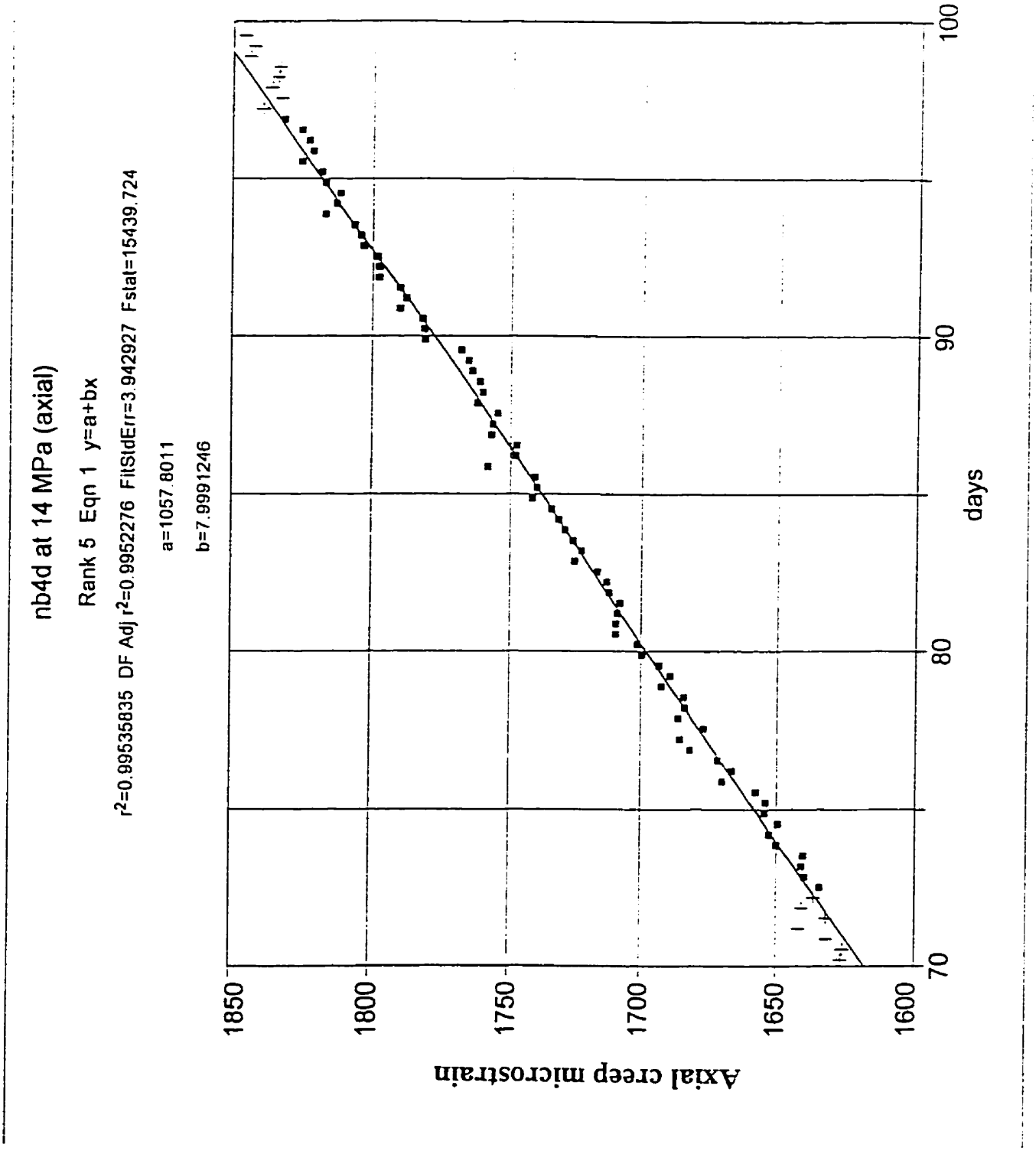


Figure 3-29. The axial microstrain versus time for specimen NB4D (14 MPa ) from 25 days' record of test with linear function fitting

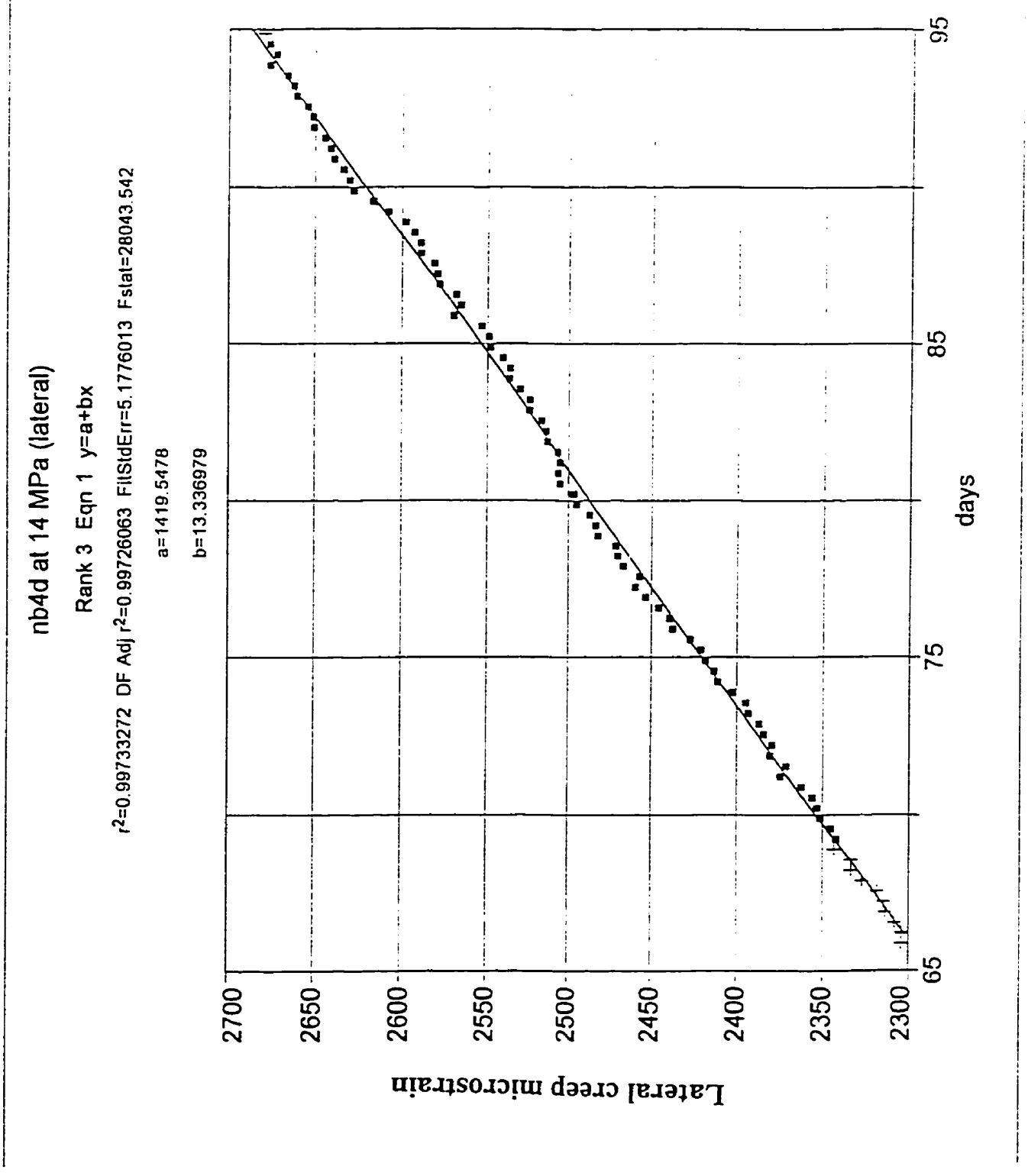


Figure 3-30. The lateral microstrain versus time for specimen NB4D (14 MPa ) from 25 days' record of test with linear function fitting

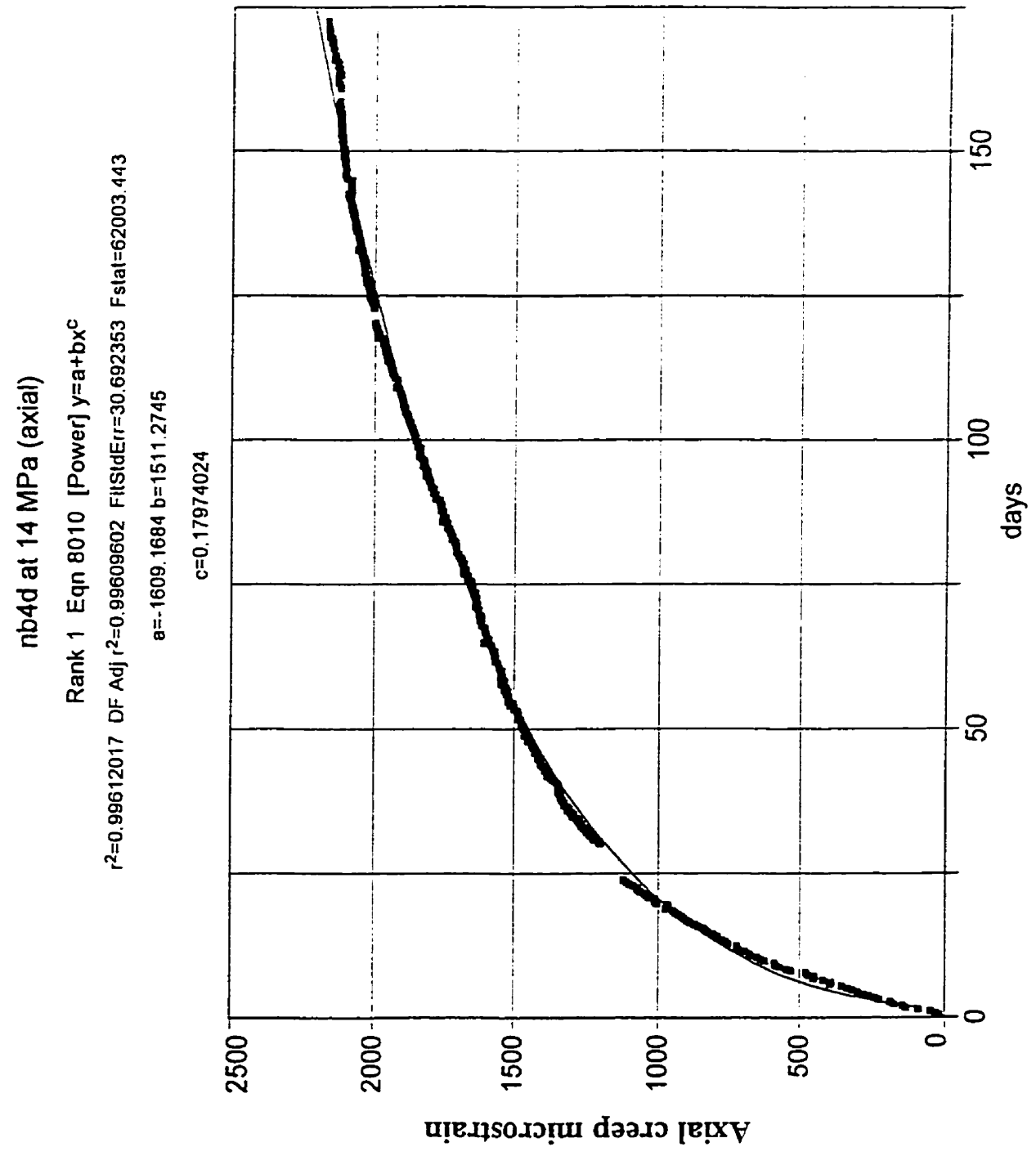


Figure 3-31. The axial microstrain versus time for specimen NB4D (14 MPa ) with power function fitting

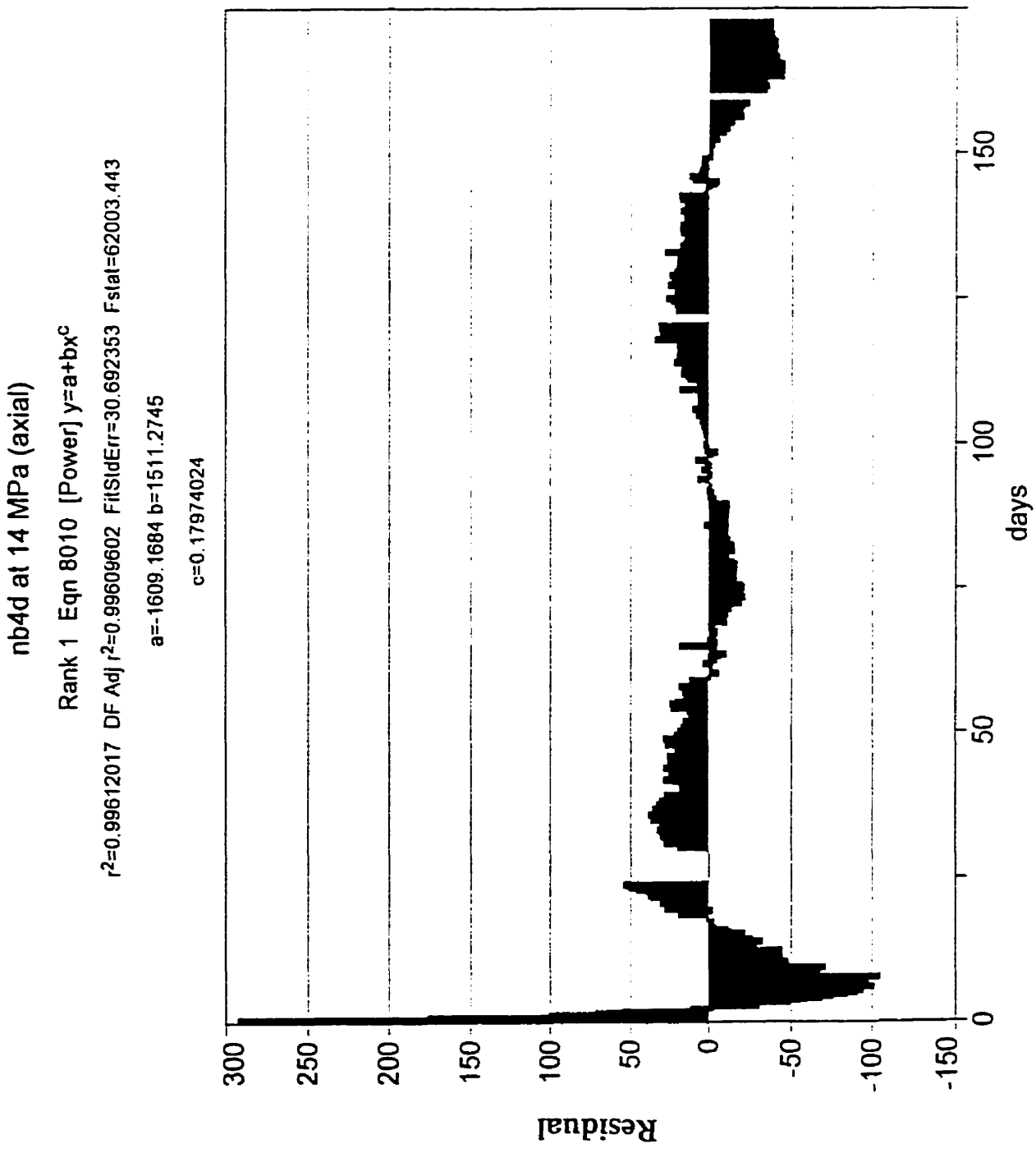


Figure 3-32. Residual versus time for specimen NB4D (14 MPa) with power function fitting

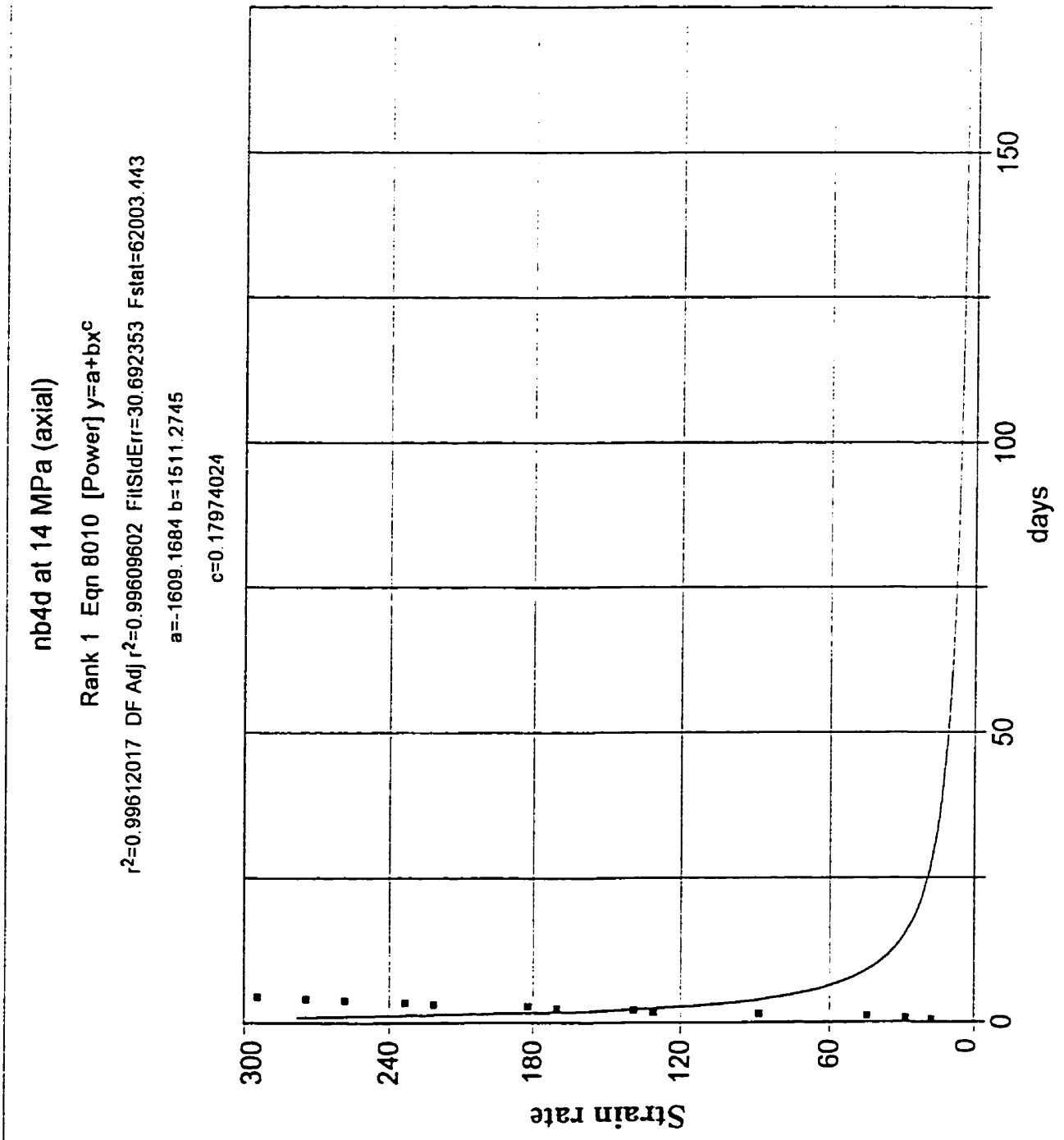


Figure 3-33. Axial strain rate versus time for specimen NB4D (14 MPa) with power function fitting

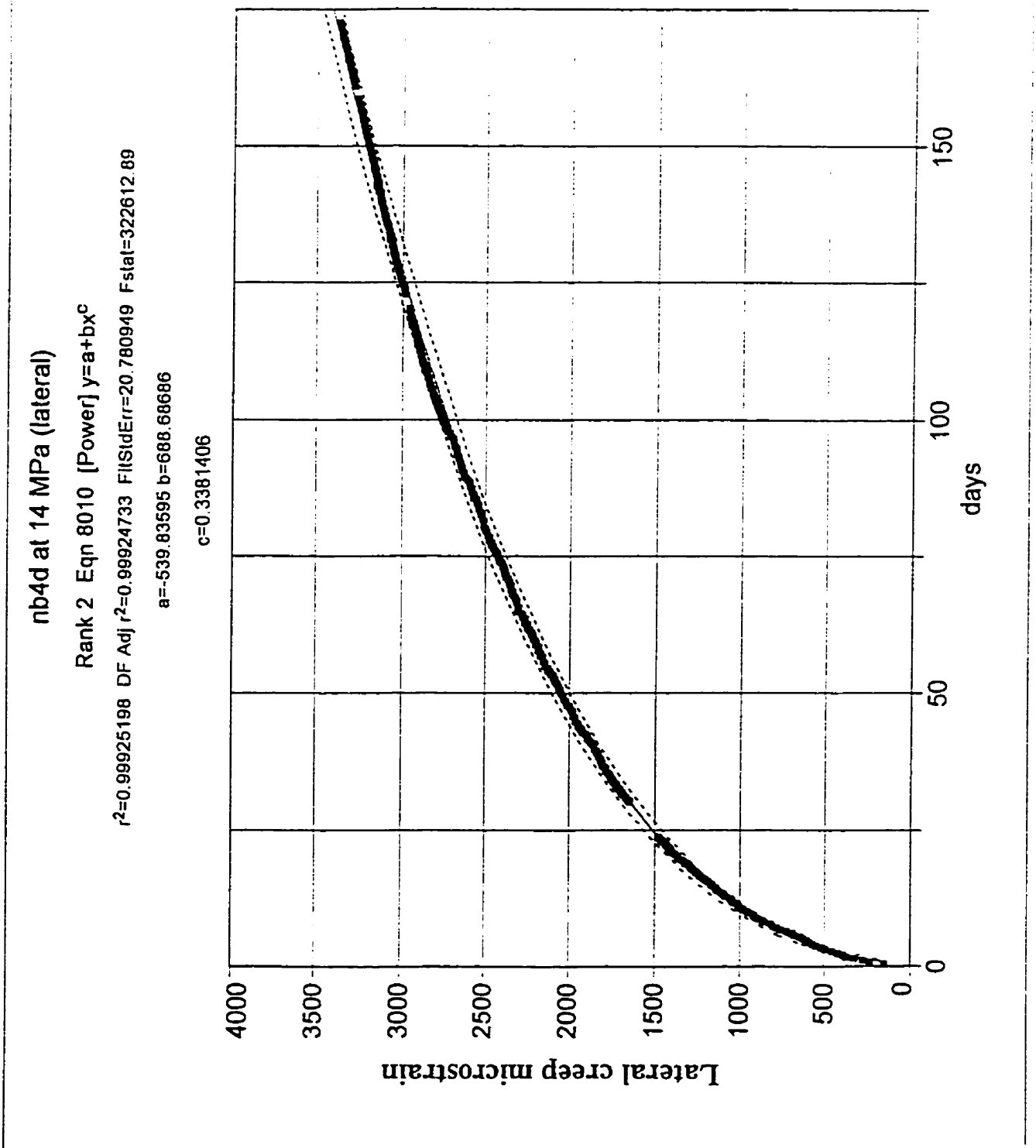


Figure 3-34. The lateral microstrain versus time for specimen NB4D (14 MPa ) with power function fitting

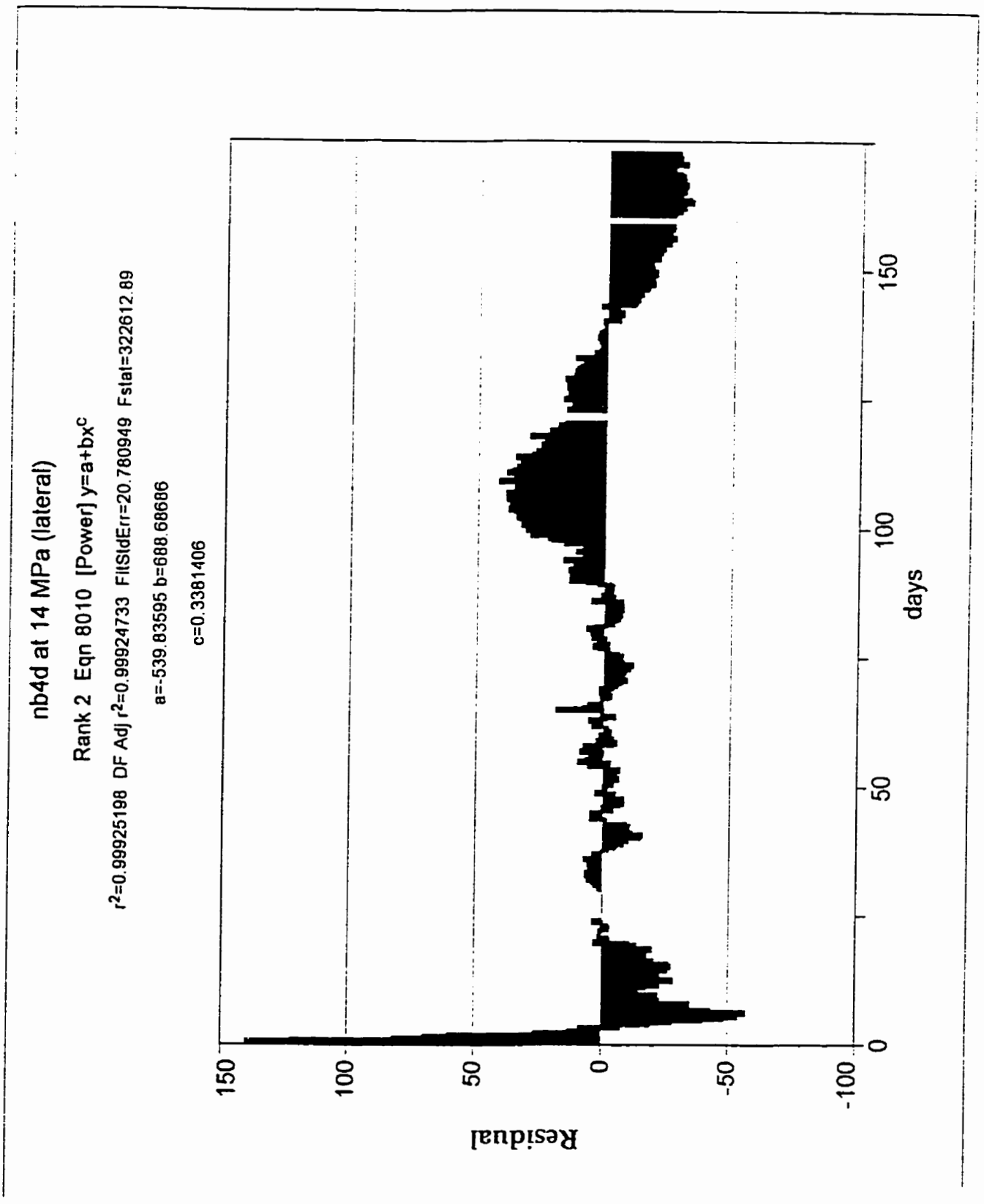


Figure 3-35. Residual versus time for specimen NB4D (14 MPa) with power function fitting

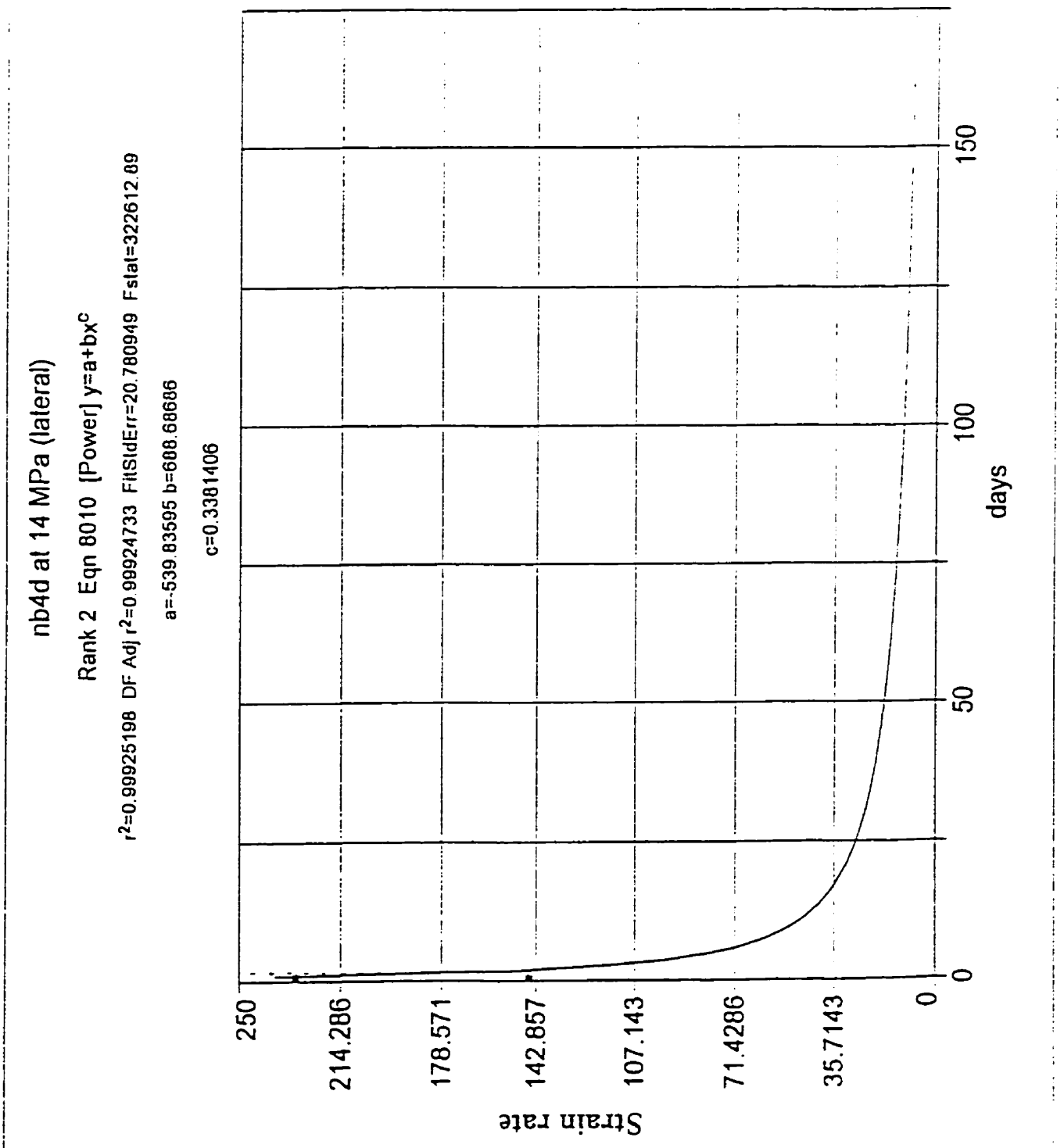


Figure 3-36. Lateral strain rate versus time for specimen NB4D (14 MPa) with power function fitting

Table 3-4. Comparison of the axial strain rate at different time intervals

| Days ⇒ | | 0.2 | 0.4 | 0.6 | 0.8 | 1.0 | 2.0 | 3.0 | 4.0 | 5.0 | 6.0 | 7.0 | 8.0 | 9.0 | 10.0 | 11.0 | 12.0 | 13.0 | 14.0 | 15.0 | 16.0 | 17.0 |
|---|---|---|---|---|---|---|---|---|---|---|---|---|---|---|---|---|---|---|---|---|---|---|
| Test No. | Stress (MPa) | Axial strain rate ($10^{-12}$/s) | | | | | | | | | | | | | | | | | | | | |
| NB6A | 3* | 16.89 | 11.79 | 11 | 10.03 | 5.86 | 5.14 | 4.79 | 4.55 | 4.37 | 4.25 | 4.15 | 4.06 | 3.97 | 3.91 | 3.85 | 3.8 | 3.77 | 3.72 | 3.7 | 3.66 | 3.64 |
| NB1A | 4 | 3.77 | 3.26 | 2.87 | 2.77 | 1.65 | 1.52 | 1.48 | 1.46 | 1.45 | 1.43 | 1.428 | 1.425 | 1.422 | 1.42 | | | | | | | |
| NB6B | 5 | – | – | – | 28.55 | 11.37 | 8.82 | 7.86 | 7.25 | 6.8 | 6.44 | 6.12 | 5.82 | 5.75 | 5.49 | 5.29 | 5.16 | | | | | |
| NB3A | 6 | 9.67 | 7.53 | 6.39 | 5.8 | 2.77 | 2.41 | 2.32 | 2.19 | 2.13 | 2.1 | 2.07 | 2.05 | 2.04 | | | | | | | | |
| NB1B | 7 | 19.49 | 15.69 | 14.44 | 13.24 | 7.03 | 6.1 | 5.51 | 5.2 | 5.02 | 4.81 | 4.69 | | | | | | | | | | |
| NB6C | 8 | – | – | – | 28.56 | 13.01 | 11.23 | 10.3 | 9.7 | 9.27 | 8.86 | 8.58 | 8.36 | 8.2 | 7.99 | 7.85 | 7.79 | 7.65 | | | | |
| NB4A | 8 | 32.19 | 10.2 | 7.23 | 6.02 | 2.39 | 2.06 | 1.93 | 1.82 | 1.78 | 1.77 | 1.75 | 1.73 | 1.7 | | | | | | | | |
| NB3B | 9 | 23.3 | 13.13 | 10.9 | 10.22 | 4.25 | 3.67 | 3.38 | 3.17 | 3.02 | 2.92 | 2.85 | 2.78 | 2.73 | 2.68 | 2.62 | 2.58 | 2.56 | 2.52 | 2.5 | 2.47 | 2.44 |
| NB3D | 9 | 11.6 | 11.37 | 11.02 | 10.56 | 9.42 | 9.38 | 9.26 | 9.1 | 8.93 | 8.76 | 8.58 | 8.41 | 8.23 | 8.06 | 7.88 | 7.71 | 7.54 | 7.37 | 7.2 | 7.06 | 6.89 |
| NB3C | 10 | 33.54 | 22.83 | 18.78 | 16.95 | 16.09 | 14.3 | 12.99 | 12.19 | 11.53 | 11.1 | 10.67 | 10.35 | | | | | | | | | |
| NB2A | 10 | 77.02 | 29.63 | 20.2 | 17.78 | 3.98 | 3.29 | 3.01 | 2.88 | 2.79 | 2.75 | 2.69 | 2.65 | 2.63 | 2.61 | | | | | | | |
| NB4B | 11 | 32.94 | 29.43 | 26 | 24.99 | 14.07 | 12.27 | 11.37 | 10.73 | 10.16 | 9.73 | 9.43 | 9.15 | 8.93 | 8.72 | 8.57 | 8.38 | 8.28 | 8.18 | 8.08 | 7.99 | 7.92 |
| NB4C | 12 | – | – | 82.36 | 61.48 | 33.18 | 26.89 | 23.08 | 20.76 | 19.02 | 17.62 | 16.24 | 15.27 | 14.66 | | | | | | | | |
| NB2B | 13 | 65.17 | 57.63 | 55.18 | 52.77 | 35.57 | 30.39 | 28.01 | 26.21 | 24.7 | 23.5 | 22.79 | | | | | | | | | | |
| NB4D | 14 | – | – | – | 83.33 | 36.47 | 29.68 | 26.56 | 24.78 | 23.4 | 22.3 | 21.56 | 20.83 | 20.21 | 19.65 | 19.2 | 18.89 | 18.56 | 18.31 | 18.08 | 17.81 | 17.56 |
| NB3E | 15 | 47.55 | 22.83 | 18.78 | 16.95 | 9.16 | 8.36 | 7.89 | 7.62 | 7.37 | 7.15 | 7.05 | | | | | | | | | | |
| NB3F | 16 | 76.43 | 66.99 | 64.41 | 55.04 | 33.86 | 24.57 | 21.92 | 20.7 | 19.72 | 18.68 | 17.5 | 16.8 | 16.21 | 15.49 | 14.92 | 14.49 | 13.96 | 13.63 | | | |

* This is a 298 days test; the strain rate at the end of test = 3.41

Table 3-5. Comparison of the lateral strain rate at different time intervals

| Days ⇒ | | 0.2 | 0.4 | 0.6 | 0.8 | 10 | 20 | 30 | 40 | 50 | 60 | 70 | 80 | 90 | 100 | 110 | 120 | 130 | 140 | 150 | 160 | 170 |
|---|---|---|---|---|---|---|---|---|---|---|---|---|---|---|---|---|---|---|---|---|---|---|
| Test No. | Stress (MPa) | Lateral strain rate ($10^{-12}$/s) | | | | | | | | | | | | | | | | | | | | |
| NB6A | 3* | 11.23 | 9.29 | 8.69 | 7.74 | 4.47 | 3.86 | 3.58 | 3.4 | 3.27 | 3.16 | 3.1 | 3.02 | 2.98 | 2.95 | 2.91 | 2.87 | 2.83 | 2.8 | 2.77 | 2.74 | 2.7 |
| NB1A | 4 | 1.66 | 1.39 | 1.24 | 1.14 | 0.58 | 0.54 | 0.53 | 0.52 | 0.51 | 0.5 | | | | | | | | | | | |
| NB6B | 5 | _ | _ | _ | 20.02 | 7.51 | 6.23 | 5.65 | 5.23 | 5.01 | 4.78 | 4.64 | 4.52 | 4.4 | 4.3 | 4.2 | 4.1 | | | | | |
| NB3A | 6 | 6.4 | 4.61 | 3.97 | 3.49 | 1.72 | 1.52 | 1.45 | 1.4 | 1.37 | 1.35 | 1.33 | 1.31 | 1.30 | | | | | | | | |
| NB1B | 7 | 40.69 | 31.58 | 22.88 | 18.08 | 7.91 | 6.66 | 6.09 | 5.66 | 5.32 | 5.09 | 5.02 | | | | | | | | | | |
| NB6C | 8 | _ | _ | _ | 18.85 | 9.05 | 7.83 | 7.2 | 6.81 | 6.52 | 6.24 | 6.0 | 5.92 | 5.85 | 5.8 | 5.53 | 5.4 | 5.28 | | | | |
| NB4A | 8 | 25.83 | 8.47 | 5.96 | 4.95 | 1.71 | 1.45 | 1.36 | 1.28 | 1.23 | 1.18 | 1.17 | 1.16 | 1.15 | | | | | | | | |
| NB3B | 9 | 16.31 | 9.2 | 7.48 | 7.08 | 2.62 | 2.29 | 2.13 | 2.03 | 1.97 | 1.91 | 1.87 | 1.83 | 1.81 | 1.79 | 1.76 | 1.74 | 1.73 | 1.72 | 1.69 | 1.68 | 1.67 |
| NB3D | 9 | 12.16 | 10.7 | 10.38 | 9.74 | 7.49 | 6.94 | 6.62 | 6.41 | 6.25 | 6.12 | 6.03 | 5.94 | 5.85 | 5.8 | 5.74 | 5.69 | 5.63 | 5.57 | 5.53 | 5.5 | 5.45 |
| NB3C | 10 | 34.94 | 30.35 | 28.22 | 26.84 | 18.63 | 16.37 | 14.96 | 13.96 | 13.18 | 12.68 | 12.3 | 11.9 | | | | | | | | | |
| NB2A | 10 | 107.3 | 40.3 | 27.13 | 23.69 | 4.74 | 3.75 | 3.43 | 3.29 | 3.22 | 3.18 | 3.13 | 3.1 | 3.09 | 3.08 | | | | | | | |
| NB4B | 11 | 37.41 | 33.05 | 28.94 | 27.69 | 14.85 | 12.77 | 11.72 | 11.0 | 10.44 | 10.0 | 9.66 | 9.4 | 9.28 | 8.99 | 8.81 | 8.7 | 8.51 | 8.4 | 8.29 | 8.19 | 8.1 |
| NB4C | 12 | _ | _ | 85.72 | 75.79 | 42.32 | 36.12 | 32.2 | 29.93 | 28.3 | 26.92 | 26.31 | 25.5 | 24.4 | | | | | | | | |
| NB2B | 13 | 56.56 | 50.54 | 47.04 | 43.33 | 26.66 | 22.55 | 20.62 | 19.28 | 18.21 | 17.23 | 16.7 | | | | | | | | | | |
| NB4D | 14 | _ | _ | _ | 113.5 | 49.3 | 40.48 | 36.06 | 33.49 | 31.69 | 30.18 | 29.2 | 28.19 | 27.8 | 26.7 | 26.2 | 25.6 | 25.1 | 24.7 | 24.4 | 23.9 | 23.5 |
| NB3E | 15 | 92.45 | 46.39 | 38.07 | 34.06 | 15.9 | 14.25 | 13.31 | 12.64 | 12.16 | 11.8 | 11.6 | | | | | | | | | | |
| NB3F | 16 | 292.9 | 279.3 | 275.1 | 254.9 | 201 | 173.7 | 164.4 | 158.9 | 154.9 | 150.4 | 146 | 143 | 141 | 138 | 135.7 | 133.7 | 131.3 | 130.2 | | | |

* This is a 298 days test; the strain rate at the end of test = 2.42

Table 3-6 shows the relationship of stress and strain rate over 60 days for each specimen separately. In general, the value of strain rate increases with the applied uniaxial stress with one exception of NB3E at 15 MPa. As mentioned before, maintaining the constant load at high stress is difficult and frequent load adjustments were required. There is also the danger of the strain gauges failing to record the true strains due to debonding.

Figure 3-37 shows the lateral strain rate curves as a function of stress for several times. These values were obtained from the fitted power curves. Although the times represented range widely between 0.2 days (5 hours) and 110 days, the shapes of the curves are very similar and the offsets due to different times is not as large as one would one expect. Figure 3-38 gives the axial strain rate for the same times.

The stress dependence of the axial strain rate seems to broadly follow the power function (Figure 3-39). In logarithmic space, it shows the expected linear trend. The slope of the linear functions (the exponent of stress in the power function) is 2.4. (A value of 3 has been proposed for creep that is controlled through dislocation-climb (Cadek, 1987)). One cannot fit a single straight line to the lateral strain rate data. This may be because the lateral strain rate could be affected by contributions coming from both the plastic and the brittle mechanisms (Duncan, 1993). Figure 3-40 shows the two-line interpretation. The exponent of stress for the low stress line is 0.4 and for the other is about 5.

Table 3-6. Axial and lateral strain rates at 60 days

| test number | constant stress (MPa) | strain rate ($10^{-12}$/s) | |
|---|---|---|---|
| | | Axial | Lateral |
| NB1A | 4 | 1.43 | 0.5 |
| NB1B | 7 | 4.81 | 5.09 |
| NB2A | 10 | 2.75 | 3.18 |
| NB2B | 13 | 23.5 | 17.23 |
| NB3A | 6 | 2.1 | 1.35 |
| NB3B | 9 | 2.92 | 1.91 |
| NB3C | 10 | 11.1 | 12.68 |
| NB3E | 15 | 7.15 | 11.8 |
| NB3F | 16 | 18.68 | 150.4 |
| NB4A | 8 | 1.77 | 1.18 |
| NB4B | 11 | 9.73 | 10.0 |
| NB4C | 12 | 17.62 | 26.92 |
| NB4D | 14 | 22.3 | 30.18 |
| NB6A | 3 | 4.25 | 3.16 |
| NB6B | 5 | 6.44 | 4.78 |
| NB6C | 8 | 8.86 | 6.24 |

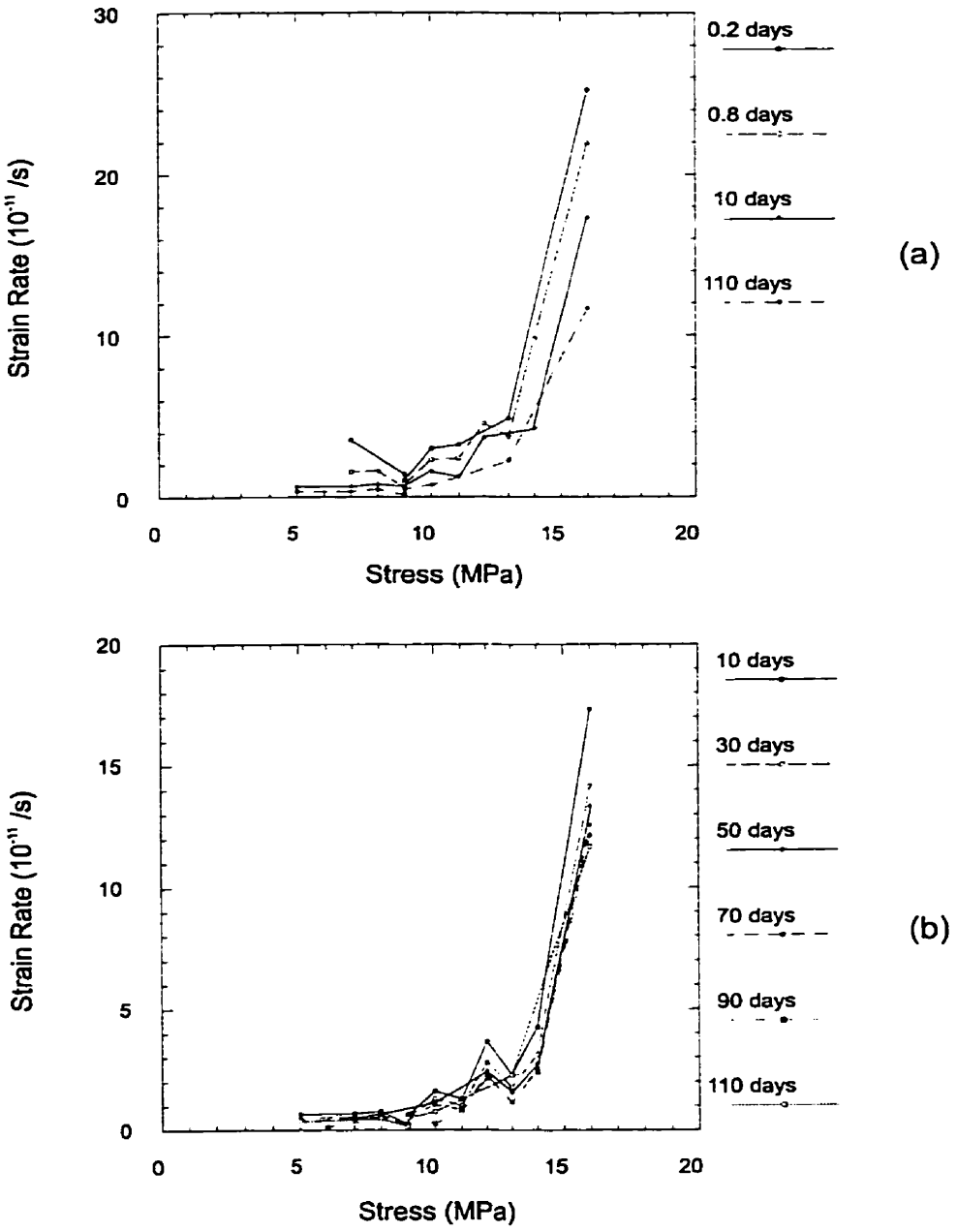


Figure 3-37. Lateral strain rate curves at different stress levels (without the first stress level); (a) at 0.2, 0.8, 10 and 110 days (b) at 10, 30, 50, 70, 90and 110 days.

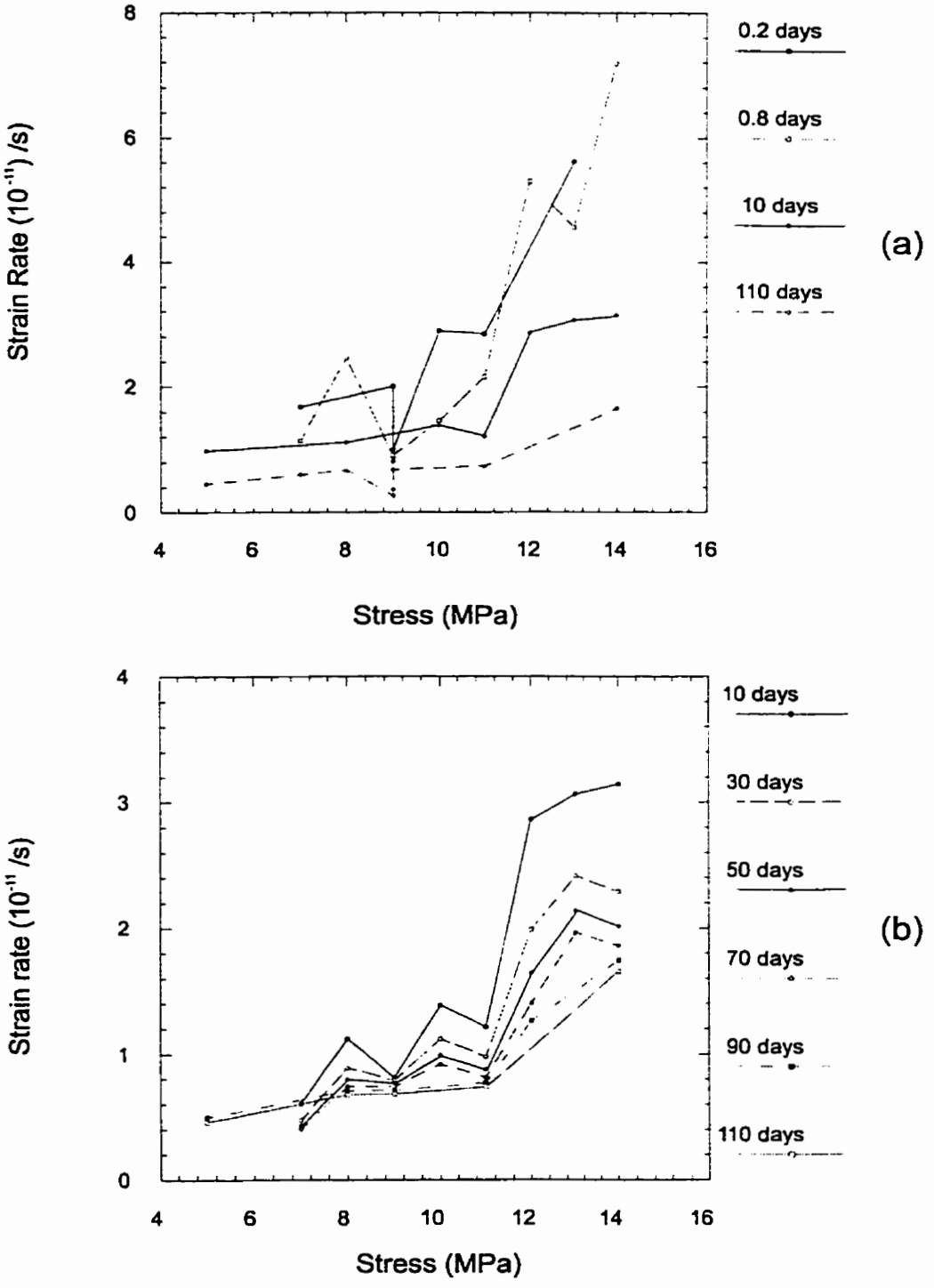


Figure 3-38. Axial strain rate curves at different stress levels (without the first stress level); (a) at 0.2, 0.8, 10 and 110 days (b) at 10, 30, 50, 70, 90and 110 days.

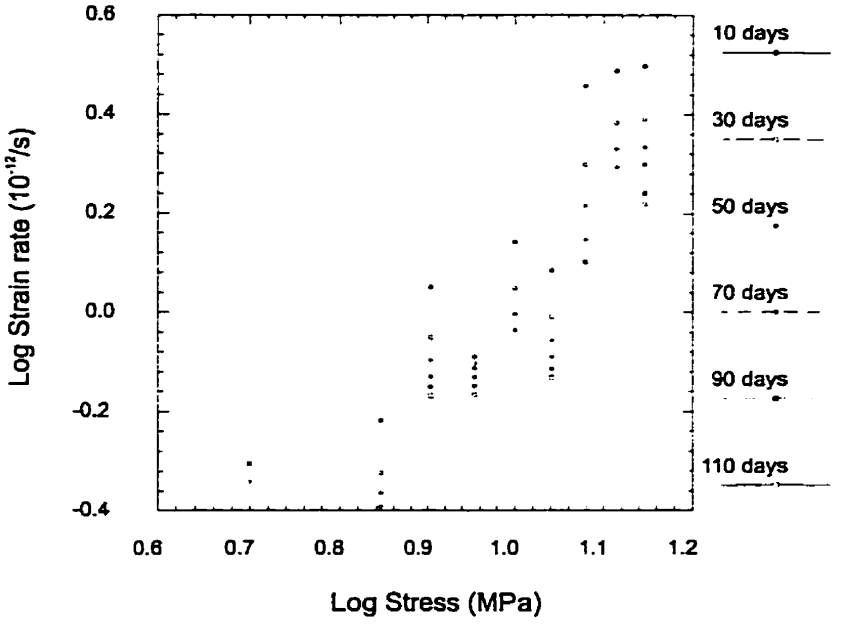


(a)

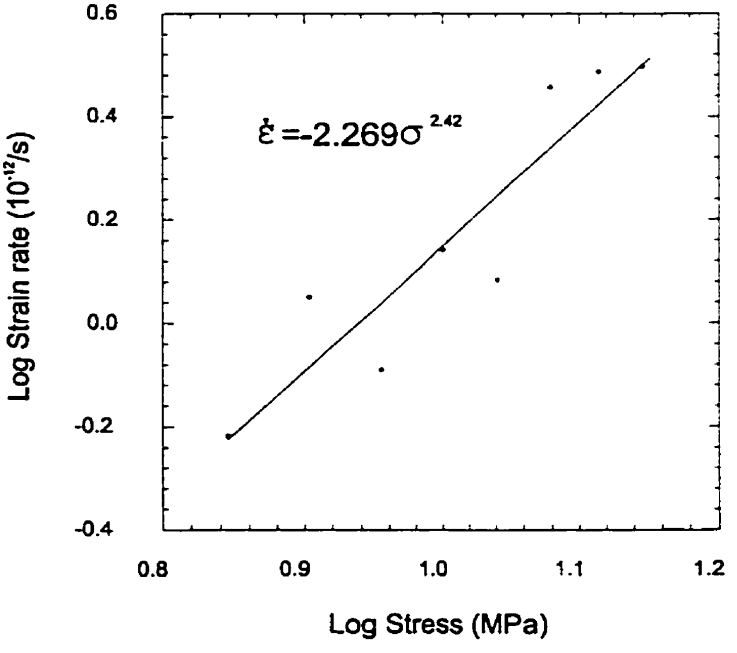


(b)

Figure 3-39. The stress dependence of the axial strain rate; (a) the axial strain rate for all specimen without the first load at 10, 30, 50, 70, 90 and 110 days (b) the relationship of stress and strain rate at 10 days.

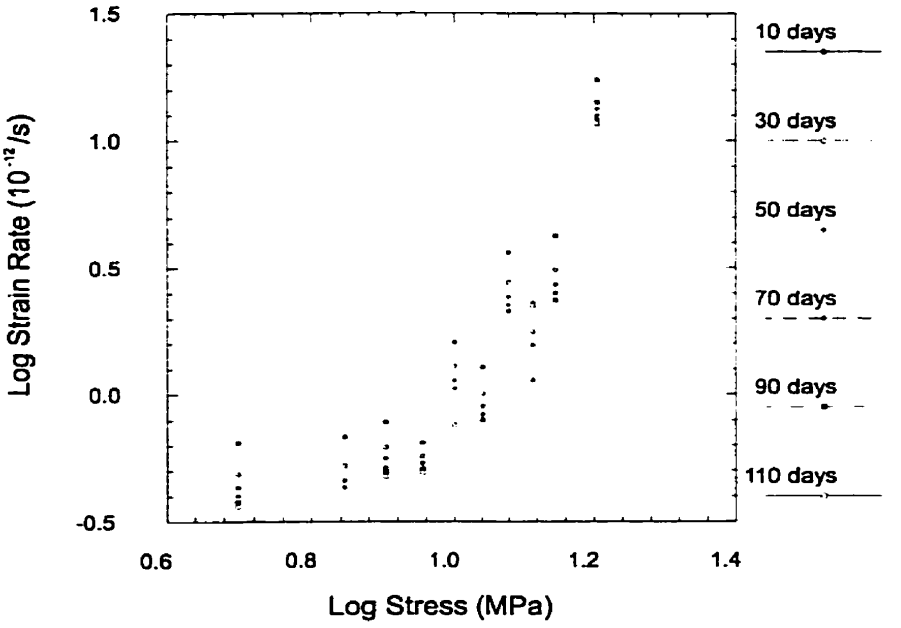


(a)

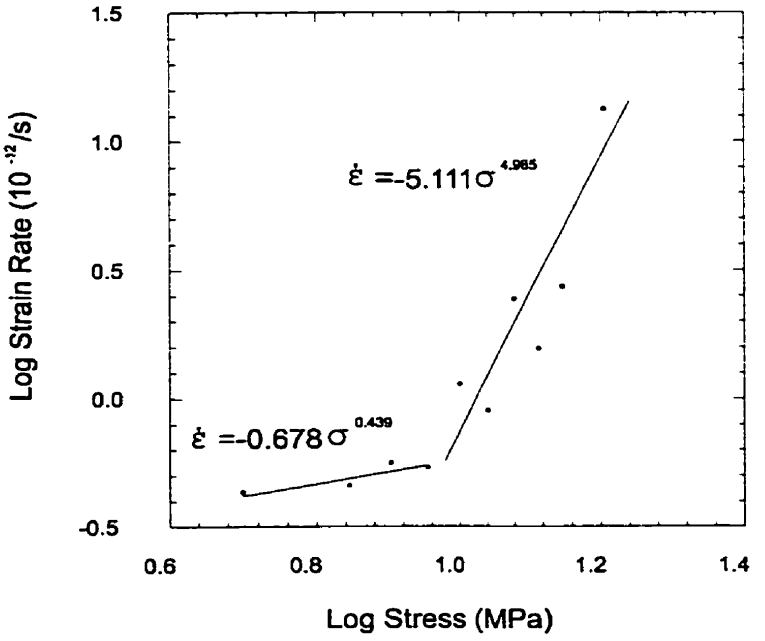


(b)

Figure 3-40. The stress dependence of the lateral strain rate; (a) the lateral strain rate for all specimen without the first load at 10, 30, 50, 70, 90 and 110 days (b) the relationship of stress and strain rate at 50 days.

Table 3-7 shows the exponent of stress of the power function of creep at different intervals. Regardless the time, the exponent is around 2.27 for the axial strain rate and 4.93 for the lateral strain rate.

Table 3-7. The exponent of stress in the power function representing the stress-strain rate relationship

| Days ⇒ | 10 | 30 | 50 | 70 |
|---|---|---|---|---|
| Strain Rate ($x10^{-12}$/s) | Exponent of stress in the power function | | | |
| Axial | 2.42 | 2.3 | 2.2 | 2.17 |
| Lateral | 4.901 | 4.879 | 4.985 | 4.94 |

## 3. 5 Summary

1. The creep strain in all the creep tests conducted on New Brunswick potash was found to be greater than the loading strain (minimum time of tests was 68 days). The average creep strain is about 60% of total strain in the axial and 70% in the lateral direction. Potash deformation is the most time dependent among all the other rock types.
2. The creep curves from this research may be characterised by two stages of time-dependent deformation: primary creep where strain attenuates rapidly with time, and a stage during which the creep strain attenuates slowly or may even appear to be constant. The change from the first to the second stage is gradual, with the first stage lasting about 20 days. The longest test NB6A at 3 MPa lasted for 298 days (Figure 3-41 and 3-42) and only in this case steady-state may have been indicated during the last 15 days. Even then, it is also possible that the instrumentation is not sensitive enough to record changes at this low load. The second and third loading phases on the same specimen, NB6B and NB6C at 5 and 8 MPa, lasted for 120 and 172 days without displaying a steady-state phase. Even though creep tests were carried out at high stress as well (NB3E at 15 MPa and NB3F at 16 MPa), tertiary strain did not appear in this study (Figure 3-43).

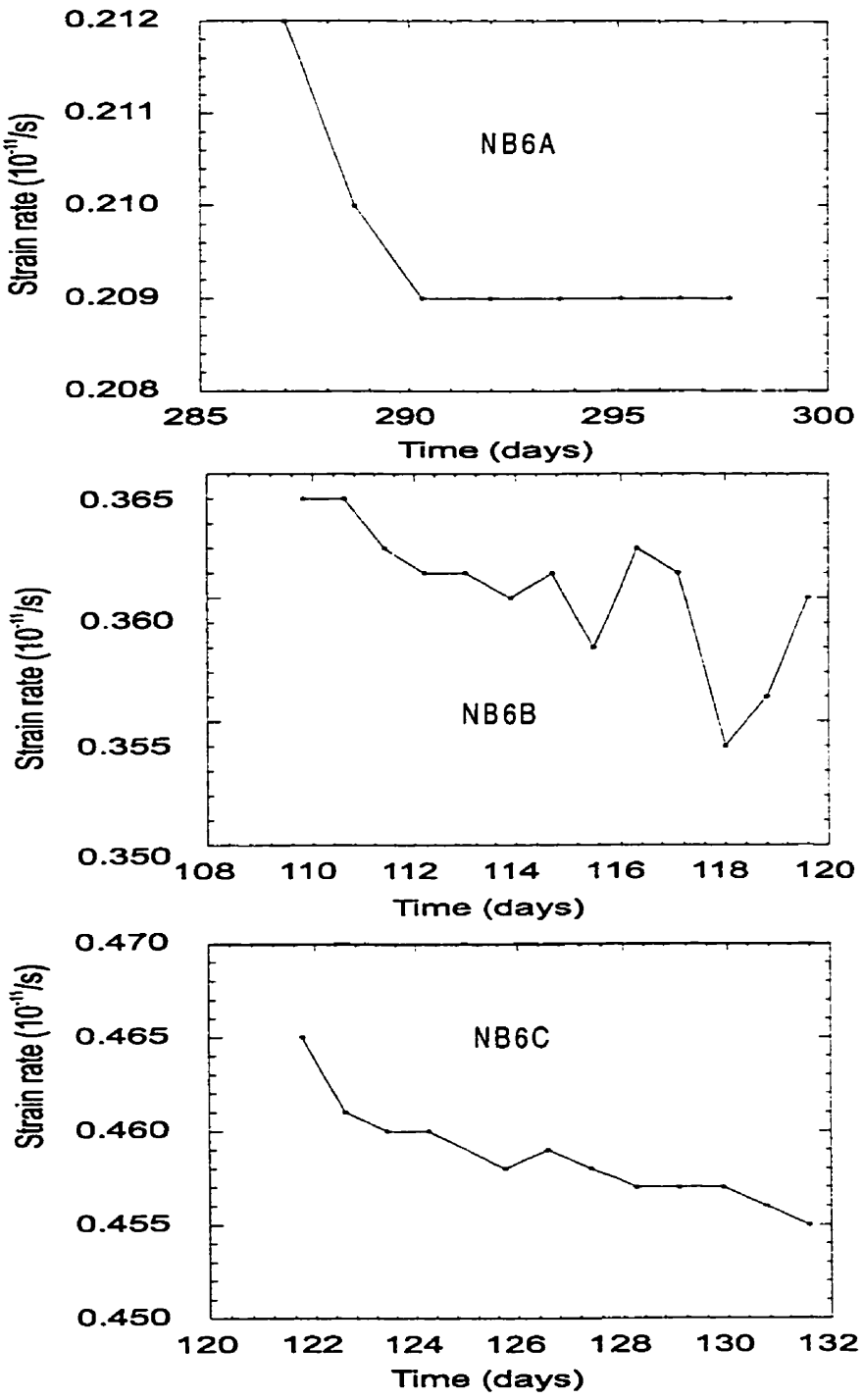


Figure 3-41. The axial strain rates; (a) 3 MPa, (b) 5 MPa and (c) 8 MPa.

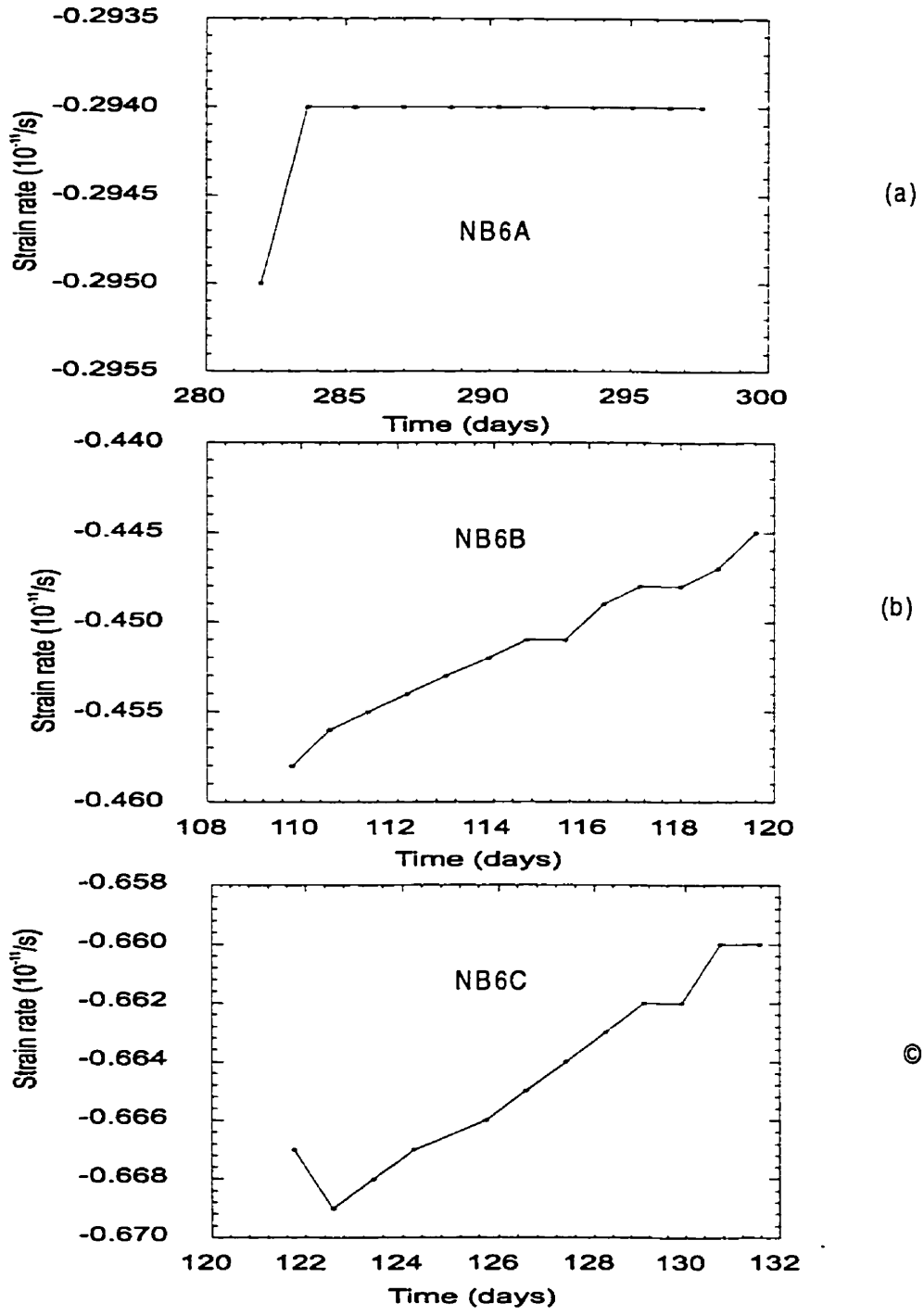


Figure 3-42. Lateral strain rate at for specimen PCA92-6; (a) NB6A at 3 MPa, (b) NB6B at 5 MPa and (c) NB6C at 8 MPa.

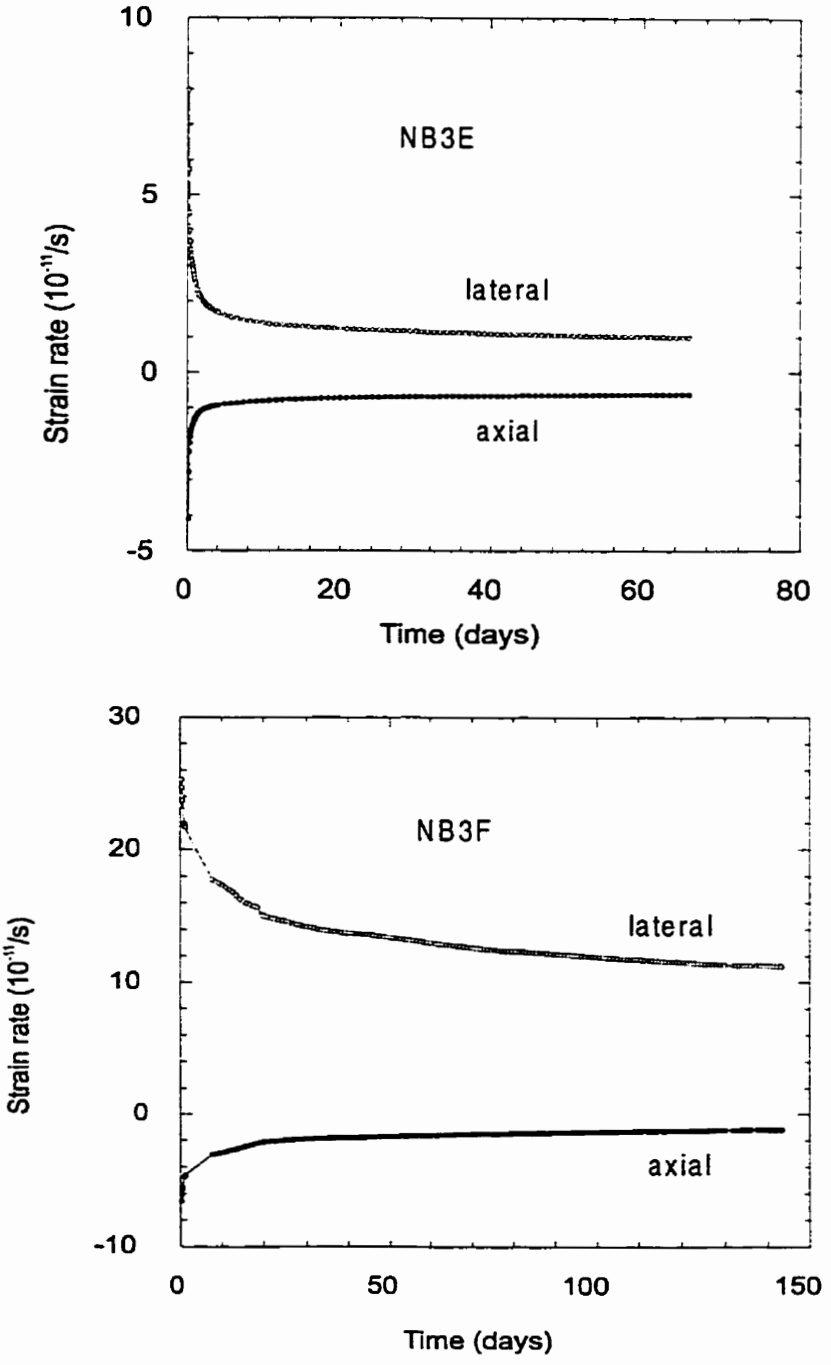


Figure 3-43. The strain rates for specimen NB3 at high stresses; (a) NB3E at 15 MPa and (b) NB3F at 16 MPa.

3. The power function seems to fit strain rate vs. stress relationships rather well. In logarithmic space, the axial strain rate shows the expected linear trend. The exponent of the stress (slope of the straight line in logarithmic space) is around 2.3. The lateral strain rate cannot be described through a simple linear relationship. At low stress, the strain rate changes but little with stress; at high stress the rate increases steeply. The bilinear interpretation of Duncan and Lajtai (1993) for Saskatchewan potash seems to apply in this case as well. The exponent of stress for the low stress line is 0.4 and 4.93 for the high stress line. The exponent changes but little with time. Practically the same exponents were found between 10 and 70 days duration. This would probably apply to longer duration as well, but little data are available in that range. The most probable reason for the need for a bilinear interpretation is that the lateral strain reflects both the plastic and the brittle strain, with the brittle strain controlling the slope of the high stress line.
4. The creep strain in response to the first loading of a new specimen is anomalously high. In contrast, the strain rates are anomalously low. Most of this "excess" strain occurs early in the test; it is almost instantaneous rather than creep strain. The cause for this is not known. It is probably due to sample disturbance.
5. Two mechanisms of deformation operate under the creep of potash: plastic and brittle. Plastic creep appears only above the yield stress. It does not, however, take place at a constant volume (Table 3-8 and Table 3-9). Below the yield stress, the volumetric strain is usually positive (compression). In two tests, however, dilation

was observed. The two exceptions were from first loading, where sample disturbance may have contributed to this behaviour. Below the yield stress, one would not expect creep deformation to occur at all. The reader is reminded however that potash is a heterogeneous material where strain is produced at many sites (different minerals and the grain boundaries between them) and possibly at different rates. Some may yield earlier than the overall yield stress, or crack at stresses below the overall crack initiation point. The low stress line of the bilinear interpretation of lateral strain rate, with its shallow slope, is probably a reflection of this pre-yield point deformation. Both the plastic and the brittle mechanisms of deformation must therefore be involved in setting the slope of the high stress line.

Table 3-8. Comparison of the volumetric strain at end of test (below yield stress)

| Specimen No. | Test No. | Constant Stress (MPa) | Duration (days) | Volumetric strain (με) | |
|---|---|---|---|---|---|
| | | | | at the beginning | at the end |
| PCA92-1M | NB1A | 4 | 102 | -100 | -430 |
| | NB1B | 7 | 68 | 80 | 110 |
| PCA92-3M | NB3A | 6 | 91 | -100 | -440 |
| PCA92-6M | NB6A | 3 | 298 | 300 | 940 |
| | NB6B | 5 | 120 | 20 | 290 |
| LS-61-19 | TP19 | 2 | 21 | 10 | 75 |
| LS-61-41 | TP41 | 1 | 21 | 10 | 60 |

Table 3-9. The volumetric strain at end of the creep test above the yield stress

| Specimen No. | Test No. | Constant Stress (MPa) | Duration (days) | Volumetric Strain (με) |
|---|---|---|---|---|
| PCA92-3M | NB3B | 9 | 171 | -700 |
| PCA92-3M | NB3C | 10 | 96 | -260 |
| PCA92-5M | NB4B | 11 | 176 | -1200 |
| PCA92-5M | NB4C | 12 | 96 | -650 |
| PCA92-2M | NB2B | 13 | 68 | -250 |
| PCA92-5M | NB4D | 14 | 172 | -1750 |
| PCA92-3M | NB3E | 15 | 71 | -4000 |
| PCA92-3M | NB3F | 16 | 143 | -4500 |

6. In the loading and creep stages of deformation, the axial and lateral strains behave differently. During the loading stage, the axial strain tends to be larger than the lateral strain, following the functional relationship of $\varepsilon_L = 1.12 \times 10^{-4} \varepsilon_A^{2.05}$. During creep, if the stress is larger than the crack initiation stress, the reverse situation exists. The lateral strain is larger than the axial strain. The creep strain follows the relationship $\varepsilon_L = 6.1 \times 10^{-2} \varepsilon_A^{1.32}$.

# CHAPTER 4

# DECREMENTED-STRESS AND REPEATED CREEP TESTS

## 4.1 Introduction

The incremented-stress path is not representative of many practical operations, such as temporary storage of petroleum products, or the isolation of nuclear waste. The process of petroleum product storage, for example, presents a series of variable loading conditions induced by the initial excavation and through subsequent stress redistribution during the filling and emptying process. The stress history will vary from location to location in the rock mass and will encompass several stress reversals.

Sensitivity of the creep to previous stress history has been noted in metal (Krempl, 1974). The influence of previous stress history has been observed to decrease with the increase in time between subsequent loading, suggesting that memory may disappear or at least fade with time.

Guessous et al (1987) indicated that the creep response of salt was strongly affected by the pre-loading history of the sample. The nature of this effect depended upon the intensity of pre-loading, and its magnitude was a function of the creep stress level.

Senseny (1984) performed some creep tests on salt rock. The specimen was initially loaded to 16 MPa for only a few minutes, then decreased to 10.3 MPa. He found that the steady-state strain rate measured was similar to those measured in experiments where the stress was held constant at 10.3 MPa for the whole test period. Therefore, he concluded that

for incremented-load experiments, the steady-state strain rate was independent of stress history and was only a function of the current stress. However, others do not support this claim. Wawersik (1982) performed creep tests on Salado salt by subjecting the specimens to a stress of 20.3 MPa before and after a creep test at the higher stress of 30.6 MPa. The duration of tests was 45, 50, and 28 days, respectively. He noted that the creep rate after the stress drop from 30.6 MPa to 20.3 MPa was only 1/10 of the rate experienced during the 20.3 MPa run before the stress drop. The problem of memory effects will be re-examined here relying on the creep tests that involved both incremented and decremented-stress procedures using the same stress levels.

## 4.2 Experimental Procedure

The experimental environment and the measuring system were the same as described in Chapter 3. The stress-decrement and the repeated tests were performed on specimens PCA92-3M (NB3) and PCA92-6M (NB6).

### 4.2.1 Creep tests under decremented-stress loading

In the NB3 series (Table 4-1) of specimen PCA92-3M, the stress-increment procedure was interrupted by reducing the load from 10 to 9 MPa. Previously to the 10 MPa series the specimen was creeping at 6 and then 9 MPa. This now provides an opportunity to compare two 9 MPa tests lasting just over 170 days, one on the increment and the other on the decrement side. The other comparable series was performed on specimen PCA92-6M (NB6). This specimen already underwent creep at 3, 5 and 8 MPa 6 months before. Now

this sequence is repeated twice, first through incrementing and then decrementing the load. The loading steps were 0 $\Rightarrow$ 3 $\Rightarrow$ 5 $\Rightarrow$ 8 $\Rightarrow$ 5 $\Rightarrow$ 3 MPa, lasting for 15, 20, 20, 24 and 26 days, respectively.

Table 4-1. Decremented-stress creep tests

| Specimen No. | Test No. | Loading condition | Constant stress (MPa) | Stress history (MPa) | Duration (Days) |
|---|---|---|---|---|---|
| PCA92-3M (NB3) | NB3A | An incremented load series through 6->9->10 MPa is interrupted with a drop in the creep load back to 9 MPa | 6 | 0 $\Rightarrow$ 6 | 91 |
| | NB3B | | 9 | 6 $\Rightarrow$ 9 | 171 |
| | **NB3C** | | **10** | 9 $\Rightarrow$ 10 | 96 |
| | **NB3D** | | **9** | 10 $\Rightarrow$ 9 | 173 |
| | NB3E | | 15 | 9 $\Rightarrow$ 15 | 71 |
| | NB3F | | 16 | 15 $\Rightarrow$ 16 | 143 |
| PCA92-6M (NB6) | NB6E | This specimen is reused now after a 6-month rest in the unloaded condition. Before the rest, it was subjected to a 3->5->8 MPa creep run | 3 | 0 $\Rightarrow$ 3 | 15 |
| | NB6F | | 5 | 3 $\Rightarrow$ 5 | 20 |
| | **NB6G** | | **8** | 5 $\Rightarrow$ 8 | 20 |
| | **NB6I** | | **5** | 8 $\Rightarrow$ 5 | 24 |
| | **NB6J** | | **3** | 5 $\Rightarrow$ 3 | 26 |

### 4.2.2 Repeated creep tests

Repeated creep tests, tests using the same uniaxial load (Table 4-2), were carried out on two specimens: PCA92-3M (NB3) and PCA92-6M (NB6). The original creep test of the NB3 series (NB3A) was performed under a uniaxial stress of 6 MPa and this was repeated in NB3H. Between these two tests, the specimen underwent additional creep tests with the full load path being 6->9->10->9->15->16 MPa. After the last, the 16 MPa test, the specimen was unloaded for 6 months and then reloaded to 6 MPa for 7 days (NB3H) then to 15 MPa (NB3I) for 10 days. During the unloading period, the specimen was stored in the same temperature and humidity environment as during the creep test. From this creep series, come two repeated tests, one at 6 and the other at 15 MPa.

In the NB6 test series (already described under stress-decremented creep tests) repeated creep tests are available at 3, 5 and 8 MPa. This specimen was initially subjected to a 3->5->8->0 MPa load path during tests NB6A, NB6B and NB6C. Similarly to creep series NB3, the NB6 specimen was unloaded after the 8 MPa test for 6 months and kept without load in the standardised creep environment. Through this series, there are three tests at 3 and 5 MPa and two at 8 MPa.

Because of the 6 month time delay involved between subsequent loading for some procedures but not for others, there is also a chance to throw some light on the presence or absence of the memory effect suggested by Kremple (1974).

Table 4-2. The repeated creep tests

| Specimen No. | Test No. | Test condition | Constant Stress (MPa) | Stress History (MPa) | Duration (Days) |
|---|---|---|---|---|---|
| PCA92-3M (NB3) | *NB3A* | Original Test | *6* | 0 ⇒ 6 | 91 |
| | **NB3E** | | **15** | 6 ⇒ 9 ⇒ 10 ⇒ 9⇒ 15 | 71 |
| | 6 month of rest in unloaded condition | | | | |
| | NB3H | Repeated Test | *6* | 0 ⇒ 6 | 7 |
| | **NB3I** | | **15** | 6 ⇒ 15 | 10 |
| PCA92-6M (NB6) | NB6A | Original Test | *3* | 0 ⇒ 3 | 298 |
| | **NB6B** | | **5** | 3 ⇒ 5 | 120 |
| | NB6C | | 8 | 5 ⇒ 8 | 132 |
| | 6 month of rest in unloaded condition | | | | |
| | NB6E | Repeated Test | *3* | 0 ⇒ 3 | 15 |
| | **NB6F** | | **5** | 3 ⇒ 5 | 20 |
| | NB6G | | 8 | 5 ⇒ 8 | 20 |
| | **NB6I** | | **5** | 8 ⇒ 5 | 24 |
| | NB6J | | *3* | 5 ⇒ 3 | 26 |

## 4.3 Experimental Results

### 4.3.1 Decremented-stress creep test on specimen NB3

The loading history of specimen NB3 is shown in Figure 4-1(a). Figure 4-1(b) gives the axial strain, while Figure 4-2 (b) shows the changes in the lateral strain with time. Figure 4-3 and Figure 4-4 shows the axial, lateral and volumetric strains for the 9->10->9 MPa sequence (NB3B, NB3C and NB3D). Both 9 MPa tests lasted about 170 days. From Table 4-3, the axial and the lateral strains of NB3D (second 9 MPa) are only 12% and 10% of those measured at the end of NB3B (first 9 MPa run). Similar change is observed in the volumetric strains. Figure 4-5 and 4-6 shows the strain rates. In contrast to the amount of creep strains, the axial and the lateral strain rates increased significantly during the second 9 MPa run with respect to the first 9 MPa run. At the end of the second 9 MPa test, the axial strain rate increased to 3 times and the lateral to 5 times of the rates experienced during the first 9 MPa run.

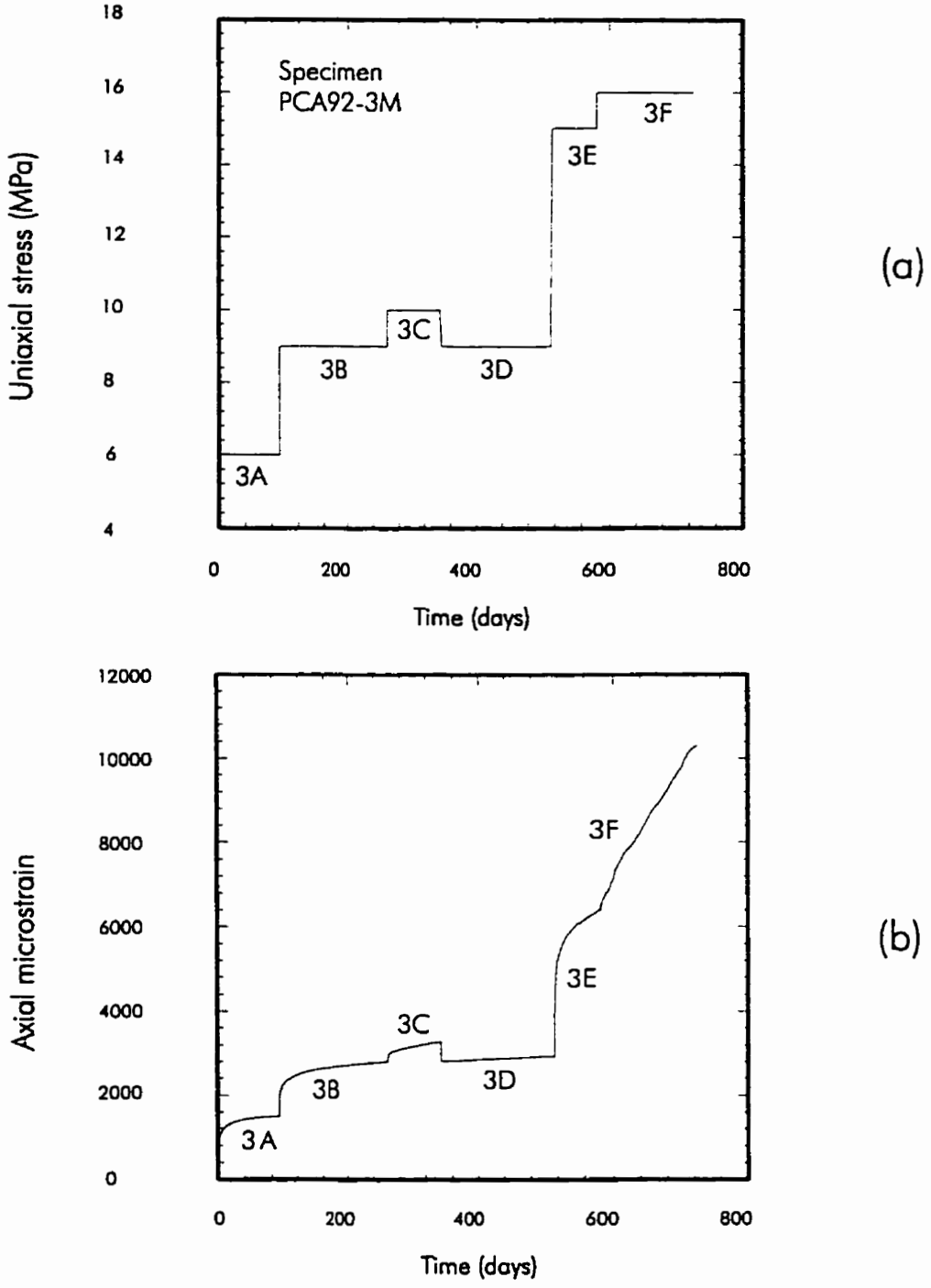


Figure 4-1. Specimen PCA92-3M; (a) stress history (b) axial strain.

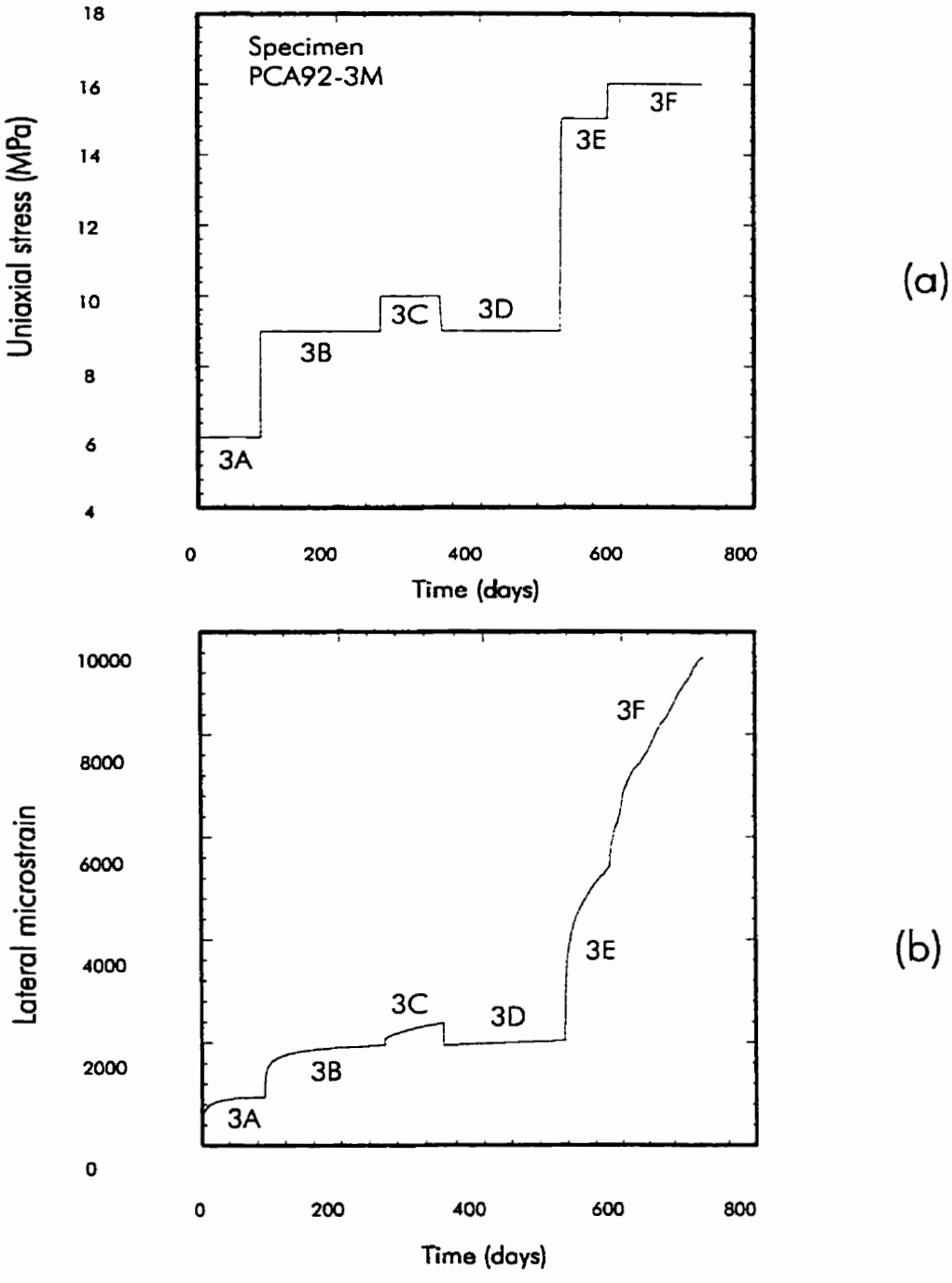


Figure 4-2. Specimen PCA92-3M; (a) stress history (b) lateral strain.

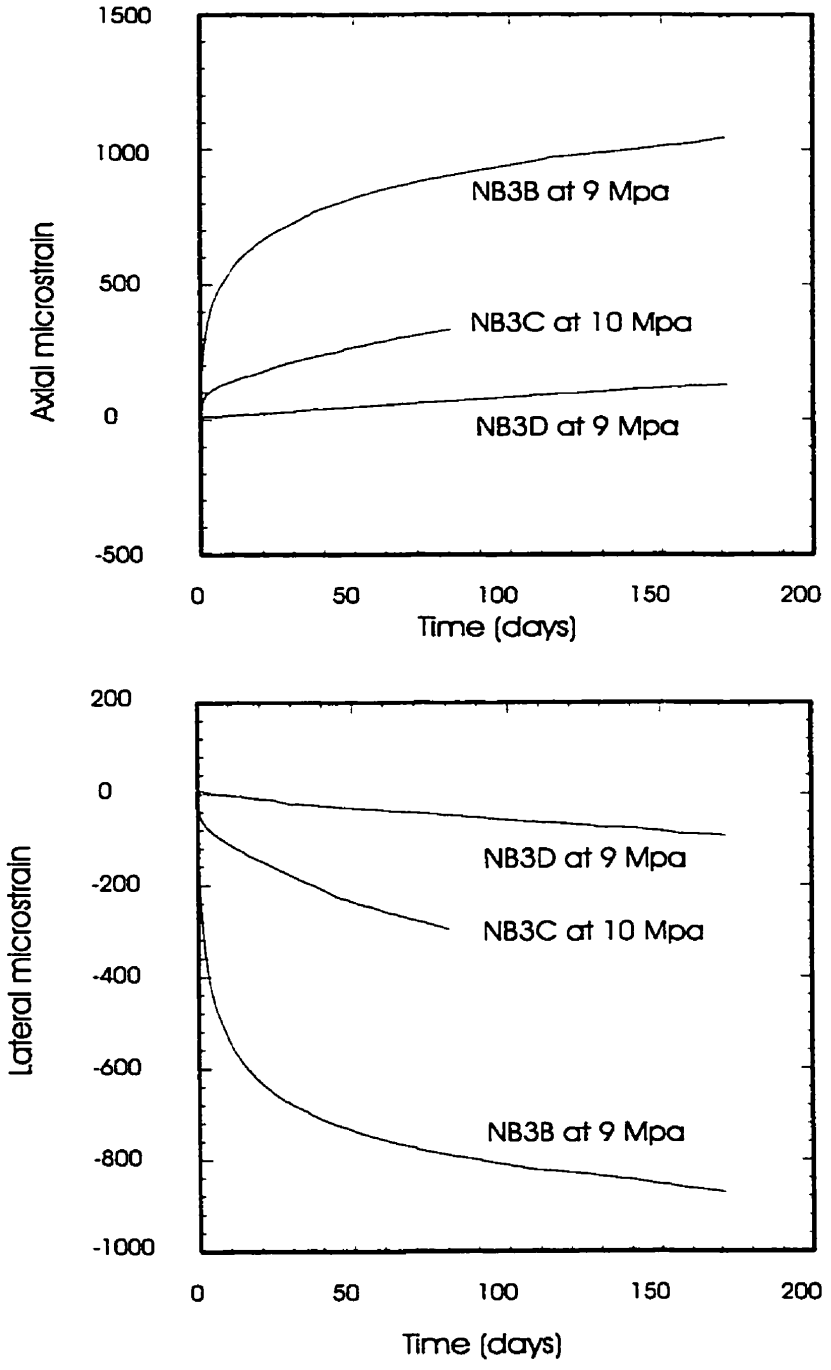


Figure 4-3. Strain for NB3B, NB3C and NB3D; (a) axial and (b) lateral.

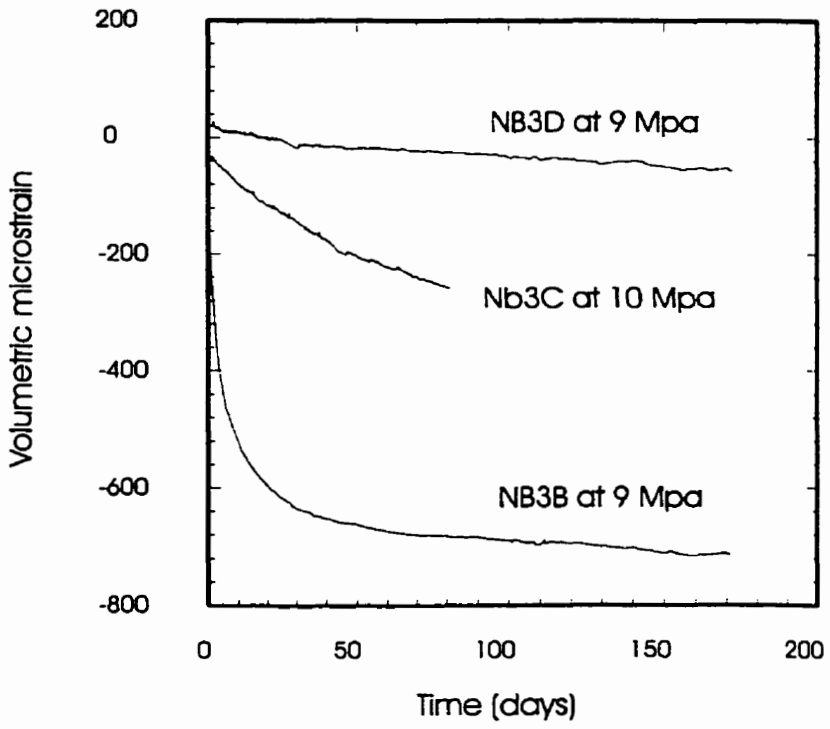


Figure 4-4. Volumetric strain for NB3B(9 MPa), NB3C(10 MPa) and NB3D(9 MPa).

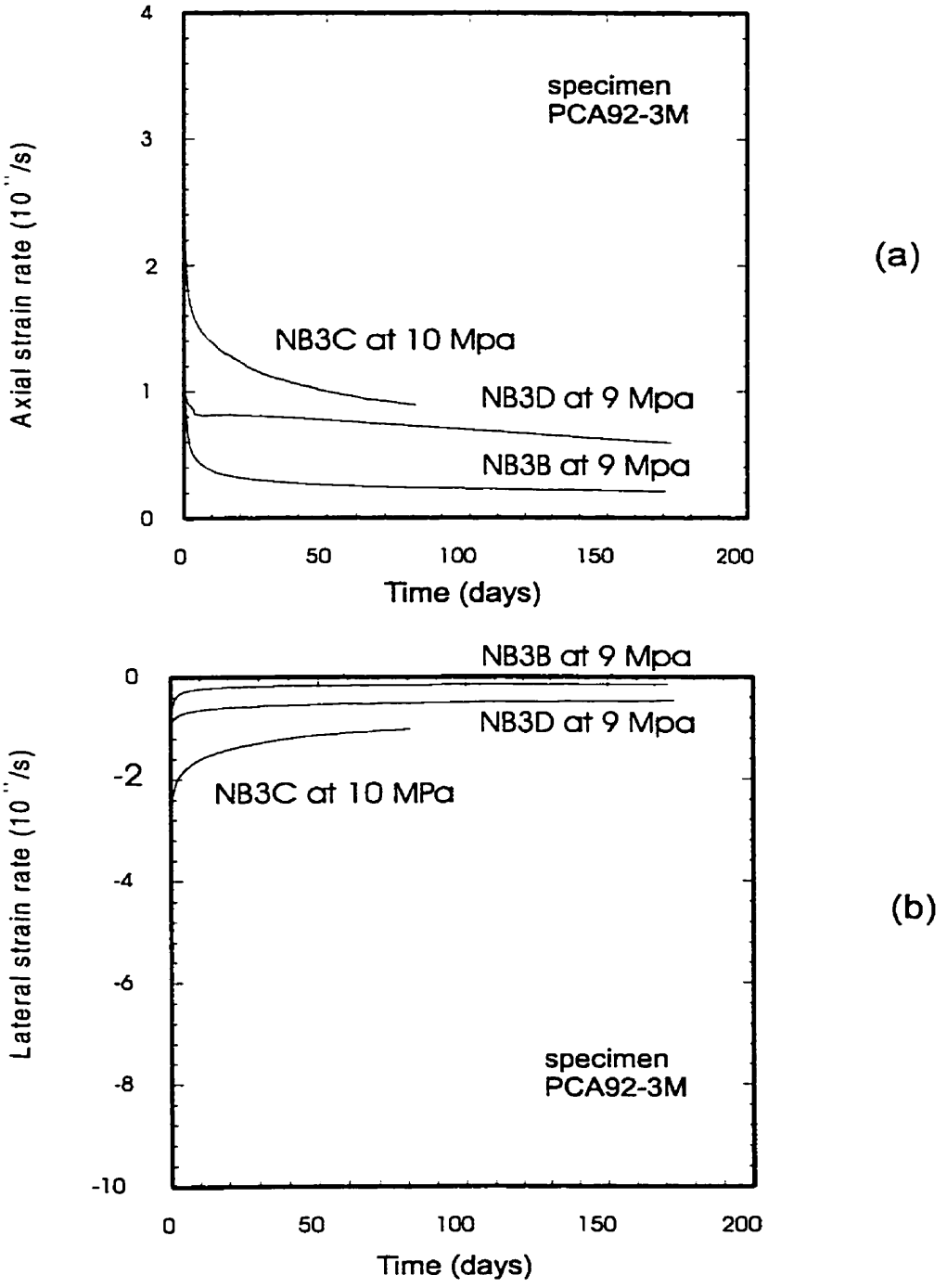


Figure 4-5. Strain rate for NB3B, NB3C and NB3D; (a) axial and (b) lateral.

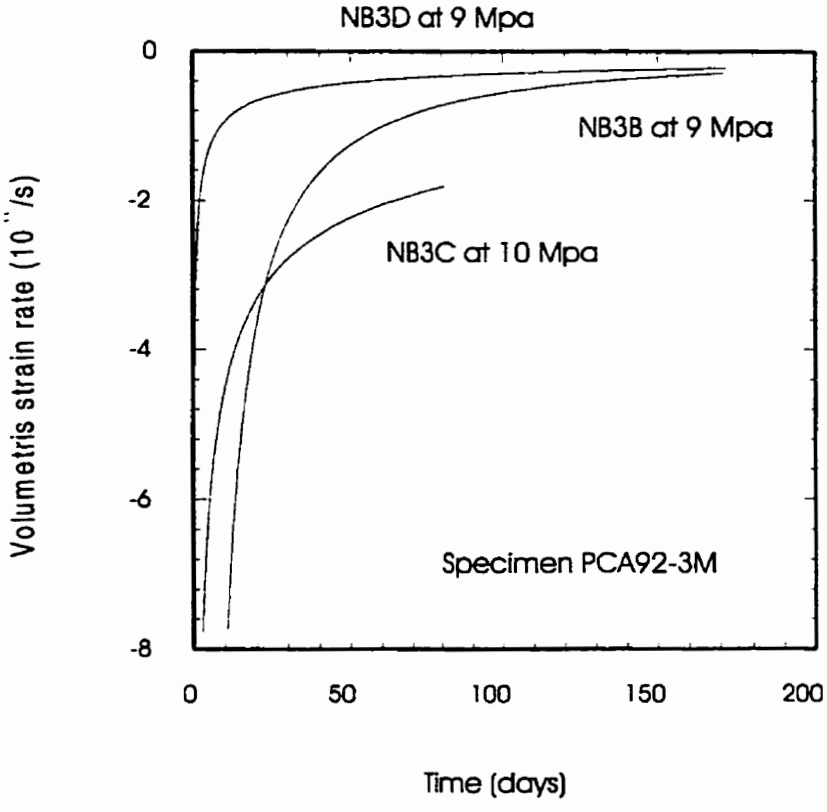


Figure 4-6. Volumetric strain rate for NB3B, NB3C and NB3D.

**Decremented-stress test on specimen NB6**

This specimen had a stress history of 0->3->5->8->0 (6 months delay) 0->3->5->8->5->3->0 (Figure 4-7(a)). The axial, lateral and volumetric strains for the sequence subsequent to the 6-month delay were plotted against time in Figure 4-7(b) and Figure 4-8. Similarly to the NB3 experience, the symmetrically decremented stresses generated less strain than the incremental stresses in both axial and lateral directions. However, the gap between corresponded strain values is substantially less. Comparing the strain values (Table 4-3 and 4-4) for the tests following the 6-month rest, the axial and the lateral strains of NB6I (second 5 MPa) are 89% and 86% of those measured at end of NB6F (first 5 MPa). The axial and lateral strains of NB6J (second 3 MPa) are 24% and 58% of those measured at end of NB6E (first 3 MPa). Figure 4-9 and 4-10 shows the strain rates. Similarly to the experience with specimen NB3, the axial and the lateral strain rates of second loading at 3 and 5 MPa (NB6I and NB6J) are larger those of the first loading at 3 and 5 MPa (NB6E and NB6F). The axial strain rates of the 5 MPa test increased at end of the test 2 times and the lateral 2.5 times. For 3 MPa, the axial and the lateral strain rates did not change at all (Table 4-4).

Comparing now the tests involved in the two incremented-stress legs separated by the 6-month rest, evidence is found for the "fading memory" and this will be discussed in the following section.

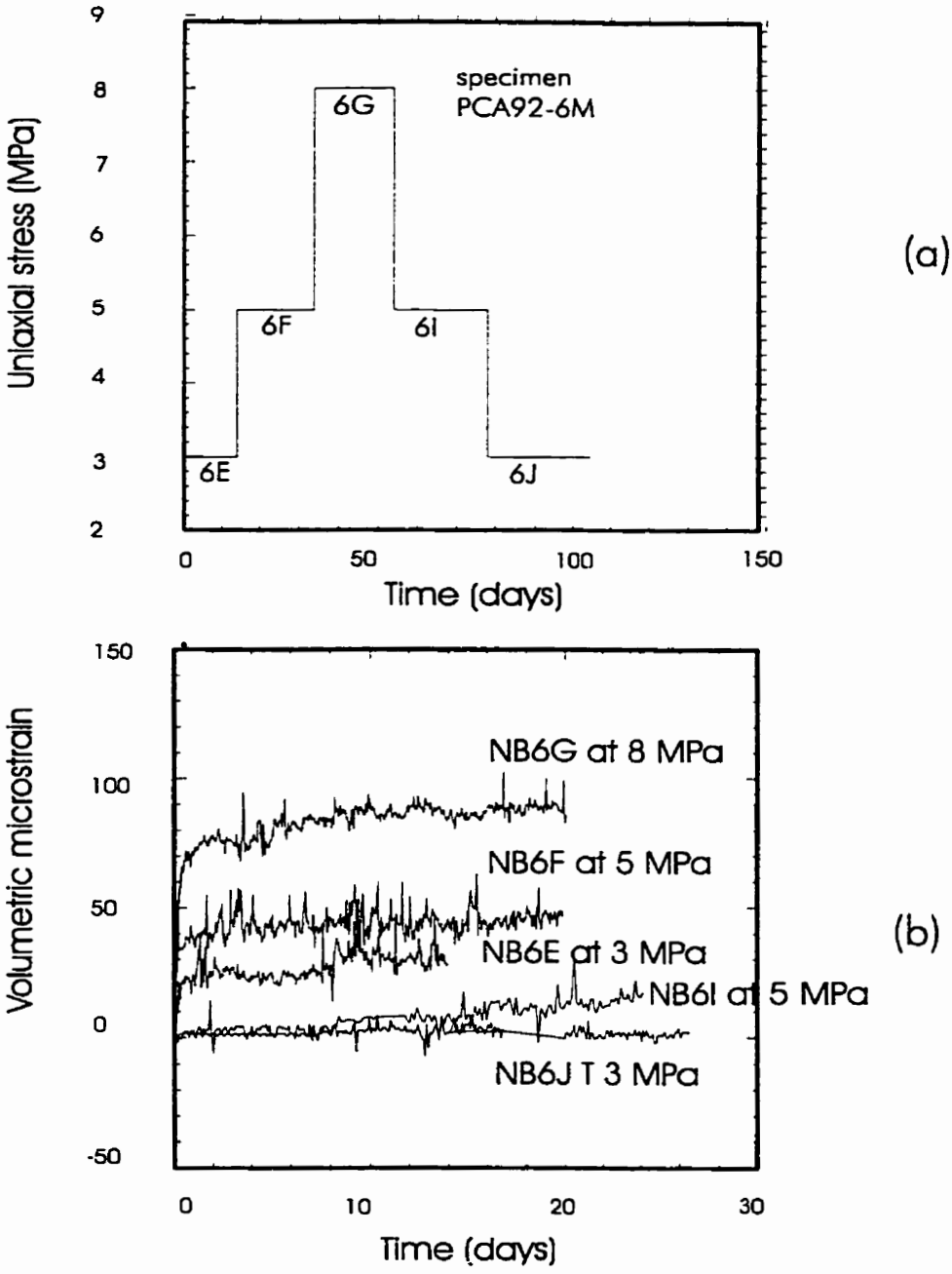


Figure 4-7. Specimen PCA92-6M; (a) stress history and (b) volumetric strain.

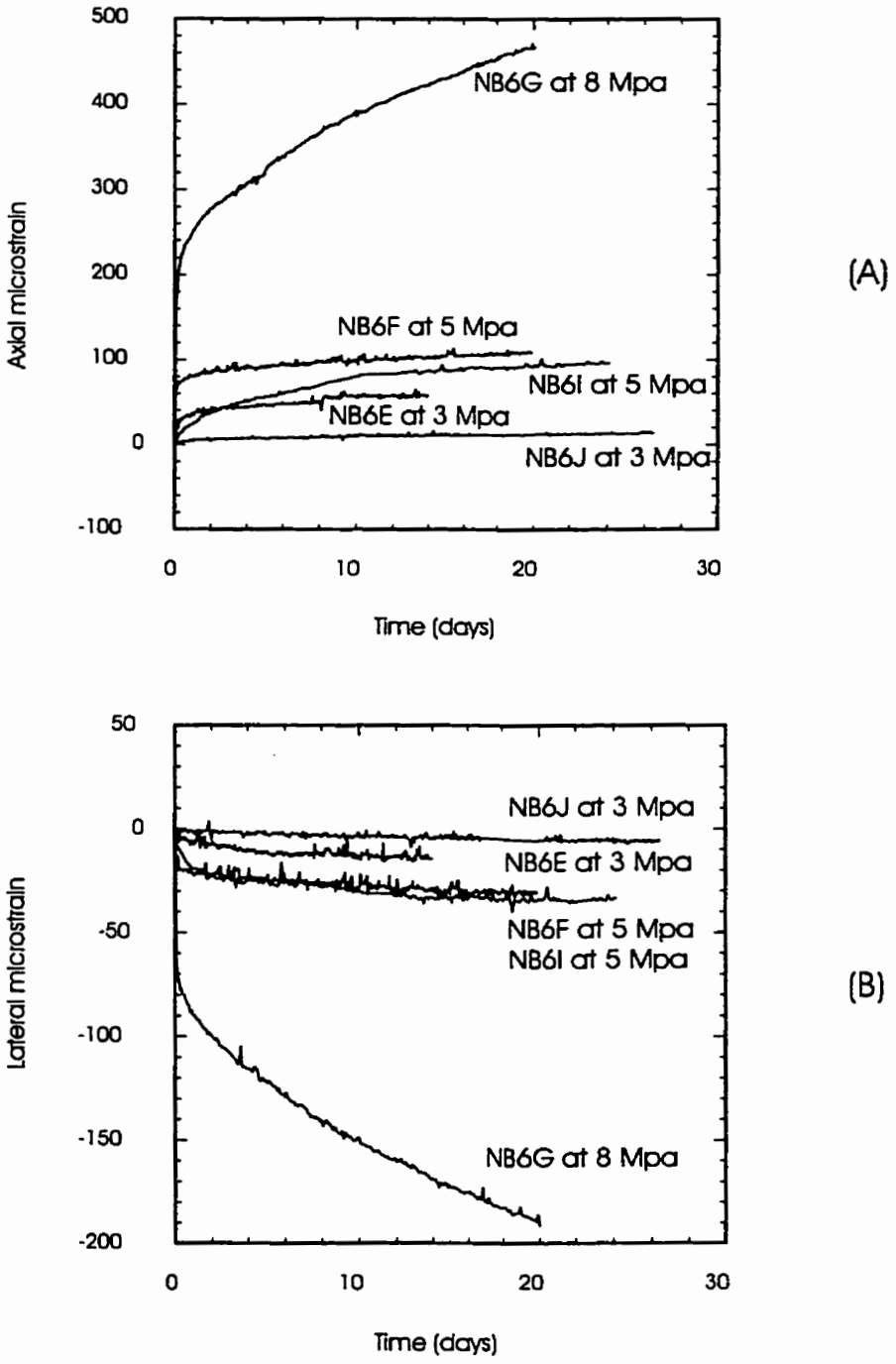


Figure 4-8. Axial and lateral strains for NB6E, NB6F, NB6G, NB6I and NB6J using different stress path; (a) axial and (b) lateral.

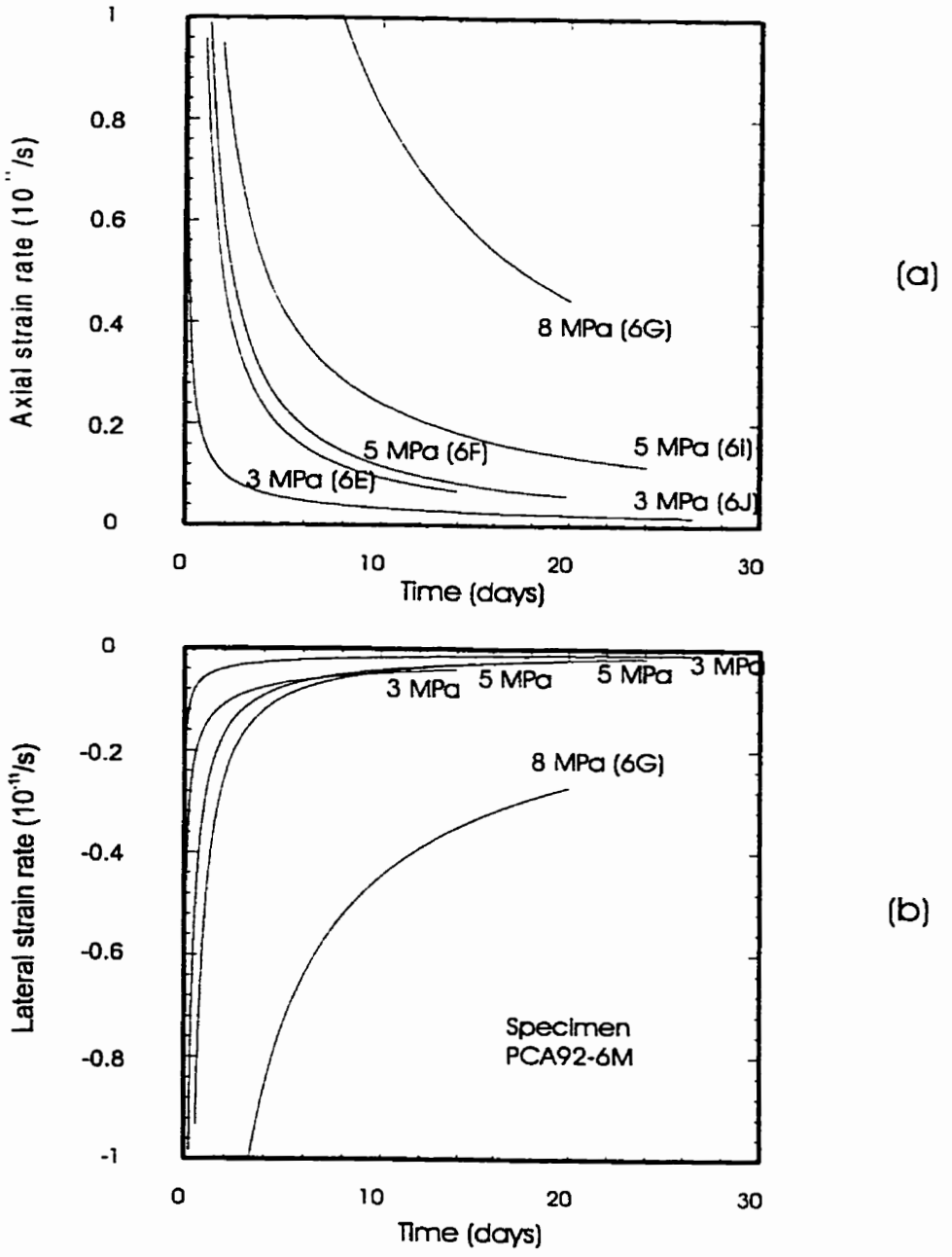


Figure 4-9. Strain rate for specimen PCA92-6M; (a) axial and (b) lateral.

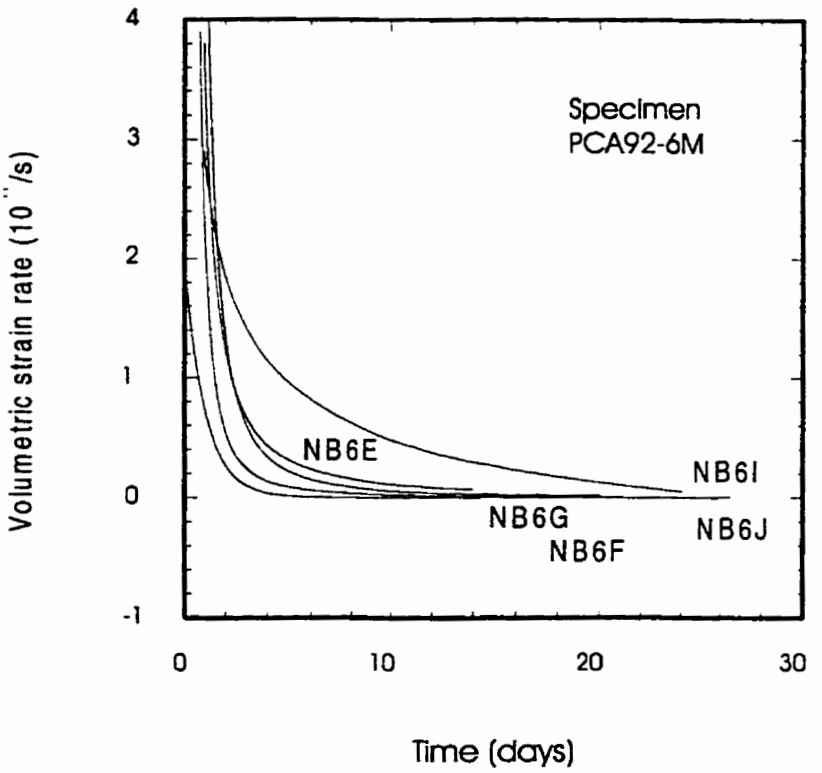


Figure 4-10. Volumetric strain rate for specimen PCA92-6M.

Table 4-3. Strain rates (at end of test) in the decremented-stress creep tests

| Test No. | Constant Stress (MPa) | Elapsed Time (Days) | Axial Strain (με) | Lateral Strain (με) | Axial strain Rate ($10^{-12}$/s) | Lateral strain Rate ($10^{-12}$/s) |
|---|---|---|---|---|---|---|
| NB3B | 9 | 171 | 1045 | 870 | 2.32 | 1.16 |
| **NB3C** | **10** | 96 | **340** | **300** | **10.44** | **11.6** |
| **NB3D** | **9** | 171 | **125** | **90** | **6.96** | **5.8** |
| NB6E | 3 | 15 | 54 | 12 | 0.23 | 0.11 |
| NB6F | 5 | 20 | 110 | 35 | 0.7 | 0.23 |
| **NB6G** | **8** | 20 | **335** | **141** | **4.87** | **3.25** |
| **NB6I** | **5** | 20 | **98** | **30** | **1.39** | **0.58** |
| **NB6J** | **3** | 15 | **13** | **7** | **0.23** | **0.11** |

Table 4-4. Comparing strains and strain rates during the incremented and the decremented-stress legs in ratio form (decremented/incremented)

| Specimen No. | Constant Stress (MPa) | Axial strain | Lateral strain | Axial Strain rate | Lateral Strain rate |
|---|---|---|---|---|---|
| NB6 | 3 | 0.24 | 0.58 | 1.0 | 1.0 |
| | 5 | 0.89 | 0.86 | 2 | 2.5 |
| NB3 | 9 | 0.12 | 0.10 | 3 | 5 |

### 4.3.2 Repeated creep tests on specimen NB6

The NB6 creep series has two 3->5->8 series separated by a 6-month rest period. In Figure 4-11, the axial and the lateral strains obtained from the before-rest creep tests (NB6A, NB6B, and NB6C) described in 3.3.5 are compared with those obtained from the after rest 3->5->8 series (NB6E, NB6F, NB6G). The data are compared at 15 days for NB6A and NB6E and at 20 days for NB6B, NB6C, NB6F and NB6G (Figure 4-11). The repeated creep tests produced less axial and lateral strains. Figure 4-12 and Figure 4-13 shows the strain rates. The strain rate for the repeated creep test (after the 6-month rest) is lower than that belonging to the first, original test (Table 4-5). This can now be contrasted with the repeated tests of the decreasing-stress leg of NB6I and NB6J. The later tests here show higher strain rates.

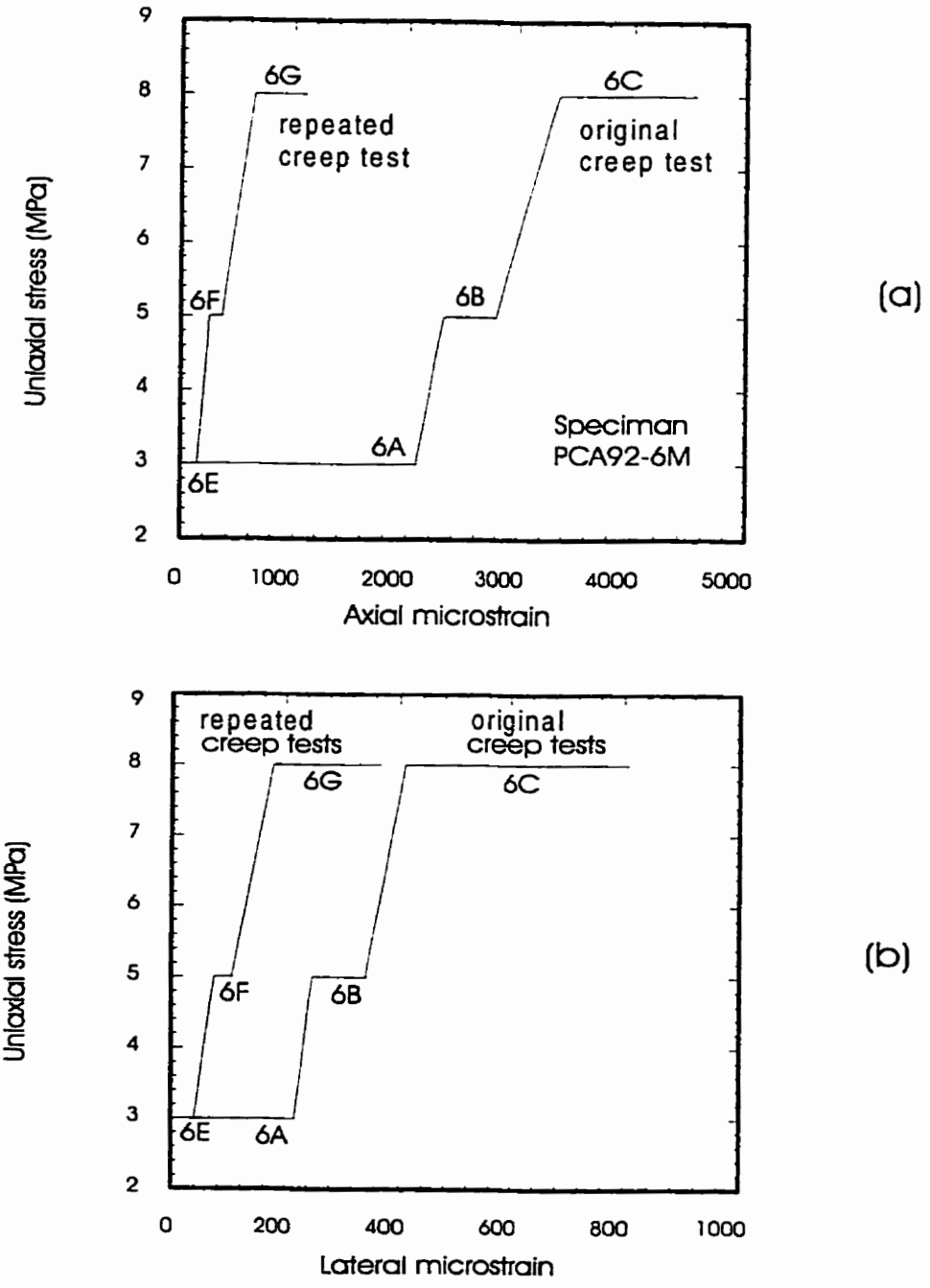


Figure 4-11. Summary plots of original and repeated creep tests for specimen PCA92-6M; (a) the axial strain and (b) the lateral strain.

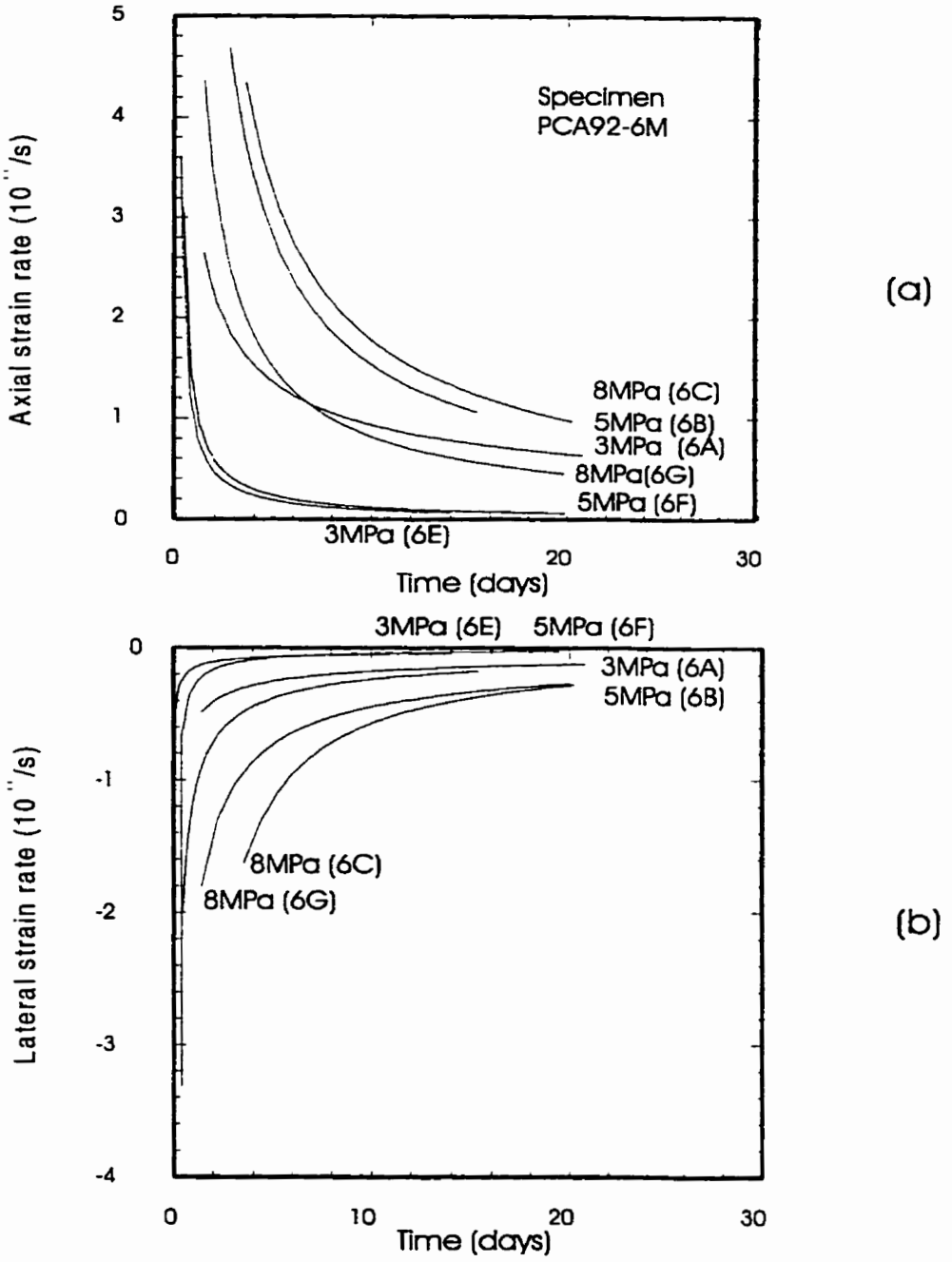


Figure 4-12. Strain rates for specimen PCA92-6M subjected to 0⇒3⇒5⇒8⇒5⇒3⇒0 MPa stress path; (a) axial and (b) lateral.

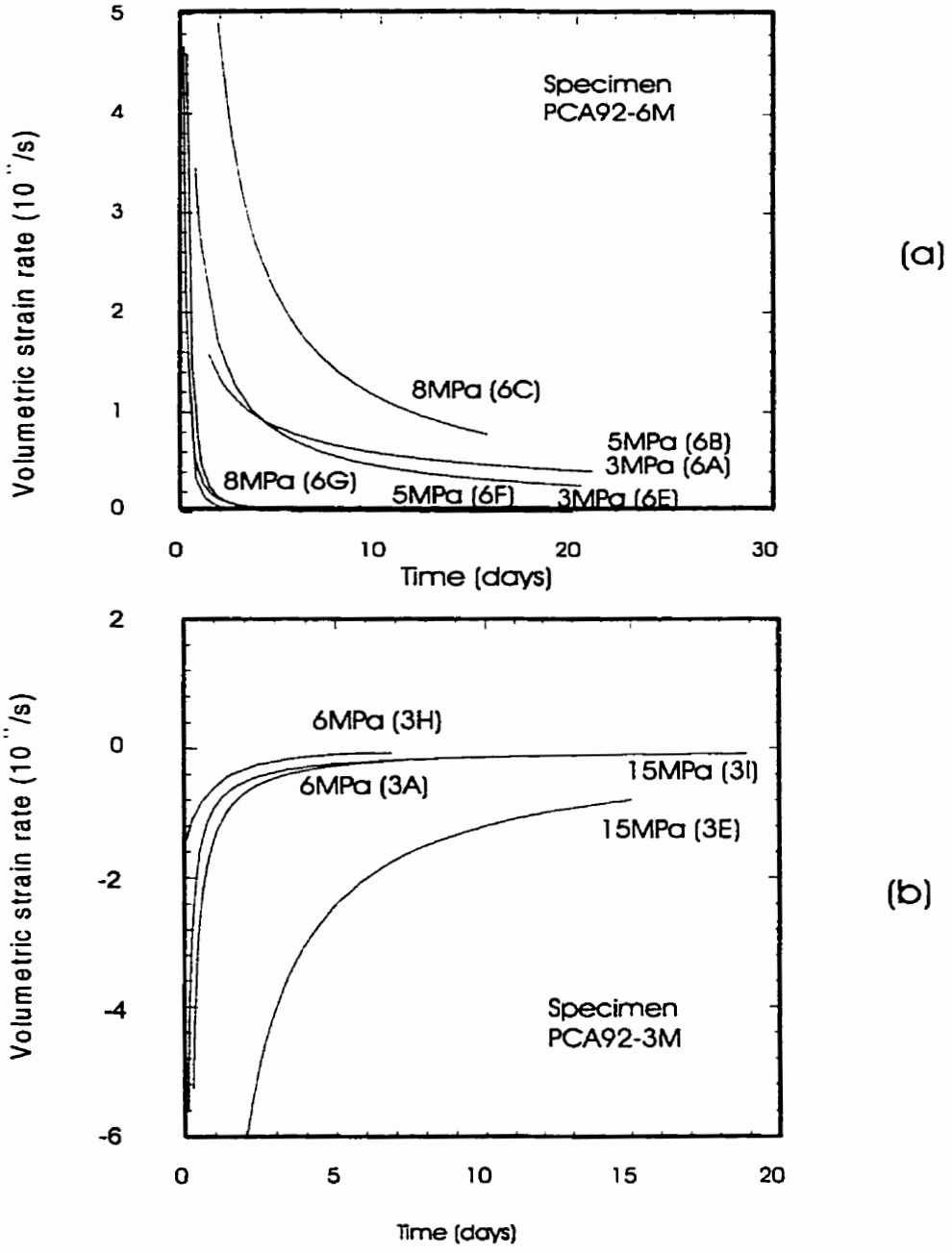


Figure 4-13. Volumetric strain rates for the original and the repeated tests; (a) specimen PCA92-6M and (b) specimen PCA92-3M.

Table 4-5. Comparison of strains and strain rates (at end of test) in the repeated creep tests

| Test No. | Constant Stress (MPa) | Elapsed Time (Days) | Axial Strain (με) | Lateral Strain (με) | Axial Strain Rate ($10^{-12}$/s) | Lateral Strain Rate ($10^{-12}$/s) |
|---|---|---|---|---|---|---|
| NB3A | **6** (0 ⇒ 6) | 7 | 610 | 339 | 2.32 | 1.74 |
| NB3H* | **6** (0 ⇒ 6) | 7 | 100 | 32 | 0.34 | 0.21 |
| NB3E | **15** 0 ⇒ 6 ⇒ 9 ⇒ 10 ⇒ 9⇒ 15 | 10 | 1967 | 2120 | 9.28 | 16.24 |
| NB3I* | **15** (0 ⇒ 6 ⇒ 15) | 10 | 400 | 430 | 5.8 | 2.32 |
| NB6A | ***3*** (0 ⇒ 3) | 15 | 758 | 83 | 4.87 | 4.06 |
| NB6E* | ***3*** (0 ⇒ 3) | 15 | 54 | 12 | 0.23 | 0.11 |
| NB6J | ***3*** (8 ⇒ 5 ⇒ 3) | 15 | 13 | 7 | 0.23 | 0.11 |
| NB6B | ***5*** (0 ⇒ 3 ⇒ 5) | 20 | 160 | 40 | 9.28 | 6.73 |
| NB6F* | ***5*** (0 ⇒ 3 ⇒ 5) | 20 | 110 | 35 | 0.7 | 0.23 |
| NB6I | ***5*** (8 ⇒ 5) | 20 | 98 | 30 | 1.39 | 0.58 |
| NB6C | **8** (0 ⇒ 3 ⇒ 5 ⇒ 8) | 20 | 550 | 200 | 7.54 | 8.12 |
| NB6G* | **8** (0 ⇒ 3 ⇒ 5 ⇒ 8) | 20 | 335 | 141 | 4.87 | 3.25 |

* after 6 month rest in unloaded condition

**Repeated tests on specimen NB3**

Figure 4-14 shows summary plots of the axial (a) and the lateral (b) strain from the original creep tests (NB3A and NB3E) and the repeated creep tests (NB3H and NB3I) on the same specimen NB3. A six-month rest is involved between the two sets. The data plotted in Figure 4-14 refers to 7 days for NB3A and NB3H, and 10 days for NB3E and NB3I. These plots show a similar trend to that described for specimen NB6. Figure 4-15 shows the axial and the lateral strain rates. Similar results were obtained for NB3. If a 6-month rest period is involved, the strain rates are lower in the later tests (Table 4-5). If no rest period is involved it is the later tests that have the higher rates.

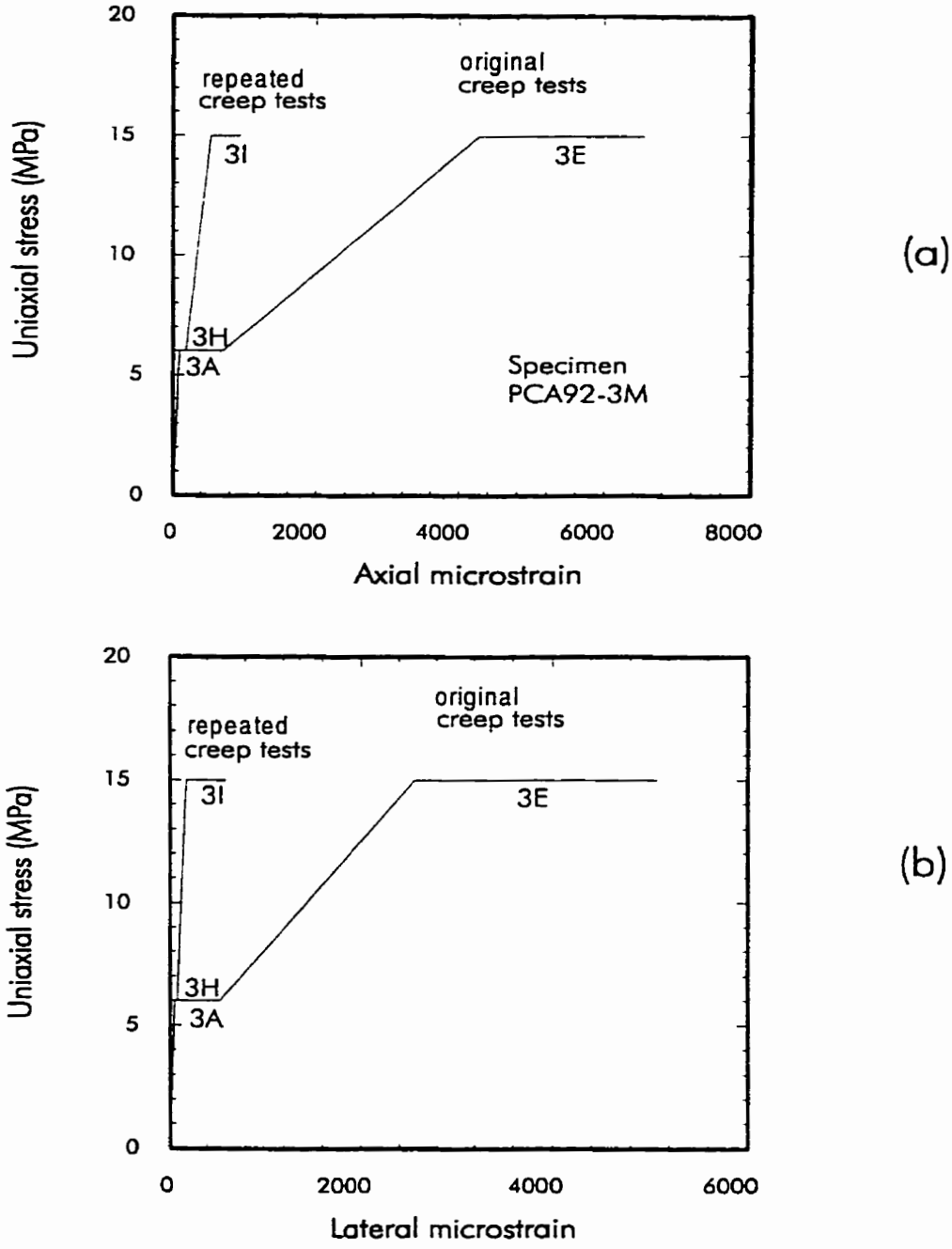


Figure 4-14. A summary plots of the original and the repeated tests for specimen PCA92-3M; (a) axial and (b) lateral.

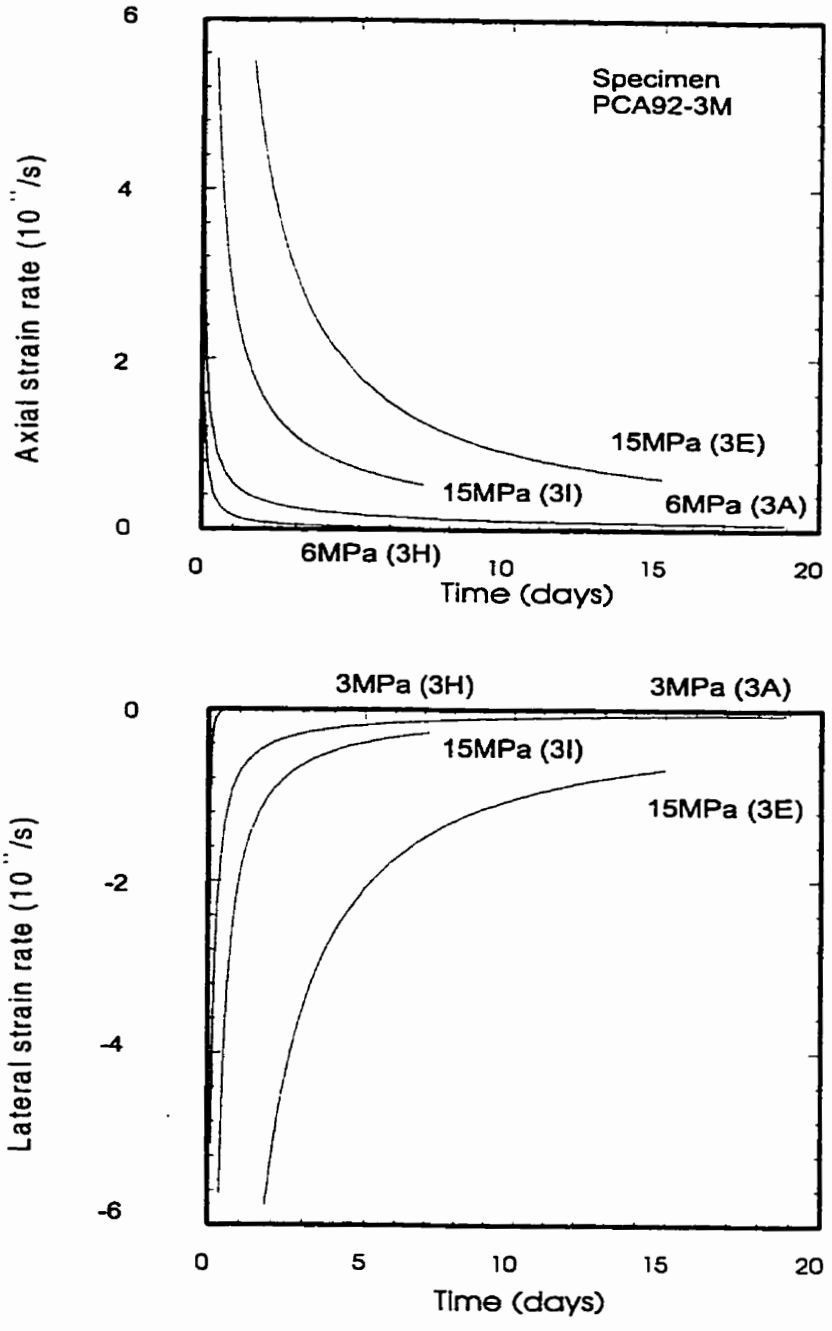


Figure 4-15. Strain rates for specimen PCA92-3M for the original and the repeated tests; (a) axial and (b) lateral.

## 4.4 Discussion of Experimental Results

### 4.4.1 Deformation in decremented-stress creep tests

The axial, lateral and volumetric strains measured from three decremented-stress creep tests are illustrated in Table 4-3 and Figures 4-1, 4-2, 4-3, 4-4 (specimen NB3), 4-7 and 4-8 (specimen NB6). Serving as a reference, the corresponding strains of the incremented-stress tests are presented in the same Figures. The experimental results show that the strains and the strain rates through a stress-increment and a stress-decrement procedure with the same load-path are not the same. The strains obtained in subsequent loading in the stress-increment run are larger than those obtained though a stress-decrement series. The strain rates are just the opposite. The rates obtained though a stress-decrement procedure are higher than those in a stress-increment procedure. The difference in strains and strain rates between the two procedures increases with stress. It is smaller when the stress is less than about 8 MPa and increases above this.

Figure 4-5 shows the data obtained from specimen NB3, which was subjected to 9 MPa before and after an intermediate loading stage of $\sigma$ = 10 MPa. The creep rate at 9 MPa after the stress decrement from 10 to 9 MPa is substantially higher than it was before the stress increment to 10 MPa. This observation is not consistent with the results reported by Senseny (1984). Senseny claimed that the steady-state strain rate is independent of stress history and is a function of the current stress only. But both Wawersik's (1982) and our results show that the strain rate depends on the stress history.

The stress-increment/decrement series of NB3 and NB6 come from a continuous loading series; there was no rest period between the incremented and decremented stress

legs of the loading path. The conclusions reached above must therefore be treated with caution. The decremented-stress leg could still be under the influence of structural changes that occurred during the earlier incremented-stress leg. If a rest period were inserted, the memory could have faded and the results could have been quite different.

### 4.4.2 Deformation in repeated creep tests

The axial and lateral strains produced though a repeated creep test (Figure 4-11 and 4-14) are always smaller than the strains obtained in the original test. How the strain rates react is somewhat more complicated (Figures 4-12, 4-13, 4-15 and Table 4-3 and 4-5). When the repeated tests (NB3H, NB3I, NB6E, NB6F and NB6G) follow a 6 month rest period in an unloaded condition, the measured strain rates in the repeated test are less than those recorded in the original test (NB3A, NB3E, NB6A, NB6B and NB6C). When the creep test is repeated (NB3D and NB6I) without unloading, the strain rate in the repeated test is higher than in the original test (NB3B and NB6F). Clearly, a memory-effect is indicated here. The tested specimen seems to have some ability to recover with time. However, the nature and extent of this recovery have not been investigated yet.

## 4. 5. Chapter summary

1. The strains and strain rates at the same creep stress, but produced through incremented-stress and decremented-stress procedures are not necessarily the same. If the decremented stress leg follows the incremented stress leg without interruption (no unloading and rest), both the axial and the lateral strains are lower and the corresponding strain rates higher during the decremented stress leg. The difference in strains and strain rates between the two procedures are smaller when the stress is less than about 8 MPa, but the gap increases substantially above this. If there is a rest period separating the increment and decrement sides a "fading-memory" effect could produce different, but presently unknown results.
2. The results of the stress-increment and stress-decrement procedures are not consistent with the claim of Senseny (1984) that the strain rate is independent of the loading path, but consistent with the findings of Wawersik (1982). According to Wawersik and the present study, the strain rate depends on the stress history.
3. The strain produced though a repeated creep test is always smaller than the strain of the original test. However, the strain rate follows a different trend. When the repeated test follows a 6-month rest at no stress, the strain rate is less than in the original test. When there is no rest between the two repeated creep tests, the strain rate is higher in the repeated than in the original test. A memory effect is indicated.

# CHAPTER 5

# CONCLUSIONS AND RECOMMENDATIONS

## 5.1 Conclusions

The purpose of this work was to investigate the characteristics of creep in New Brunswick potash and Thailand potash. This was achieved by loading cylindrical specimens through various stress paths in a constant temperature and humidity environment and under uniaxial compressive stresses ranging from 3 to 16 MPa, with loading periods lasting between 7 and 298 days. Most of the data come from incremented-stress procedures using the same specimen. There were, however, a few decremented-stress steps and a number of creep tests were repeated using the same load.

The experiments have demonstrated that salt rocks are sensitive to time effects. The average creep strain is about 60% of total strain in the axial and 70% in the lateral direction.

The creep curves produced through this study may be characterised by two stages: an early stage during which the strain rate attenuates rapidly. This phase lasts about 20 days. During the second phase the strain rates still attenuates, but the rate of change is quite small. By definition both phases are part of the primary stage of creep. No strong case can be made for the existence of steady-state creep either in the axial or the lateral direction. The only arguable case is NB6A with a creep load of 3 MPa and test duration of 298 days. After about 3 months of testing, the measured strain rate was relatively constant, but very small, close to the resolution of the measuring system. The tertiary stage did not appear in this

study and none of the specimens failed. Tests were usually terminated after the strain sensors became inoperative.

Although there is creep at any stress, the amount of time-dependent strain increases rapidly above the yield point around 8 MPa. Until cracking is initiated around 12 MPa, most of the strain occurs in the axial direction. Above the crack initiation point, lateral dilatancy, brought on by axial microcracking, dominates the creep process.

In all the stress-increment procedures, the first step in the loading path yields anomalously high strains, strains that are always higher than those produced during the second and sometimes the third loading step. The cause for this is not quite clear. It may be due to stress effects accumulated by the rock during its natural life (both stressing and stress relief) and to sample disturbance during sample retrieval and preparation.

Because no steady-state creep was observed, the strain rate is a function of time. In general, the change in rate after about 20 days is quite small in comparison to the scatter obtained from multiple tests. Following tradition, the strain rate versus stress relationship is modelled using the power function. The exponent of stress for the axial strain rate is about 2.3 and these changes but little for tests that are longer than about 20 days. There was more difficulty in fitting the power function to the lateral strain rate. At low stress, under 10 MPa, the lateral strain rate is very small, around the resolution of the instrumentation. Fitting only the rates above 10 MPa produces a power function with a stress exponent of 4.93.

Strains and strain rates obtained through a stress-increment or stress-decrement procedure using the same loading steps are significantly different. In a stress-decrement run,

the strains are lower and the rates higher than in the stress-increment procedure.

When a single creep test is repeated under the same environmental and loading conditions, the strains measured during the second test are always lower. The strain rates follow a more complex pattern depending on the time elapsed between the two tests. If the second test follows immediately after the first test is finished and the specimen is unloaded, the strain rate in the second test is higher than in the first. On the other hand, if a considerable delay is involved between the two tests (6 months in this case), it is the rate in the first test, which is the higher. It appears that the effects of the earlier loading history fade with time.

## 5.2 Recommendations for Further Research

Potash rock is a very complex material. As part of the salt rock group, it is the only rock type that has the capability to deform in a plastic manner. Its deformation, instantaneous and long-term, develops through both plastic and brittle mechanisms. Because of this extra complexity, it is very sensitive to environmental conditions; temperature and humidity are perhaps the most important. These effects have not been examined here; testing was at constant temperature and humidity. A separate research program would be needed to investigate the effect of both temperature and humidity.

The stress-path involved in a practical application is often complex. The present investigations into the effect of different stress-paths are sufficient only to signal the potential influence of a previous stress history. A research program that has a better balance

of stress-increment and stress-decrement procedures would be required to establish the relationship between the two loading procedures.

The specimens coming into the laboratory were tested as they were. The anomalous strains obtained during the first loading step would suggest that the arriving specimen could carry the effects of a previous loading history and may have also acquired undesirable characteristics during sample preparation. These characteristics may carry over to later loading steps as well, even though this may not be obvious. Is there a way to condition specimens so that they display only the effects of a controlled testing procedure? Further research could concentrate on answering the question.

It is quite obvious from these tests that the previous stress history has a very strong effect on measured strains and strain rates. It is obvious that neither a stress-increment nor a stress decrement procedure can reproduce the strains and strain rates at a given stress that would appear through direct loading to the same stress. Is there a definable relationship among the three loading procedures: the stress-increment, the stress-decrement and the direct loading methods? The answer to this question will always be hard to obtain, as the amount of work that it would require would be enormous.

Another element that this work has barely touched on concerns the memory effect. Letting the specimen rest after subjecting it to a loading procedure gave different results. The rest period was 6 months in this case. What is the rate and amount of recovery from a loading situation as a function of rest time? The answer to this question could come from an appropriately designed research project.

# REFERENCES

Bieniawski, T. Z.1967. Mechanism of brittle fracture of rock. Int. J. Rock Mech. Min. Sci, 4, 395-430.

Cadek, J. 1987. The back stress concept in power law creep of metals: a review, Material Science and Engineering, 94, 79-82.

Carter, N. L. And Hansen, F. D. 1983. Creep of rocksalt. Tectonophysics, 92, 275-333.

Cruden, D. M. 1971. The form of the creep law for rock under uniaxial compression, Int. J. Rock Mech. Min Sci., 8,105-126.

Duncan, E.J.S. 1990. Deformation and strength of Saskatchewan potash rock. Ph.D thesis, Department of Civil Engineering, The University of Manitoba, Winnipeg.

Duncan, E.J.S. and Lajtai, E.Z. 1993. The creep of potash salt rocks from Saskatchewan, Geotechnical and Geological Engineering, 11, 159-84.

Francis T. Wu and Leon T. 1975. Microfracturing and deformation of Westerly granite under creep condition, Int. J. Rock Mech.. Min. Sci. & Geomech. Abstr., 12, 167-173.

Guessous, Z., Ladanyi, B., and Gill, D. E. 1984. Effect of sampling disturbance on laboratory determined properties of rock salt. Proceeding 2nd Conf. on the Mechanical behaviour of salt, Hannover, Germany.

Guessous, Z., Gill, D. E., and Ladanyi, B. 1987. Effect of simulated sampling disturbance on creep behaviour of rock salt. Rock Mechanics and Rock Engineering, 20, 261-275.

Handin, J., Russel, J. E. And Carter, N. L., 1985. Experimental deformation of rock salt, American Geophysical Union, Monograph.

Hardy, H. R. 1958. Time -dependent deformation and failure of geologic materials. Colo. Sch. Mines Q. 54, 135.

Heard, H. C., 1972. Steady-state flow in polycrystalline halite at pressure of 2 kilobars, in flow and fracture of rocks, American Geophysical Union, Geophysical Monograph, 16, 191-210.

Hendron, A. J. 1968. Mechanical properties of rocks, in Rock Mechanics in Engineering Practice (K. C. Stagg and O. C. Zienkiewicz, Eds), Wiley, New York.

Herrmann, W. And Lauson, H. S. 1981. Analysis of creep data for various natural rock salts, Report SAND81-2567, Sandia Nationa; Laboratories, Albuquerque, New Mexico.

Hobbs, D. W. 1970. Stress-strain-time behaviour of a number of coal measure rocks. Int. J. Rock Mech. Min. Sci. 7: 149-170.

Horseman, S. 1988. Moisture content - a major uncertainty in storage cavity closure prediction, in The Mechanical Behaviour of Salt - Proceedings of the First Conference, (edited by H.R. Hardy and M. Langer), Pennsylvania State University, Trans Tech Publications, Clausthal, Federal Republic of Germany. 53-68.

Krempl, E. 1974. Cyclic creep - an interpretive literature survey. WRC Bulletin. 195: 63-123.

Ladanyi, B., Gill, D. E. 1983. In situ determination of creep properties of rock salt. Proceedings 5th Cong. I. S. R. M., Melbourne, vol. 1, A219-A225.

Lajtai, E.Z. and Duncan, E.J.S. 1988. The mechanism of deformation and fracture in potash rock, Canadian Geotechnical Journal, 25, 262-78.

Lajtai, E.Z., Carter, B.-J. and Duncan, E.J.S. 1994. En echelon crack-arrays in potash salt rock, Rock Mechanics and Rock Engineering, 27, 89-111.

Le Comte P. 1965. Creep in rock slat. J. Geol. 72, 469.

Li, Y. 1995. Creep and relaxation of 4 kinds of rock under uniaxial compression tests, Chinses Journal of Rock Mechanics and Engineering, Vol. 14, No. 1, 39-47.

Lux, K.H. and Rokar, R. 1984. Laboratory investigations and theoretical statements as a basis for the design of caverns in rock salt formation, in The Mechanical Behaviour of Salt - Proceedings of the First Conference, (edited by H.R. Hardy and M. Langer), Pennsylvania State University, Trans Tech Publications, Clausthal, Federal Republic of Germany. 275-310.

Patchet, S.J., 1970. Rock Mechanics studies associated with the development of a deep potash mine, Ph.D Thesis, Department of Mining Engineering, University of Newcastle upon Tyne.

Pomeroy C. D. 1956. Creep in coal at room temperature. Nature, Lond. 178, 279-280.

Reynolds T.D. and Gloyna E.F. 1961. Creep measurements in salt mines. Proc. 4th Symp. Rock Mech., H.L. Hartman Ed., (Penn. State Univ.), 11-17.

Roux A.J.A. and Denkhaus H.G. 1954. An investigation into the problem of rock bursts-An oprational research project. J. chem. metall. min. soc. S Afr. 55, 103-24.

Saito M. 1965. Forecasting the time of occurrence of a slope failure. Proc. 6th Int. Conf. Soil Mech. Found. Engrg. 2, 537-41.

Saito M. 1969. Forecasting time of slope failure by tertiary creep. Proc. 7th Int. Conf. Soil Mech. Found. Engrg. Mexico, 677-83.

Senseny, P. E. 1988. Creep properties of four salt rocks. Proceedings, Second Conference on the Mechanical Behaviour of Salt, Hardy and Langer (eds), Trans Tech Publications, Clausthel, Germany, 431-444.

Senseny, P. E., 1984. Specimen size and stress history effects on creep of salt, Proceedings of the 1st Conference on the Mechanical Behaviour of Salt, Pennsylvania State University, Pennsylvania, Trans Tech Publications, 369-79.

Singh, D. P. 1975. A study of creep of rock. Int. J. Rock Mech.. Min. Sci. & Geomech. Abstr. 12, 271-276.

Vyalov, S. S. 1970. Creep in rock. Proceeding of the second congress of the international Society for Rock Mechanics, Beograd, 2-5.

Vyalov, S. S. 1973. Long term failure of frozen soil as a thermal activated process. Proc. U.S.S.R. Contribution, 2nd Int. Conf. on Permafrost, Yakutsk, U.S.S.R. Washington, D.C., 222-228.

Wang, B. and Sun, M. 1989. The study of creep characteristic in rock mass of Xiaolongdi. Proceedings of the Rock Mechanics in Geological Engineering, Jiaozuo, China, 115-125.

Wawersik,W. R. 1972. Time-dependent rock behaviour in uniaxial compression. Rock Mechanics. 85-106.

Wawersik, W. R. et al. 1982. Excavation design in rock salt-laboratory experiments, material modelling and validations. ISRM Symposium, Aachen. 1345-1356.

Wawersik, W. R. 1985. Determination of steady state creep rates and activation paraweters for rock salt. ASTM STP 869. 72-92.

Woodford, D. A. 1969. Measurement and interpretation of the stress dependence of creep at low stress, Mat. Sci. Engr. 4: 146-154.

# IMAGE EVALUATION
# TEST TARGET (QA-3)

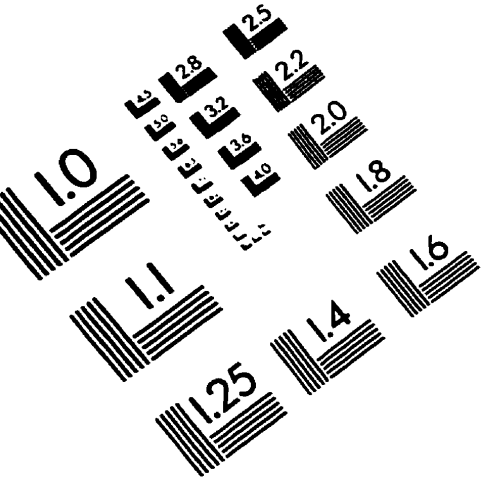


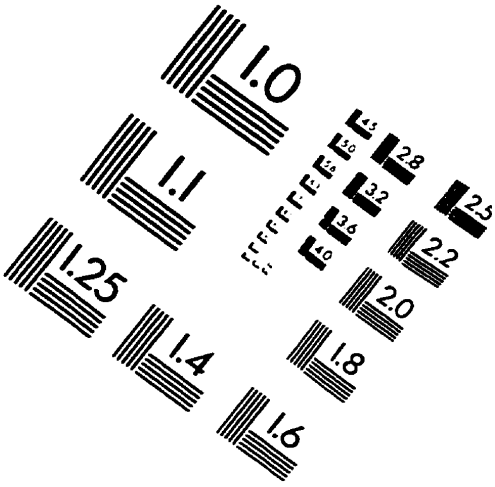


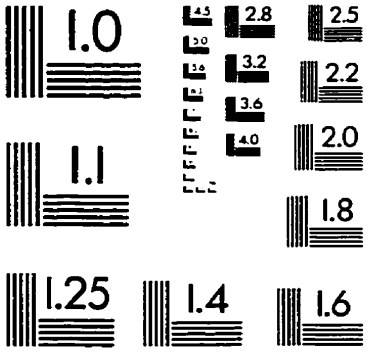


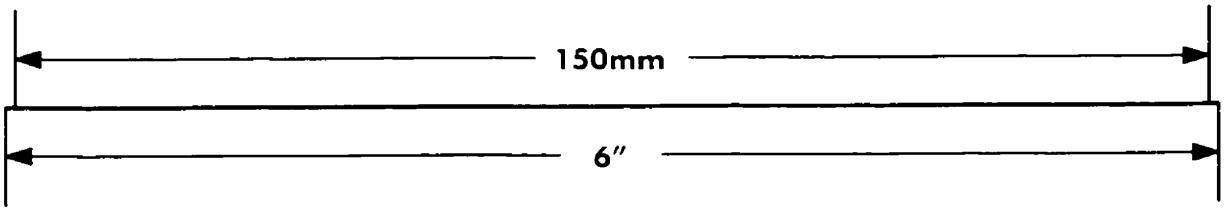


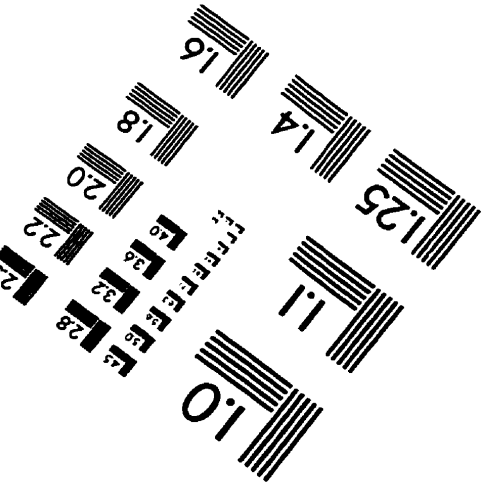


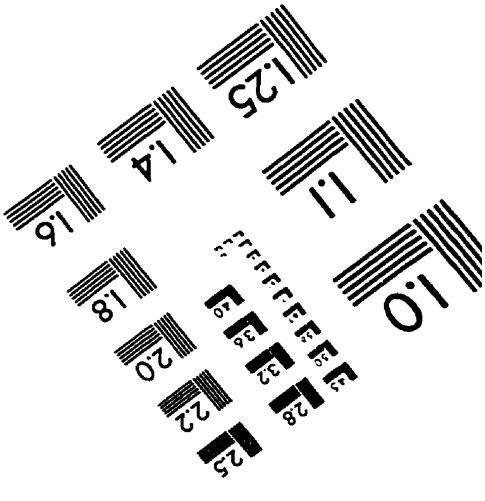


APPLIED IMAGE, Inc
1653 East Main Street
Rochester, NY 14609 USA
Phone: 716/482-0300
Fax: 716/288-5989